8-30-2013 12:00 AM

Insights into the Function of the FATC Domain of Saccharomyces Cervisiae TRA1 via Mutation and Suppressor Analysis

Samantha A. Pillon
The University of Western Ontario

Supervisor
Dr. Chris Brandl
The University of Western Ontario

Graduate Program in Biochemistry
A thesis submitted in partial fulfillment of the requirements for the degree in Master of Science

INSIGHTS INTO THE FUNCTION OF THE FATC DOMAIN OF *Saccharomyces cerevisiae* TRA1 via MUTATION AND SUPPRESSOR ANALYSIS

By: Samantha A. Pillon

Graduate Program in Biochemistry

A thesis submitted in partial fulfillment of the requirements for the degree of

Master of Science

The School of Graduate and Postdoctoral Studies

The University of Western Ontario

London, Ontario, Canada

August 2013

Abstract

The regulation of transcription is an important cellular function because it is the first step in gene regulation. In *Saccharomyces cerevisiae*, two protein complexes, SAGA and NuA4, act as regulators of transcription. A common protein shared between these two complexes, called Tra1, regulates transcriptional activation through its interaction with gene specific transcriptional activators. Tra1 is a member of the PIKK family of proteins, which are characterized by FAT, PI3K and FATC domains. The FATC domain encompasses the terminal 33-35 residues of the protein. Two mutations within the FATC domain, *tra1-L3733A* and *tra1-F3744A*, result in slow growth under stress conditions. Partially dominant mutations in the gene encoding Tti2, a 421 residues component of the TTT chaperone complex, suppressed these phenotypes. **My goal was to further characterize the role of the FATC domain of Tra1 by determining which residues are important for function, and characterize how these relate to the *TRA1-TTI2* interaction.** I created alleles of *tra1* which convert the terminal residue to serine (*tra1-F3744S*) or arginine (*tra1-F3744R*), an allele with the two terminal residues inverted (*tra1-WF-FW*), and alleles which resulted in deletions of one or two residues (*tra1-Δ1*and *tra1-Δ2). tra1-WF-FW* supported cell viability, whereas *tra1-F3744S* supported cell viability in the presence of the *tti2-F328S* suppressor. Slow growth at 37°C resulting from Tra1-WF-FW was also suppressed by *tti2*. Tra1-F3744S grew slowly at 37°C and on 6% ethanol in the presence of the suppressor. *tra1-F3744R, tra1-Δ1,* and *tra1-Δ2* would not support viability in the presence or absence of the suppressor.

To better understand the structure and function of Tti2, truncation mutations were created to identify essential regions of Tti2. These truncation mutations were assessed by analyzing cell viability, protein expression levels, and interaction with Tti1 and Tel2, two other members of the

TTT complex. Only Tti2-53-421 (containing residues 53-421) supported viability and retained its ability to interact with Tel2 and Tti1 at near wildtype levels. Tti2-53-238 and Tti2-1-238 interact with Tel2 but do not support viability. All of the other mutations did not support viability and showed minimal binding affinity to Tti1 and Tel2.

A terminal mutation of another PIKK family member, Mec1 (*mec1-W2368A*) also results in slow growth at 37°C. Interestingly, the *tti2-F328S* suppressor does not suppress the *mec1-W2368A* phenotype. Using bioinformatics approaches, I identified *rpn3-L140P*, encoding a component of the proteasomal cap, as a suppressor of *mec1-W2368A*.

Keywords: Tra1, TRRAP, Tti2, Mec1, ATR, Rpn3, SAGA, NuA4, ASTRA, yeast, genetics, transcription.

Acknowledgements

I would especially like to thank Dr. Chris Brandl, my supervisor, for all of his guidance and assistance over my two years as a graduate student in his lab. Due to his expertise and patience I have come to grow and learn as a scientist. I would also like to thank him for performing all of the tetrad dissections referred to in this work.

Thank you to my advisory committee, Dr. Eric Ball, Dr. Greg Gloor and Dr. Megan Davey for their advice regarding experiments and project ideas. I would also like to thank Dr. Gloor and Jean Macklaim for their time and patience while teaching me computer programming and bioinformatics. Their expertise and advice was crucial in elucidating the suppressor found in this thesis.

I thank all of the Brandl lab members, past and present, for their assistance, support, and energy in making the lab an enjoyable work environment. Thank you to Julie Genereaux for all of her help with implementing and improving my laboratory techniques. Thank you to Dominik Dobransky, Simon Lam, Kyle Hoffman, Lance DaSilva, Aaron Simkovich, Serina Dai, Cameron Rogers, Matthew Renaud, Adam Magill, and Michael Obeda for their encouragement and help throughout my time in the lab.

Thank you to Lance DaSilva, Tom Kolaczyk, Stephanie Zukowski, and Michelle Gabriel for proof reading this thesis.

Thank you to my friends and family for their unwavering support and encouragement. Thank you to my parents (David and Lilianna) and my two sisters (Sylvia and Monica) for always being there when things got tough and for helping in any way that they could. Thank you to Monica and my dad, David, for proof reading my thesis.

Thank you to the University of Western Ontario for the Western Graduate Research Scholarship (WGRS) that paid for my tuition.

Table of Contents

List of Tables

List of Figures

Table of Abbreviations

Abbreviation	Meaning
ASTRA	Assembly of Tel, Rvb, and Atm-like kinase
ATP	Adenosine Triphosphate
CBP	Calmodulin Binding Protein
DNA	Deoxyribonucleic acid
DOC	Sodium Deoxycholate
EDTA	Ethylenediaminetetraacetic acid
FAT	FRAP, ATM, TRRAP
FATC	FRAP, ATM, TRRAP, C-terminus
FRB	FKBP12 Rapamycin Binding
G	Gram
HAT	Histone Acetyltransferase
HEAT	Huntintin, Elongation factor 3, A subunit of protein phosphatase 2A and Tor1
HSP90	Heat Shock Protein 90
IDV	Integrated Density Value
Indel	INsertion or DELetion
kDa	Kilodalton
L	Litre
MDa	Megadalton
mRNA	Messenger RNA
µg	Microgram
µL	Microliter
mg	Milligram
mL	Millilitre
NuA4	Nucleosomal Acetyltransferase of histone H4
PCR	Polymerase Chain Reaction
PIC	Preinitiation complex
PI3K	Phosphatidylinositol-3-kinase
PIKK	Phosphatidylinositol-3-kinase related kinase
PMSF	Phenylmethylsulfonyl fluoride
PVDF	Polyvinylidene fluoride
RNA	Ribonucleic acid
RNAPII	RNA polymerase II
SAGA	Spt-Ada-Gcn5-acetyltransferase
SAM	Sequence Alignment/Map
SC	Synthetic Complete
SDS	Sodium Dodecyl Sulfate
SDS PAGE	Sodium Dodecyl Sulfate PolyAcrylamide Gel Electrophoresis

SLIK	SAGA-like complex
SNP	Single Nucleotide Polymorphism
TAF	TATA-binding protein associated factor
TBP	TATA-binding protein
TBS	Tris Buffered Saline
TBST	Tris Buffered Saline with Tween 20
TCA	Trichloroacetic acid
TE	Tris-EDTA
TFII	Transcription Factor II
TPR	TetratricoPeptide Repeat
TRRAP	TRansformation/tRanscription domain-Associated Protein
TTT	Tel2-Tti1-Tti2
YPD	Yeast Peptone Dextrose

Chapter 1: Introduction

1. Prelude

PIKKs are a family of proteins involved with cell transcription regulation, DNA repair, and nutrient-signalling in eukaryotic cells. The FATC domain of the PIKK protein family has been a subject of interest for many years because it is thought to play a role in the kinase activity of PIKK protein function. Interestingly, an essential PIKK, known as Tra1 in yeast, does not show kinase activity; however, its FATC domain remains an important region of the protein. Tra1 is a 3744 residue protein and member of essential acetyltransferase complexes including SAGA and NuA4. Both SAGA and NuA4 function in transcriptional activation of genes under stress conditions. Previous studies examined the effect of altering the FATC domain of Tra1, revealing that cells containing mutations to the FATC domain display slow growth under stress conditions or are inviable. These Tra1 FATC domain mutations include a substitution of the terminal phenylalanine to an alanine (*tra1-F3744A)*, a leucine to an alanine (*tra1-L3733A*), and an addition of glycine to the C-terminus (*tral-G3745*). Interestingly, a mutation in Tti2, *tti2-F328S*, rescues the slow growth phenotypes of *tra1-F3744A* and *tra1-L3733A* (*tra1-G3745* is inviable). Tti2 is implicated in the proper folding of proteins since it is a component of the TTT complex, which associates with HSP 90, and R2TP/prefoldin complex. This led to the hypothesis that one role of the FATC domain is for proper folding of Tra1. Notably, Tti2 and Tra1 are both components of a group of associated proteins named ASTRA. The Brandl lab is interested in trying to elucidate the function of Tra1. **The goal of my thesis is to further characterize the role of the FATC domain of Tra1 by determining which residues are important for function, and characterize how these relate to the *TRA1-TTI2* interaction.**

My introductory chapter covers topics central to Tra1 and its binding partners. These areas include: (1) an overview of transcription activation and chromatin remodelling, (2) the PIKK protein family, particularly their general structure and cellular function, (3) Tra1-containing protein complexes and their functions, (4) a summary of the current knowledge of the role of Tra1 determined by mutational studies, and (5) the role of Tti2 in the cell including its suppression of *tra1* alleles. Mec1, another PIKK protein harbouring kinase activity, is also discussed in my introduction as experiments on Mec1 can be used to validate and complement findings in Tra1.

2. Transcriptional Activation and Chromatin Remodelling

Transcription is the first step for protein expression within the cell. Efficient transcription activation is necessary for the cell to produce proteins in response to cell growth, differentiation and environmental change. The first step in transcription is the formation of the preinitiation complex (PIC) at the promoter (Wandelt and Grummt, 1983). PIC assembly involves localizing transcription factors to the target promoter. These transcription factors include TFIIA, TFIIB, TFIID, TFIIE, TFIIF, and TFIIH, which are assisted with their localization to the promoter by TATA binding proteins (TBP) (Ranish *et al.*, 1999; Reinberg and Roeder, 1987; Flores and Reinberg, 1992). TBP, along with TFIID, TFIIA and TFIIB, bind DNA at the promoter region (Reinberg and Roeder, 1987; Ranish *et al*., 1999). TBP, TFIIB and TFIIF are necessary for recruiting RNAPII (RNA polymerase II) to the promoter (Killeen *et al*., 1992). TFIIE and TFIIH (one component of which is a helicase) function to separate and stabilize the DNA strands (Holstege *et al*., 1996). This separation and stabilization is important for future steps in transcription including promoter clearance and RNAPII elongation (Maxon *et al*., 1994;

Holstege *et al*., 1996). The nucleosomes surrounding the gene must be altered to allow these factors access to DNA. Histone acetyltransferases play a part in this process (Mizzen *et al*., 1996).

Chromatin remodelling is the name given to the process of altering nucleosomes. A nucleosome consists of DNA encircling a histone octamer, composed of two molecules of each of histone H2A, H2B, H3, and H4, approximately twice, (Luger *et al*., 1997). In addition to transcription regulation, chromatin remodelling is involved in processes such as DNA repair, DNA replication and chromosome segregation (reviewed by Clapier and Cairns, 2009). There are two principal methods of gaining access to genes enveloped in nucleosomes. The first is by moving, removing, or exchanging histones in an effort to change the nucleosome structure in an ATP dependent manner (Clark *et al*., 1992; Adam *et al*., 2001). An example of histone exchange would be switching a histone H2A particle for a histone Htz1 variant at the transcriptional start site for RNA PolII recruitment (Adam *et al*., 2001). The second is through post-translational modifications, such as acetylation or methylation, which is thought to elicit a "histone code" (Strahl and Allis, 2000; Noma *et al*., 2001). These modifications can disrupt the interaction between DNA and the histone allowing access of other transcription factors to the promoter, as well as recruiting cofactors to the promoter that specifically recognize the modified histones (Strahl and Allis, 2000; Noma *et al*., 2001). Methylation can also repress transcription by condensing the chromatin (Strahl and Allis, 2000; Rea *et al.*, 2000). The complexes with which Tra1 associates contain histone acetyltransferase activity and in the case of SAGA also deubiquitylation (Rodríguez-Navarro, 2009). Its role in chromatin modification complexes is one reason that Tra1/TRRAP is an interesting target for drug therapy.

3. PIKK Protein Family

The phosphoinositide-3-kinase related kinase (PIKK) family of proteins function as kinases within various cell signalling pathways (reviewed by Keith and Schreiber, 1995). These PIKK proteins include Tel1 (yeast)/ATM (human), Mec1/ATR, DNA-PKcs (human), SMG-1 (human), Tra1/TRRAP, and Tor/mTOR (Keith and Schreiber, 1995). The pathways which involve PIKKs are largely those required for stress response. Mec1/ATR, Tel1/ATM and DNA-PKcs are implicated in the pathways related to DNA damage, such as single stranded gaps and double stranded breaks (Weinert *et al*., 1994; Jackson, 1996). SMG-1 plays a role in mRNA nonsense-mediated decay and Tor/mTOR is required for nutrient-dependent signalling (Yamashita *et al*., 2001; Barbet *et al*., 1996).

The general structure of PIKKs includes five domains: a HEAT domain, a FAT domain, an FRB domain, a PI3K domain, and a FATC domain (**Figure 1)** (Knutson and Hahn, 2011). The HEAT (Huntington, Elongation factor 3, A subunit of protein phosphatase 2A and Tor1) domain consists of multiple HEAT repeats strung together at the N-terminus of the protein (Brewerton *et al*., 2004; Perry and Kleckner, 2003). These HEAT repeats are a known motif for protein-protein interactions (Ruediger *et al.,* 1994). The FAT (FRAP, ATM, TRRAP) domain also consists of HEAT repeats as well as TPR (tetratricopeptide) repeats, and together form an alpha helical domain that take on a "C" shape and wraps around the PI3K domain (Yang *et al*., 2013). The FAT domain contacts the PI3K domain with residues that are conserved within mTOR orthologs and these residues are important for mTOR function (Yang *et al.,* 2013). The FRB (FKBP12 Rapamycin Binding) domain is formed by four alpha helices and sits within the PI3K domain in mTOR (Yang *et al*., 2013) The FRB domain is a regulatory domain since it can inhibit

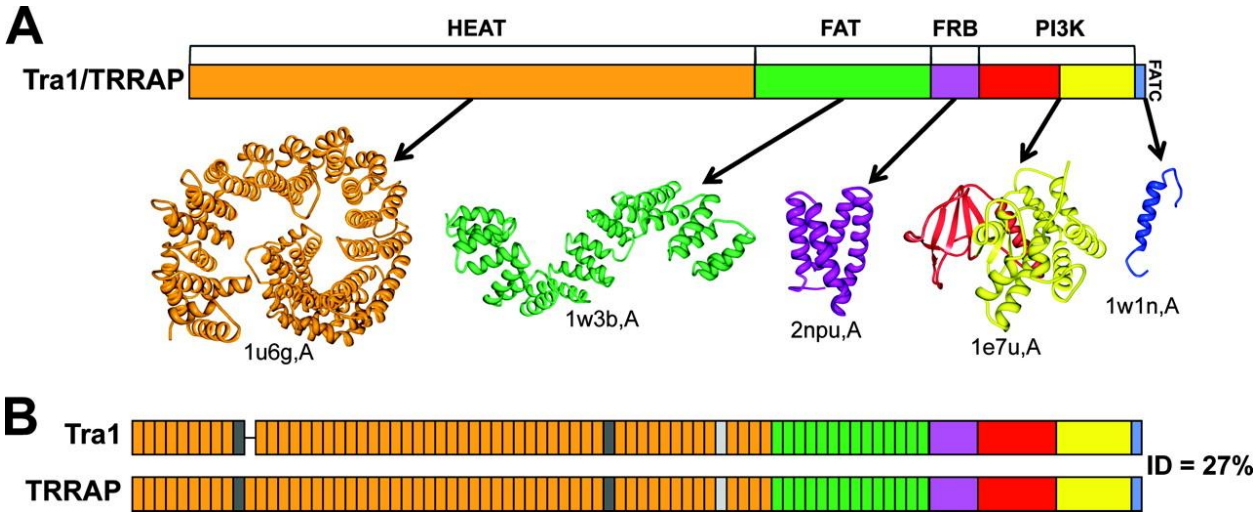

Figure 1. Schematic of the arrangement of the domains in wildtype Tra1. ***A***. The orientation of the domains within Tra1/TRRAP is outlined with the projected secondary structure underneath. ***B.*** The differences between the domain orientation of Tra1 and TRRAP are shown. Knutson and Hahn, (2011).

mTOR function when it is bound by rapamycin and FKBP12 (reviewed by Huang *et al*., 2003). The PI3K domain resembles the PI3K lipid kinases (Berndt *et al.,* 2010; Lempiäinen and Halazonetis, 2009; Yang *et al*., 2013) and consists of two lobes, the N-terminal lobe and the C-terminal lobe, with a cleft region between the two lobes where ATP can bind (Yang *et al*., 2013). Lastly, the FATC (FAT C-terminus) domain is a small 33-35 residue domain at the C-terminus of the PIKK proteins and consists of alpha helices (Dames *et al.,* 2005; Yang *et al*., 2013). In mTOR, the FATC domain contains cysteine residues which were thought to form a loop between the helices (Dames *et al*., 2005). The formation of a loop within the FATC domain was not seen in the mTOR crystal structure by Yang *et al.,* (2013). The role of the FATC domain is crucial for stability and kinase function of the PIKK proteins which contain kinase activity (Morita *et al*., 2007; Jiang *et al*., 2006; Rivera-Calzada, 2005). Interestingly, the FATC domain is so highly conserved among some of the PIKKs that they are interchangeable (Sommer *et al*., 2013). For example, the FATC domain of Tel1/ATM can be replaced by the FATC of DNA-PKcs, Tra1/TRRAP, or Tor/mTOR (Jiang *et al*., 2006; Sommer *et al*., 2013). This does not hold true for all PIKKs since the FATC domain of Tel1/ATM cannot replace the FATC of Mec1/ATR or Tor/mTOR (Takahashi *et al*., 2000; Mordes *et al*., 2008).

4. Transcriptional Regulators: Complexes associated with Tra1

a. SAGA

The SAGA (Spt-Ada-Gcn5 Acetyltransferase) complex was first identified in *S. cerevisiae* and is a large 1.8 MDa complex with 19 subunits (**Figure 2)**. As stated in Rodríguez-Navarro (2009), SAGA is modular with histone acetyltransferase (HAT), deubiquitylation, mRNA export, and promoter recruitment modules. The largest subunit within SAGA is Tra1.

A

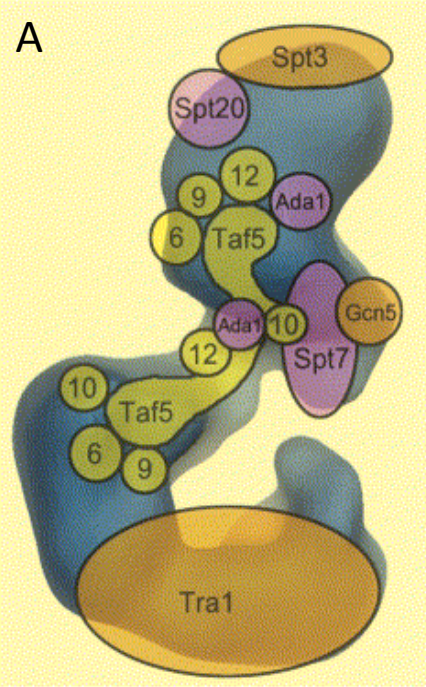

B

SAGA Subunits	
Ada1	Spt20
Ada2	Sus1
Ngg1/Ada3	Taf5
Gcn5	Taf6
Sgf11	Taf9
Sgf29	Taf10
Sgf73	Taf12
Spt3	Tra1
Spt7	Ubp8
Spt8	

Figure 2. Schematic of the SAGA (Spt-Ada-Gcn5 Acetyltransferase) complex. **A.** The structure of SAGA was determined using electron microscopy. Tra1 is positioned at the edge of the complex. Wu *et al*., (2004). **B.** A list of all the subunits in SAGA.

Within the SAGA complex, Tra1 is thought to play an integral role in transcriptional activation via interactions with gene specific activators (Fishburn *et al*., 2005).

The Spt3 and Spt8 proteins within the SAGA complex aid in transcriptional regulation by recruiting TATA-binding proteins (Eisenmann *et al*., 1992; Eisenmann *et al*., 1994). Both have been shown to directly interact with TBP proteins (Dudley *et al*., 1999a; Bhaumik and Green, 2002). Interestingly, Spt3 and Spt8 can also repress transcription (Belotserkovskaya *et al*., 2000). How these proteins distinguish between transcription activation and repression remains unknown.

The structural integrity of the SAGA complex is achieved by a group of proteins called SPT (SuPressor of Ty) and TAF (TATA-binding protein-Associated Factor) proteins and Ada1 (Sterner *et al*., 1999; Grant *et al*., 1998a). The structural module is composed of Spt7, and Spt20; while the TAF proteins include Taf5, 6, 9, 10, and 12 which also have a role in the general PolII transcription factor TFIID (Sterner *et al*., 1999; Grant *et al*., 1998a). An *spt7* deletion strain showed a loss of SAGA complex integrity revealing the subunit's importance for SAGA formation (Wu and Winston, 2002).

The histone acetyltransferase (HAT) module in SAGA includes Ngg1, Ada2, Gcn5, and Sgf 29 (Horiuchi *et al.,* 1995; Balasubramanian *et al*., 2002; Samara and Wolberger, 2011). In particular, this module of SAGA acetylates histone H3 at K9, K14, K18, and K23 as well as having some activity on histone H4 and histone H2B (Grant *et al*., 1999; Pray-Grant *et al*., 2005). Gcn5 is the main catalytic subunit, Ngg1 is important for assessing lysine specificity and Ada2 aids with the complex's catalytic activity (Balasubramanian *et al*., 2002). In addition to transcription activation, acetylation of the nucleosomes aids in transcription elongation.

Releasing DNA from the nucleosome helps to increase RNAPII processivity (Govind *et al*., 2007). As stated by Budillon *et al*., (2007), acetylation is multifaceted and known to play several other roles in the cell aside from chromatin remodelling, such as the regulation of protein function (Budillon *et al.*, 2007).

The SAGA complex also modifies chromatin through deubiquitylation by Ubp8, Sgf11, Sus1, and Sgf73 (Koutou *et al*., 2010). Ubp8 is the catalytic protein of the module and Sgf73 links the module to the rest of the SAGA complex (Henry *et al*., 2003; Khöler *et al*., 2008). SAGA deubiquitylation occurs on histone H2B in yeast (Daniel *et al*., 2004). When the deubiquitylation activity of the SAGA module is disrupted, the methylation of histone H3 is also affected (Henry *et al.*, 2003). This highlights the complexity of the SAGA deubiquitylation function. Alone Ubp8 lacks deubiquitylation activity and requires the presence of the other module components which most likely causes a conformational change in the protein (Bonnet *et al*., 2008; Lee *et al*., 2005). Without Sgf73, the deubiquitylation complex is no longer bound to SAGA yet the deubiquitylation complex retains its activity (Khöler *et al*., 2006). This suggests a role for the deubiquitylation module outside of SAGA (Khöler *et al*., 2006). As well, Sus1 is involved with mRNA export and interacts with the TREX2 RNA export complex (Khöler *et* al., 2008). While it is unclear whether Sus1 acts in the TREX2 complex with other SAGA constituents, the dual roles of Sus1 connect SAGA to mRNA transport (Khöler *et al.,* 2008).

There is an alternate form of SAGA in *S. cerevisiae* called SLIK (SAGA-Like) (Pray-Grant *et al*., 2002). SAGA and SLIK share many of the same proteins including Tra1. Additionally, SLIK also contains acetylation and deubiquitylation activity which is catalyzed by Gcn5 and Ubp8, respectively (Pray-Grant *et al*., 2005). Notably, SLIK differs from SAGA in

that the Spt7 within SLIK contains a C-terminal truncation and Spt8 is not included in the complex (Belotserkovskaya *et al*., 2000; Pray-Grant *et al*., 2002).

b. NuA4

NuA4 (NUcleosome Acetyltransferase of histone H4), an essential 1.3MDa transcription regulatory complex in *S. cerevisiae*, also includes Tra1 (Allard, 1999). NuA4 contains acetyltransferase activity and is involved in transcription activation and the DNA repair pathway (reviewed in Doyon and Cote, 2004). The NuA4 complex contains approximately 13 proteins in *S. cerevisiae* and approximately 15 associated proteins in mammalian cells (**Figure 3**) (Doyon and Cote, 2004). Eaf1 acts as the NuA4 complex scaffold much like Spt7 in SAGA; in the absence of Eaf1, the structural integrity of NuA4 is lost (Auger *et al.*, 2008; Chittuluru *et al*., 2011). The catalytic component of NuA4 is the acetyltransferase Esa1, an essential protein in yeast (Tip60 in mammalian cells) (Allard, 1999). NuA4 specifically acetylates K5, K8, K12, and K16 on histone H4 and it also acetylates lysine residues on histone H2A *in vivo* (Allard, 1999). There are three other proteins, Epl1, Eaf6, and Yng2 (EPC1, mEAF6, and ING3, respectively, in mammalian cells), that work in subcomplex with Esa1 to allow for acetyltransferase activity (Doyon and Cote, 2004; Lu *et al*., 2009). Together with Esa1, this complex is named piccolo NuA4 (Boudreault *et al*., 2003). As a full complex, NuA4 only acetylates histones at specific genes; however, piccolo NuA4 has broader acetylation function (Boudreault *et al*., 2003). To access the DNA wrapped around histone H2A, NuA4 works in tandem with the Swr1 complex, which removes histone H2A and replaces it with the histone H2A variant Hzt1 (H2A.Z in mammalians) (Kobor *et al*., 2004). This is followed by NuA4 acetylation at the N-terminal tail of the histone (Keogh *et al*., 2006).

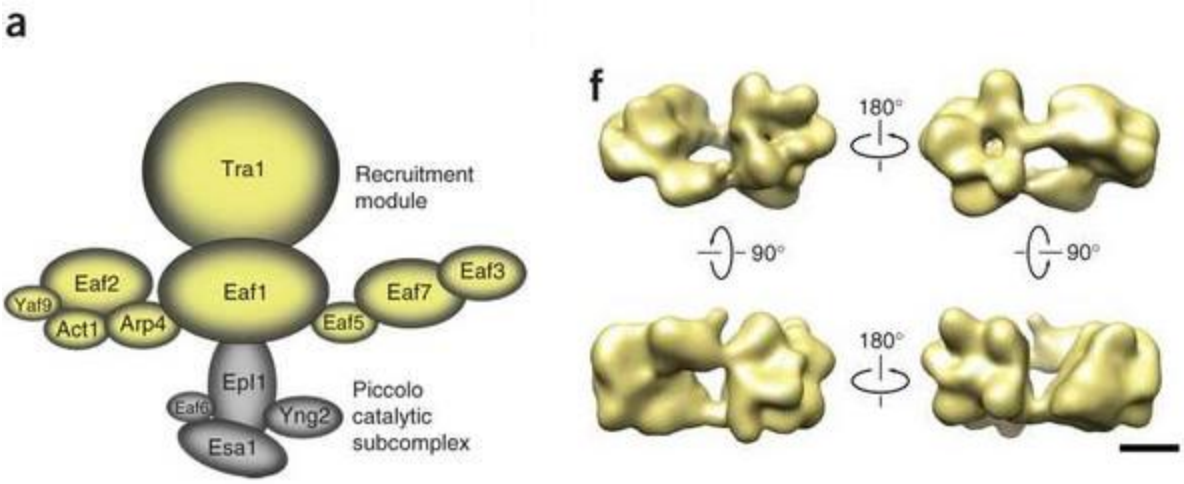

Figure 3. NuA4 schematic of the organization of the subunits and EM image of NuA4. ***A.*** A schematic image of the organization and orientation of the subunits of the NuA4 complex where Tra1 is bound to Eaf1 (From Chittuluru *et al*., 2011, based off of Doyon and Cote, 2004). ***F.*** Electron microscopy image of the NuA4 complex shown from each side. Chittuluru *et al*., (2011).

Much like its role in SAGA, Tra1 is involved with transcriptional regulation in NuA4 (Brown *et al*., 2001). Tra1 recruits the NuA4 complex to gene-specific promoter regions (Brown *et al*., 2001). Once recruited to the promoter, NuA4 acetylates histones and transcription can be activated (Brown *et al*., 2001; Doyon and Cote, 2004).

Arp4 and Esa1 are necessary for the recruitment of the NuA4 complex at sites of chromatin remodelling to signal DNA repair (Brown *et al*., 2001; Steinboeck *et al*., 2007). Esa1 acetylation by NuA4 is required in the repair of double stranded breaks (Bird *et al*., 2002). Arp4, which typically binds histones, recognizes the phosphorylated histone H2A at the site of the break (Bird *et al*., 2002; Downs *et al*., 2004). Esa1 and Apr4 directly interact and together recruit NuA4 to the site of a double stranded break (Steinboeck *et al*., 2007).

The presence of Tra1/TRRAP in multiple complexes, illustrates the versatility and importance of Tra1/TRRAP in the cell.

c. ASTRA

ASTRA (ASsembly of Tel, Rvb, and Atm-like kinase) is the name given a group of seven associated proteins, Rvb1, Rvb2, Asa1, Tel2, Tti1, Tti2, and Tra1/TRRAP, each of which is essential (Shevchenko *et al*., 2008). The ASTRA proteins were found to interact via a set of co-immunoprecipitation experiments (Shevchenko *et al*., 2008; Stirling *et al*., 2011). The function of ASTRA within the cell is unclear but preliminary studies suggest that the components are required for chromosome integrity (Stirling *et al*., 2011). However, there are some questions that remain with regard to the function and even the existence of ASTRA, since the intact complex has not been isolated.

Rvb1 and Rvb2 are members of the AAA+ (ATPases Associated with diverse cellular Activities) protein family and partner with various chaperone and chromatin remodelling complexes (Shen *et al.*, 2000; Kanemaki *et al.*, 1999; Makino *et al.*, 1998). These AAA+ proteins function in several cellular pathways including DNA repair and transcription (Shen *et al.*, 2000). Tel2, Tti1, and Tti2 together form a complex called the TTT complex (Hurov *et al.*, 2010). Tti1 and Tti2 were both identified as proteins involved in the DNA damage response pathway (Hurov *et al*., 2010). In the absence of Tti1, cells cannot arrest in G2 phase or stop DNA replication in the response to irradiation (Hurov *et al*., 2010). Asa1 is a protein involved in telomere maintenance along with Tel2 and Tti1 (Stirling *et al*., 2011). In addition to its telomeric role, Asa1 is thought to aid the TTT complex with the biogenesis of various PIKKs (Stirling *et al*., 2011).

The TTT complex interacts with PIKKs, particularly newly synthesized PIKKs (Takai *et al*., 2010). This interaction is short lived and thought to be an important step in the formation of PIKKs (Takai *et al*, 2010). HSP90 (heat shock protein 90) also interacts with the TTT complex, supporting the hypothesis that the TTT complex is a chaperone (Takai *et al*., 2010). HSP90 and the TTT complex are both required for the proper maturation of the newly synthesized PIKKs (Takai *et al*., 2010). All three proteins, Tti1, Tti2, and Tel2, are required to form a stable complex (Hurov *et al.*, 2010, Takai *et al*., 2010).

5. Tra1/TRRAP

Tra1 is a 433 kDa essential protein with roles in the SAGA complex, the NuA4 complex, and ASTRA as well as some independent functions (Saleh *et al*., 1998; Hoke *et al*., 2008; Helmlinger *et al*., 2011; Stirling *et al*., 2011). Its human homologue TRRAP (TRansformation/tRanscription

domain Associated Protein) is found in related complexes. A main characteristic of the PIKK family is that they contain a kinase domain; however, Tra1 does not have kinase activity (Saleh *et al.,* 1998). While no enzymatic activity of Tra1/TRRAP has been determined, mutation studies show that the PI3K domain is important for Tra1 function. A mutation was created in the Tra1 PI3K domain and converts a serine followed by two arginines to three alanines in Tra1 at positions 3413-3415 (*tra1-SRR3413-3415AAA*). *tra1-SRR3413-3415AAA* results in slow growth at 37°C, on 6% ethanol, and 5µg/mL of Calcofluor white plates grown at 30°C (Mutiu *et al*., 2007). In addition to its slow growth defects, it was found that this mutation resulted in generation dependent telomere shortening (Mutiu *et al*., 2007). It is unknown whether this effect is direct or indirect (Mutiu *et al.*, 2007).

A modelled structure of the FATC domain from Tor1 depicted its C-terminus pointing in towards the active site of the protein (Lempiäinen and Halazonetis, 2009). The model shows the activation site residues from the PI3K domain forming a pocket. This pocket includes the FATC domain and the ATP binding site (Lempiäinen and Halazonetis, 2009). The structure of DNA-PKcs was also modelled by Sibanda *et al.* (2010), and it showed a similar interaction between the FATC domain and the PI3K domain. It was not until recently that a crystal structure was solved for a portion of a PIKK protein, mTOR (Yang *et al.*, 2013). This crystal structure presents the FATC domain of mTOR looping back to interact with the PI3K domain, similar to the modelled structures (Yang *et al.*, 2013; Sibanda *et al.*, 2010; Lempiäinen and Halazonetis, 2009). Analysing the crystal structure of mTOR shows the FATC domain surrounding the activation loop (**Figure 4**) (Yang *et al*., 2013).

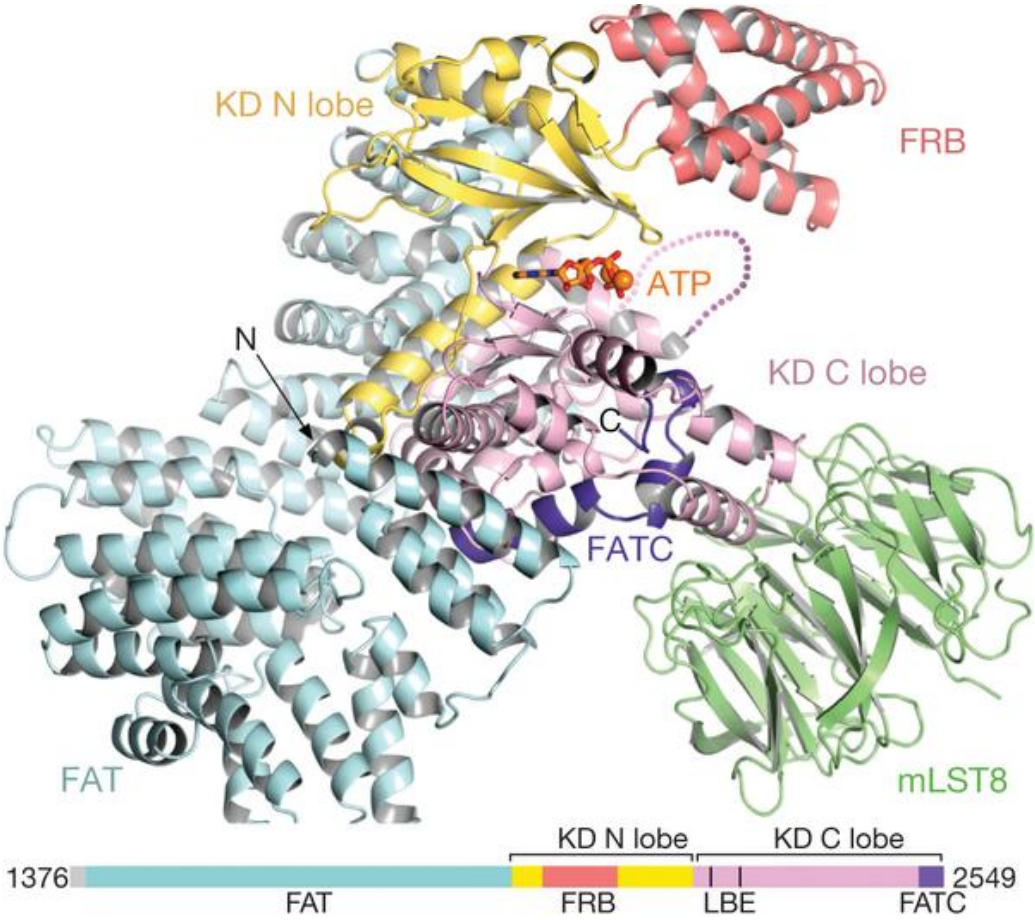

Figure 4. Crystal Structure of mTOR in complex with Lst8. The crystal structure of the FAT, FBR, PI3K, and FATC domains of mTOR are shown. The FATC domain is dark purple, the ATP residue is orange and the C-terminal lobe of the PI3K kinase domain is light purple. The C-terminal end of the FATC domain wraps around the C-terminal lobe of the PI3K domain. Yang *et al.,* (2013).

To better understand the role of the Tra1 FATC domain, mutagenesis experiments were performed. Two mutations were created within the FATC domain of Tra1. A mutation from a leucine to an alanine at position 3733 in Tra1 was generated (*tra1-L3733A*) (Hoke *et al*., 2010). This mutation showed slow growth when grown under stress conditions such as on YPD (yeast peptone dextrose) plates grown at 37°C, on plates containing either 6% ethanol, 5µg/mL of Calcofluor white, or 1nM rapamycin (**Figure 5**) (Hoke *et al*., 2010). The C-terminal residue of Tra1 was mutated from a phenylalanine to an alanine (Tra1-F3744A) (Genereaux *et al*., 2012). The Tra1-F3744A mutation showed slow growth under the same conditions as Tra1-L3733A (**Figure 5**) (Hoke *et al*., 2010). This growth sensitivity demonstrates the importance of the C-terminus of the FATC domain. Interestingly, the leucine at position 3733 is highly conserved among Tra1/TRRAP from various species and among differing PIKKs, and the terminal residue of the PIKKs is always large and hydrophobic but not always phenylalanine (**Figure 6**) (Hoke *et al*., 2010*).* A third mutation where a glycine residue was added to the C-terminus of Tra1 was created to determine its effect on Tra1 and cell viability (Hoke *et al*., 2010). The addition of the C-terminal glycine residue resulted in inviability (Hoke *et al.*, 2010), further supporting the notion that the C-terminal residues of Tra1 are important for function.

The C-terminal mutations of Tra1 can be suppressed by both intragenic and extragenic mutations. Tra1-N3677D and Tra1-T3716A, found in the PI3K domain and FATC domain, respectively, rescued the slow growth phenotype of Tra1-L3733A when cells were grown on 4% ethanol at 30°C (Hoke *et al.*, 2010). Moreover, novel extragenic mutations were found to suppress both the phenotypes resulting from Tra1-L3733A and Tra1-F3744A (Genereaux *et al.*, 2012). Tti2-F328S and Tti2-I336F will suppress both of the Tra1 C-terminal mutations and based on the known chaperone functions of Tti2 are thought to function by stabilizing and assisting in

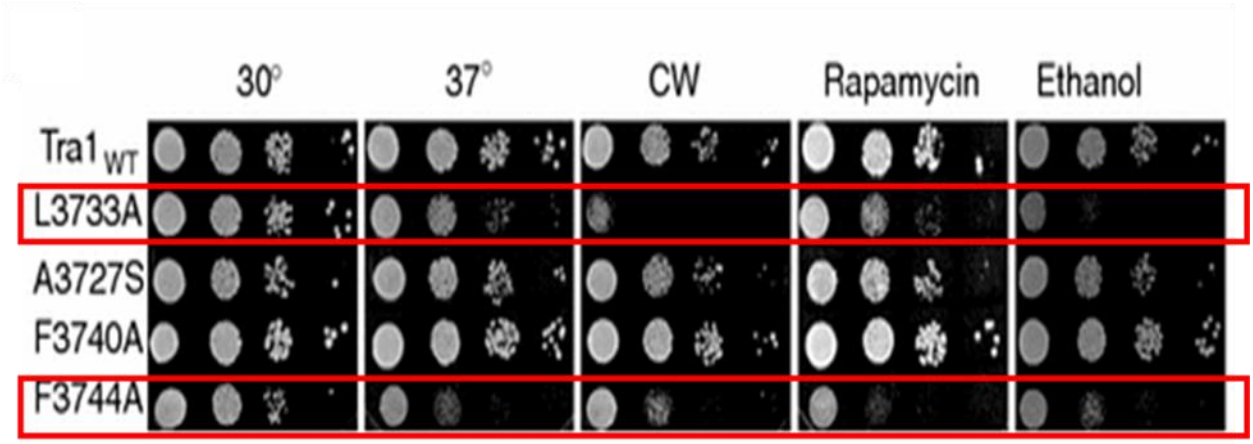

Figure 5. Phenotype of *tra1-F3744A* and *tra1-L3733A* under various stress conditions. A serial dilution of each haploid cell cultures of each genomically integrated mutation and wildtype allele were plated onto YPD grown at 30°C or 37°C, or YPD containing 5 µg/ml Calcofluor white (CW), 1 nM rapamycin, or 6% ethanol grown at 30°C. The *tra1-F3744A* and *tra1-L3733A* are boxed in red. Hoke *et al.*, (2010).

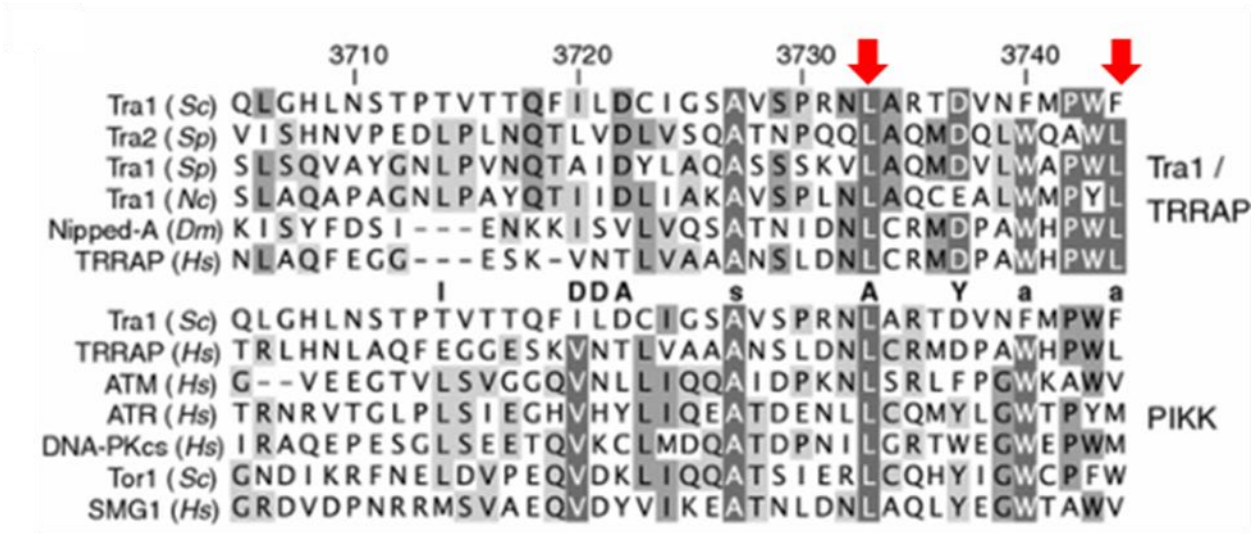

Figure 6. FATC Sequence Alignment. Using the Clustal W program, a sequence alignment of the FATC domains across various species of Tra1 (top portion) and different PIKK proteins (bottom portion) were generated. The conserved leucine residue at position 3733 and the residues at position 3744 are denoted by a red arrow. Hoke *et al*., (2010).

the folding of Tra1/TRRAP thus implicating the FATC domain in these processes (Genereaux *et al*., 2012).

Unlike *Saccharomyces cerevisiae*, *Schizosaccharomyces pombe* contains two copies of Tra1, Tra1 and Tra2. Tra1 is a component of SAGA and ASTRA and Tra2 a component of NuA4 (Helmlinger *et al.*, 2011). Interestingly, only Tra2 is required for cell viability (Helmlinger *et al.*, 2011). Since *tra1Δ* strains are viable, it allowed Helmlinger *et al.*, (2011) the opportunity to explore the cellular function of Tra1. Tra1 was long thought to be a scaffold protein for the SAGA complex due to its large size (Knutson and Hahn, 2011). Rather, Tra1 deletion in *S. pombe* showed that Tra1 is not required for the assembly of the SAGA complex (Helmlinger *et al.*, 2011). Secondly, it was noted that only specific genes were activated by SAGA and Tra1 (Helmlinger *et al*., 2011). Based on genome-wide expression changes and chromatin immunoprecipitation assays, SAGA was found to have both Tra1 dependent and independent recruitment to promoters (Helmlinger *et al.*, 2011). This datum suggests that Tra1 contains a specific regulatory role within SAGA. Originally, Tra1 was thought to have a global recruitment effect to promoters in the SAGA complex, but the ability for SAGA to be targeted to a promoter without Tra1 suggests that Tra1 is required for specific genes (Helmlinger *et al.*, 2011).

6. Tti2

S. cerevisiae Tti2 (Tel two interacting protein 2) is a 421 amino acid residue protein found associated with Tel2 and Tti1 in the TTT complex (Hurov *et al*., 2010) and also the putative ASTRA complex. There is a TTT complex in *S. pombe*; however, it differs slightly from *S. cerevisiae* (reviewed by Kanoh and Yanagida, 2007). In *S. pombe*, Tel2 and Tti1 are strongly

associated with one another and these two proteins are similarly important for interaction with PIKKs (Kanoh and Yanagida, 2007); however, the interaction of Tel2 with Tti2 is not as strong.

As previously stated, Genereaux *et al*., (2012) identified two *tti2* mutations that rescue the slow growth phenotype caused by Tra1-F3744A and Tra1-L3733A. The two *tti2* mutations that resulted in suppression are a phenylalanine to a serine at position 328 (Tti2-F328S) and an isoleucine to a phenylalanine at position 336 (Tti2-I336F) (Genereaux*et al*., 2012). Tti2-F328S demonstrated slightly better suppression than Tti2-I336F and was pursued with further experiments (**Figure 7**) (Genereaux *et al*., 2012). Tti2-F328S suppresses two different mutations in the FATC domain, but was unable to suppress mutations in the Tra1 PI3K domain, nor was it able to suppress the deletion of other components of SAGA, such as *spt7*and *ada2* (Genereaux *et al*., 2012). This suggests that although Tti2-F328S does not directly interact with the terminal residue of the *tra1-F3744A* mutant allele, the suppression is allele specific to Tra1 (Genereaux *et al*., 2012). Tti2 suppression was found to be partially dominant and the mechanism of the suppression is thought to be through the stabilization and folding of Tra1 (Genereaux *et al*., 2012). Western blots performed with Tra1-F3744A in the presence or absence of the *tti2-F328S* suppressor indicates that Tti2-F328S increases the level of Tra1-F3744A (Genereaux *et al*., 2012). The *tra1-F3744A* allele also reduces the protein's nuclear localization, particularly under conditions of stress (Genereaux *et al.*, 2012). In the presence of the Tti2-F328S suppressor, this effect was partially reversed (Genereaux *et al*., 2012). These results suggest that Tti2 may aid in the proper folding and stability of Tra1.

7. Mec1/ATR

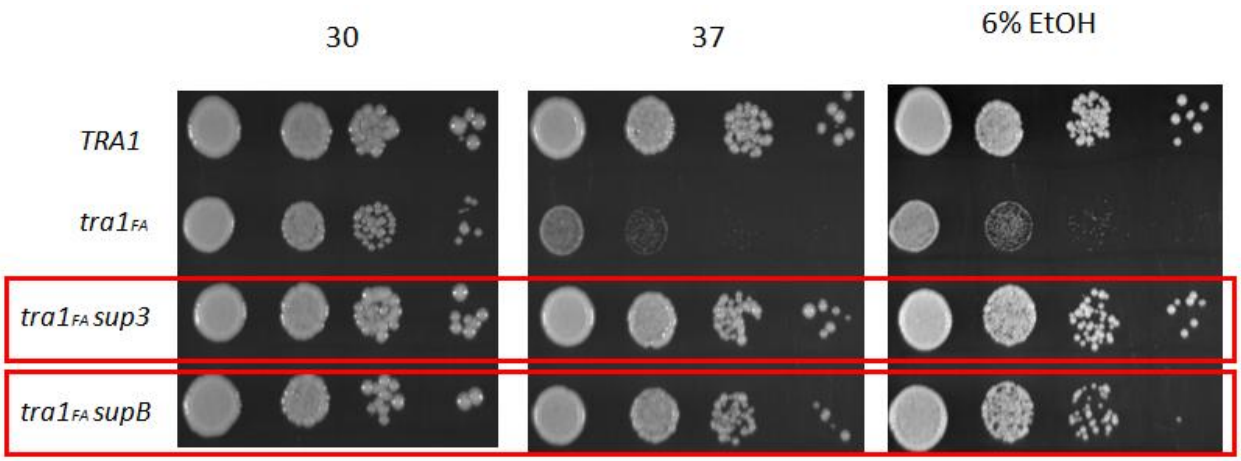

Figure 7. Suppression of *tra1-F3744A* by Tti2-F328S (Sup3) and Tti2-I336F (SupB). Genomically integrated *tra1-F3744A* haploids containing either no suppressor, Tti2-F328S (SUP3), or Tti2-I336F (SUPB) were grown to stationary phase and spotted onto either YPD grown at 30°C or 37°C, or YPD containing 6% ethanol grown at 30°C. Genereaux *et al*., (2012). A wildtype Tra1 haploid (*TRA1)* was used as a positive control.

Mec1 and its human homolog ATR are also members of the PIKK family (reviewed in Abraham 2001). Mec1 is an essential protein with a mass of approximately 273 kDa (Cortez *et al*., 2001; Brown and Baltimore, 2003). The FATC domain of Mec1 is similar to Tra1 (**Figure 8**) though some differences are noted. For example, the last two residues of Mec1 are a phenylalanine followed by a tryptophan; this is reversed in Tra1.

Unlike Tra1, Mec1 has kinase activity with substrates including Rad9 (in DNA damage), Cdc13 (in telomere recruitment), and Ies4 (in checkpoint response to DNA damage) (Emili, 1998; Tseng *et al.*, 2006; Morrison *et al*., 2007). Mec1 has several roles within the cell: maintaining the integrity of replication forks, and initiating cell cycle checkpoints and DNA repair pathways (Lopes *et al.,* 2001). Given that Mec1 plays such a crucial role at the S-phase checkpoint in the cell cycle, it is highly regulated (Friedel *et al*., 2009). Mec1 is activated under stress conditions such as DNA damage during S-phase or stalling of the replication fork (Friedel *et* al., 2009). To activate Mec1, there are three proteins that come together and form a clamp called the 9-1-1 clamp which is loaded at the site of DNA damage (Burtelow *et al.*, 2001; Majka *et al.,* 2006). RPA (replication protein A) and its co-factor, Lcd1/Ddc2 (ATR-Interacting-Protein, or ATRIP in mammalians), recruit Mec1 to the site of DNA damage (Zou and Elledge, 2003; Dubrana *et al*., 2007). Both Lcd1/Ddc2 and the 9-1-1 clamp are required for activation of Mec1 (Majka *et al.,* 2006; Delacroix *et al*., 2007). Once activated, Mec1 phosphorylates components of the DNA repair cascade. In the case of Mec1 signalling during S-phase, Mec1 interacts with a different set of proteins. Firstly, Mec1 activates Chk1 and Rad53 (or CHK1 and CHK2 in mammals) via phosphorylation (Friedel *et al*., 2009). These two kinases then continue the activation cascade leading to various outcomes such as cell cycle arrest and replication fork stabilization (Hirao *et al*., 2000; Matsuoka *et al*., 2007). Recently, Rodríguez and Tsukiyama

Figure 8. Sequence alignment of the FATC domains of *S. cerevisiae* Tra1 and Mec1 proteins using the MUSCLE sequence alignment program.

(2013) provided evidence that Mec1 may also stabilize replication forks under stress conditions by facilitating the accessibility of chromatin and increasing replication fork progression. The role of Mec1 in DNA damage response and replication fork stability makes it a possible drug target for DNA damage or cell cycle related diseases.

Due to the sequence and likely structural similarities between Tra1 and Mec1, studies of Mec1, important in their own right, also increase our understanding of Tra1. In addition, the kinase activity of Mec1 provides another assay to validate function.

Similar to Tra1-F3744A, mutations were introduced at the C-terminal end of Mec1. Mec1-W2368A and Mec1-G2369 also share the slow growth phenotype and inviability seen by Tra1-F3744A and Tra1-G3745, respectively (DaSilva *et al*., In press). Deletion mutations of Mec1 were also created at the C-terminus. The Mec1 mutations where the last amino acid (*mec1-Δ1*), the last two amino acids (*mec1-Δ2*), or the last three amino acids (*mec1-Δ3*) of *mec1* are deleted were found not to support viability (DaSilva *et al.*, In press). Western blots were performed with all five of these mutations (DaSilva *et al*., In press). From these blots, Mec1-W2368A and Mec1-G2369 were present at levels that are near wildtype, whereas the deletion mutations had lower expression with the lowest protein levels being found with the *mec1-Δ3* mutation (DaSilva *et al*., In press). With the *mec1-W2368A* and *mec1-G2369* mutations, both mirroring the results of the *tra1-F3744A* and *tra1-G3745* mutations, it would be expected that the Tti2-F328S suppressor could rescue the Mec1-W2368A slow growth phenotype. However, the Tra1-F3744A suppressor, Tti2-F328S, does not rescue the Mec1-W2368A phenotype (Genereaux *et al*., 2012).

Kinase assays and immunoprecipitation assays were performed to investigate the mechanism by which the *mec1* mutations reduced function (DaSilva *et al*., In press). From

immunoprecipitation experiments, it was clear that the mutations were capable of interaction with Lcd1/Ddc2 and that this was not the source of reduced function. On the other hand, all of the Mec1 derivatives showed dramatically reduced kinase activity *in vitro* with only Mec1-W2368A showing any activity above background. Together this datum clearly identifies a functional role for the C-terminal residue of Mec1.

8. Concluding Remarks

The results found from the *tra1-F3744A* experiments as well as the discovery of the Tti2-F328S suppressor were the basis of my thesis. The goals of my thesis were to determine the sequence constraints of the C-terminal residues of Tra1, address using molecular tools whether the C-terminus may have a role outside of folding, and initiate the characterization of Tti2 at the molecular level. **Specific objectives were to: (1) Characterize the role of the FATC domain of Tra1 using mutation and suppressor analysis of Tra1; (2) Determine which regions within Tti2 are required for viability, function, and interaction with the TTT complex components; (3) As a result of the parallels between Tra1 and Mec1, I also was involved in a project to identify suppressor mutations of Mec1-W2368A, to further characterize the role of the FATC domain in PIKK function.**

PIKKs have key roles in various cellular pathways, which include DNA repair, transcription activation, cell nutrient signalling and mRNA nonsense-mediated decay. In humans a defect in any one of these pathways can result in disease. A better understanding of PIKKs and their function will lead to avenues for therapies. The phenotypes of cells carrying mutations in the FATC domain demonstrate the importance of this domain for Tra1 function (Hoke *et al*., 2010).

Further exploration of this region is required to gain full comprehension of the function of the FATC domain in Tra1.

Chapter 2: Materials and Methods

1. Yeast strains

A list of the *Saccharomyces cerevisiae* strains used in this work can be found in **Table S1** under Supplemental Data. The FLAG-tagged *tra1 C-terminal* mutations were generated from strain CY4398, a diploid strain containing one of the *tra1* alleles with a 5x-FLAG tag, by genomically integrating plasmids CB2485, CB2486, CB2487, CB2488, and CB2489 (Table S3), after digestion with *Sph*I and *Sac*I. His+ transformants were sequenced to confirm the integration of *C-terminal tra1* mutations (see Section 4). The resulting heterozygous diploid yeast strains CY6497 (*tra1-F3744S*), CY6507 (*tra1-WF-FW*), CY6508 (*tra1-Δ1*), and CY6509 (*tra1-Δ2*) contained their respective FLAG-tagged *tra1 C-terminal* mutation. CY6514 (*tra1-F3744R*) was generated the same way but was integrated on the untagged allele. CY6499 (*tra1-F3744S* with *tti2-F328S*), CY503 (*tra1-WF-FW*) and CY6504 (*tra1-WF-FW* with *tti2-F328S*) were obtained by sporulating the diploid mutants (see Section 3).

CY6145 (*tti2-53*-421 on a *LEU2* centromeric plasmid) and CY6513 (*TTI2* on a *LEU2* centromeric plasmid) were created by plasmid shuffling (Section 8). CB2494 and CB2327 plasmids were transformed individually into CY6070 (*tti2* deletion strain containing *TTI2* on a *URA3* plasmid). Plasmid shuffling was used to remove CB2319 (*TTI2* with *URA3* centromeric plasmid) while retaining the *LEU2* centromeric plasmid containing either *tti2-53-421* mutation or *TTI2*. These strains were then used for growth assay experiments.

2. DNA constructs

A list of the DNA oligonucleotides and plasmids used can be found in **Table S2 and Table S3,** respectively. The *tti2* truncation mutations were generated using two different approaches. The first approach was implemented to generate the N-terminal deletions (CB2491, CB2492, CB2493, and CB2494) and the internal segment (CB2595) of *TTI2*. Oligonucleotides 6173-1, 6173-2, 6173-3, and 6223-1were created for the different N-terminal start sites and oligonucleotide 5693-2 or 6312-1 (for the internal segment) was used to amplify the C-terminal region of *tti2*. Once the region of interest was amplified using PCR, the PCR product was ligated into the pGEM T-Easy Vector® (Promega). Each pGEM plasmid was transformed into *Escherichia coli* and sequenced. From the pGEM plasmid, the *tti2* truncation region was digested using *Not*I and *Sac*I and ligated into CB2134 (9x myc tagged *TTI2* on a *LEU2* centromeric plasmid), replacing the same fragment from wildtype *TTI2* gene. The newly ligated *tti2* truncation mutations were transformed into *E. coli* and confirmed by sequencing. The remaining *tti2* variants were created by removing fragments of the *tti2* gene from CB2134 using restriction enzymes *Nde*I, *Eco*RI, or *Bst*BI. For CB2321 (*tti2-1-238)*, *Nde*I was used to cut once at the site of base pair 716. The overhang ends were processed by Klenow (Fermentas) to produce blunt ends and then re-ligated. For CB2320 (*tti2-1-165) Eco*RI was used to cut at a site 495 in *tti2* and at a site found in the polylinker of the vector. For CB2490 (*tti2-Δ108-216), Bst*BI1 was used to cut at two sites within *TTI2*, at 312 and 648. The digested vector was gel purified then re-ligated. The ligated plasmids were transformed into *E. coli* and sequenced to ensure the *tti2* truncations.

Plasmid constructs CB2485 (*tra1-F3744S*), CB2486 (*tra1-F3744R*), and CB2488 (*tra1-Δ1*) were generated in a similar manner using oligonucleotides 6238-1, 6238-2, and 6260-1, respectively, with primer 5747-1 to amplify the downstream region of the CB2147 vector from

the *tra1* gene. These PCR products were ligated into CB2151 after digestion with *Nco*I and *Sac*I and the constructs were sequenced.

For CB2487 (*tra1-WF-FW*) and CB2489 (*tra1-Δ2*) oligonucleotides 6241-1 and 4249-3, and 6260-2 and 4249-3, respectively, were used to amplify the C-terminal region of *tra1* using CB2147 as template. The PCR product was digested with *Bam*HI and *Nco*I and used in a triple ligation with a vector obtained by digesting CB2151 with *Nco*I and *Sph*I, and a second *Bam*HI and *Sph*I insert fragment from *TRA1* from base pairs 1049 to 5794. The ligations were transformed into *E. coli* and the *tra1* gene was sequenced to ensure the presence of the *tra1* mutation.

3. Viability Assays using Sporulation

For sporulation of diploid yeast strains, cells were first grown to stationary phase in one milliliter of YPD (2% peptone, 1% yeast extract, 2% dextrose). The yeast cells were washed twice with three milliliters of water before resuspending in three milliliters of 1% potassium acetate. The cells were grown for three to five days at 30°C. Tetrads were treated with 10 µL lyticase (5 µg/mL) to 30 µL of cells in 300 µL of sterile water and incubating for 12 minutes at 25ºC. The haploid spores were then dissected and grown at 25°C for three days until spore colonies appeared. The spore colonies were genotyped by plating on synthetic complete (SC) media lacking leucine plates to check for the YHR100C/*GEP4* plasmid (either CB1932 or CB2331), SC lacking uracil to check for the FLAG tag, and SC lacking histidine to check for the *tra1* allele. Spores that grew on both the leucine-depleted and histidine-depleted plates were crossed with tester *MAT a* and *MAT α* haploid strains to ensure they were haploids. The genomic

DNA of true haploids was isolated and a PCR product of the *tra1* C-terminus were sent for sequencing (see Section 4) to confirm the presence of the mutation.

4. Preparation of Genomic DNA from Yeast for Sequencing

To determine if the *tra1* mutation was correctly integrated into the yeast genome, the genomic DNA was isolated and a PCR product of the *tra1* C-terminus was sent for sequencing. Yeast cells were grown to stationary phase in five milliliters of YPD. The cells were harvested, washed once with water and resuspended in 200 µL of Hoffman Buffer (2% Triton X-100, 1% SDS, 100 mM NaCl, 10 mM Tris-Cl pH8, 1 mM EDTA), 200 µL of phenol, pH 8, and 0.3 g of acid washed 0.5 mm glass beads. The cells were vortexed for two to three minutes and then debris pellet by centrifugation at 10 000 x g for three minutes. The supernatant was collected and 2.5 times the volume of 95% ethanol was added and the sample incubated at 25ºC for 30 minutes. The samples were centrifuged again at 10 000 x g for three minutes to pellet the DNA. The RNA was removed from the genomic DNA by gel purification and extraction using phenol, pH 8.0, and chloroform isoamyl alcohol (24:1 – chloroform to isoamyl alcohol). The DNA pellet from the gel extraction was resuspended in 100 µL of water and one microliter was used for the template of the PCR to amplify the region of interest using primers 4225-7 and 4479-1 (see Section 5). The primers amplify the *TRA1* gene from base pair 10950 to 11300, which includes 65 bases downstream of the stop codon. After the region of interest is amplified, the DNA was again gel purified. DNA concentrations were determined based on the concentration of the DNA ladder and the DNA was resuspended to a concentration of 30-50ng/µL. One microliter was added into a 1:9 dilution with sterile water to send for sequencing.

5. PCR

PCR reactions contained 1 µL of template DNA (1:500 dilution of mini prep plasmid stock), 1 µL of primers (final concentration of 1.25 pmol), and 10 µL of 2x PCR-EZ D-PCR Master Mix® (Bio Basic), were added to a final volume of 20 µL. The PCR reactions begin with an incubation at 94°C for five minutes to denature the DNA, followed by 25 or 30 (for genomic DNA) cycles with incubations at 94°C for 45 seconds, 45 seconds at 54°C to anneal the primers, and an extension of 1 minute for every 1000 bases of product at 72°C.

6. Growth Assays

One colony of haploid strains CY4353 (*TRA1*), CY6499 (*tra1-F3744S* with *tti2-F328S*), CY6503 (*tra1-WF-FW*), CY6504 (*tra1-WF-FW* with *tti2-F328S)*, CY6513 (*TTI2*), or CY6145 (*tti2-53-421*) was grown to stationary phase at 30ºC in one milliliter of YPD. The culture was first diluted 100-fold then serial dilutions of 10-fold each were made. Three microliters of each dilution were plated onto YPD or YPD containing either 6% ethanol, 0.2M hydroxyurea (HU), 2nM rapamycin or 200µg/µL 6- azauracil (AU). Plates were grown at 30°C unless otherwise stated.

7. Western Blot

Ten milliliters cultures of yeast strain CY4118 (TAP-tagged *TEL2* strain*)* containing plasmids CB2320, CB2321, CB2327, CB2490, CB2491, CB2492, CB2493, CB2494, or CB2495 were grown in SC lacking leucine at 30°C to an OD_{600}~2.0. Ten milliliters of diploid strains CY6497 (FLAG tagged *tra1-F3744S)*, CY6507 (FLAG tagged *tra1-WF-FW)*, CY6508 (FLAG tagged *tra1-Δ1*), CY6509 (FLAG tagged *tra1-Δ2*), CY4419 (FLAG tagged *TRA1*), CY4421 (FLAG tagged *tra1-F3744A*), or BY4743 (untagged *TRA1*) containing plasmids CB1932 or

CB2331, were grown in YPD at either 30ºC or 37ºC until an OD_{600}~2.0. Cells were lysed using the glass bead protocol described in Hoke *et al*. (2010). Protein concentration of the cell lysate was determined using the Bradford assay reagent (BioRad). Fifty micrograms of the *tra1* mutation protein extracts or 70 µg of the *tti2*mutation protein extracts was separated by SDS-PAGE (SDS polyacrylamide gel electrophoresis) followed by transfer of the protein to a PVDF membrane and Western blotted following the protocol found in Mutiu *et al.* (2007). To probe with the anti-calmodulin binding protein (CBP) antibody, first the PVDF membrane was incubated in Casein blocking buffer (Sigma) overnight followed by a two hour incubation in anti-CBP antibody. Three four minute washes were performed using TBS (150mM NaCl and 20mM Tris, pH 7.5) before incubating the membranes in Casein blocking buffer for another two hours. The membrane was incubated in anti-rabbit IgG HRP antibody for 45 minutes. Two four minute washes with TBS and one six minute wash with TBST (TBS with 0.5% Tween 20) were performed before visualising the protein signal. The following antibodies were used: anti-c-myc (Sigma, cat#M5546) primary antibody at 1:4000, anti-FLAG (Sigma, cat#F3165) primary antibody at 1:4000, anti-Calmodulin Binding Protein (Millipore, cat#07-482) primary antibody at 1:1000, anti-mouse IgG HRP (Promega, cat#W4021) at 1:10000 , and anti-rabbit IgG HRP (Promega, cat#W4011) at 1:15000. The protein signal was visualised on film after detection with Supersignal West Pico Chemiluminescent Substrate (Thermo Scientific). The bottom half of the SDS PAGE gel was removed and stained overnight in Coomassie Brilliant Blue stain (45% methanol, 10% acetic acid, and 0.5 g/L R-250 C-Blue (BDH)) to determine the protein loading levels. The gel was destained overnight in 5% acetic acid and 40% methanol. Densitometry data was obtained using AlphaImager 3400 software (Alpha Innotech, San Leandro, CA).

8. Plasmid Shuffling

Each of the *tti2*-containing plasmids, CB2320, CB2321, CB2327, CB2490, CB2491, CB2492, CB2493, CB2494, or CB2495 was transformed into yeast strain CY6070, individually, and grown in one milliliter of SC media lacking leucine at 30°C until stationary phase. One microliter of culture was transferred to one milliliter of YPD and grown to stationary phase at 30°C to enable the loss of the *TTI2-URA3* plasmid (CB2319). Serial dilutions of each culture were made and three microliters was spotted onto 5-fluoroorotic acid (5-FOA) plates and incubated at 30°C for two days.

9. Co-immunoprecipitation experiments

Five hundred milliliter cultures of either CY4118 (*tel2*-TAP tagged) or CY4119 (*tti1*-TAP tagged) containing plasmids encoding wildtype or mutant *tti2* (CB2320, CB2321, CB2327, CB2490, CB2491, CB2492, CB2493, CB2494, or CB2495) were grown at 30°C in YPD media to an OD_{600} ~2.0-3.0. The cells were lysed in liquid nitrogen as described in Saleh *et al*., (1997). The affinity purification (co-IP) assays were performed following the protocol from Rigaut *et al*., (1999). For each immunoprecipitation, 600 µL of rabbit IgG agarose beads (Sigma) was used. Forty milligrams of protein was applied to the column for the Tel2 co-IP while 30 mg of protein was applied to the columns for the Tti1 co-IP. The protein was eluted off the IgG agarose column using 3 µL of TEV enzyme (Invitrogen) to cleave the TAP tag. The calmodulin column binding and elution steps were omitted from the protocol. Prior to separating the eluted protein on a 12.5% SDS polyacrylamide gel, the protein elution samples were precipitated using a trichloroacetic acid (TCA) (Ozols, 1990). Once the precipitated pellets were dry, 30 µL of 3x SDS loading buffer was added and the protein was separated by electrophoresis on a 12.5% SDS-PAGE gel, transferred to a PVDF membrane and immunoblotted for the proteins of

interest. Prior to blotting with anti-CBP, the protein was stripped using a stripping buffer containing 1% Tween 20 (Fisher Scientific), 15g/L glycine (Fisher Scientific), and 1g/L sodium dodecyl sulfate (SDS) (BDH). The PVDF membrane was incubated in 25mL of the stripping buffer for 10 min twice followed by two incubations in TBS (150mM NaCl and 20mM Tris, pH 7.5) for 10 min each and two incubations in TBST (TBS with 0.5% Tween 20) for 5 min each.

10. Bioinformatics analysis of *mec1-W2368A* suppressors

Nine extragenic *mec1-W2368A* suppressors were discovered by Dr. Chris Brandl and sent to Biodiversity Research Centre (University of British Columbia, Vancouver, Canada) for paired end sequencing using the Illumina platform. All of the samples were sequenced in the same lane. Barcoding and library construction was performed at Biodiversity Research Centre. The map reads and quality files were assessed using the program Bowtie (Langmead *et al.*, 2009). The reference *Saccharomyces cerevisiae* genome was downloaded from *Saccharomyces* Genome Database on March 24, 2011. The datum analysis was performed the same as described in Genereaux *et al*. (2012) with minor changes to the Perl and Shell scripts which were made to accommodate the script to the Illumina dataset (Supplemental Data, Figures S1-3). In addition to analysing the datum through the Bowtie program, one suppressor sample was also analysed using Novoalign (Hercus, 2013) to examine the sequence for any insertions or deletions. The Perl script for the Novoalign sequence analysis can be found in the Supplemental Data, Figure S4. A novoindex was created using the same *S. cerevisiae* reference genome. CY6267 (*mec1-W2368A* suppressor strain) was mated with CY6076 (*mec1-W2368A* strain) to obtain spore colonies containing the suppressor mutation. These spore colonies had a portion of the *Hkr1* gene amplified using oligonucleotides 6529-1 and 6529-2 to identify the presence of the

suppressor. The method of preparing the genomic DNA for sequencing is the same as stated in Section 4. Spore colonies without the suppressor were also sequenced as a control.

Results

Chapter 3:

1. Rationale:

Mutational analysis at the C-terminus of Tra1 was previously examined by changing the terminal phenylalanine of Tra1 to an alanine (*tra1-F3744A*) as well as adding a glycine to the C-terminus (*tra1-G3745*) (Hoke *et al.,* 2010). Both of these mutations demonstrated that the C-terminus is important for the proper function of Tra1. The *tra1-F3744A* mutation resulted in yeast strains with slow growth at 37°C, in media containing 6% ethanol and calcofluor white, among other stresses (Hoke *et al*., 2010). The protein level of Tra1-F3744A was lower than that of wildtype and this level was recovered in the presence of the Tti2-F328S suppressor (Genereaux *et al*., 2012). This increase in protein expression led to the hypothesis that the C-terminus of Tra1 is important for its folding and stability. This hypothesis is supported by the known interaction of PIKK proteins with the TTT complex (which contains Tti2) and heat shock proteins (Takai *et al*., 2010). However, when the *tra1-G3745* mutation was analysed, the results suggested that the role of the C-terminus may be more complex (Hoke *et al*., 2010). First, the addition of a glycine residue (G3745) to the C-terminus renders the cell inviable. Second, the Tti2-F328S suppressor was not able to rescue the cells containing *tra1-G3745*. This was surprising since Tti2-F328S was able to suppress another FATC mutation, *tra1-L3733A*, thus indicating that the Tti2-F328S suppressor does not function specifically at the terminal residue. Together, this raises the possibility that the C-terminus of Tra1 has a role other than in proper folding. Yang *et al*. (2013) recently solved the crystal structure of mTOR from the FAT domain through to the C-terminus. This structure clearly shows that the FATC domain of mTOR interacts with its PI3K activation loop (Yang *et al*., 2013). Yang et al. (2013), propose that the

FATC domain aids in stabilizing the activation loop. If the C-terminus of Tra1 is similarly placed, it would be in a position where it may be a functional component of the protein.

To begin to address this question, the sequence constraints at the C-terminus of Tra1 must be evaluated. To determine the sequence constraints, various mutations were constructed at the C-terminus of Tra1; these included altering the terminal phenylalanine to a serine (*tra1-F3744S*) or an arginine (*tra1-F3744R*), switching the terminal phenylalanine and the penultimate tryptophan (*tra1-WF-FW*), and deleting one or two residues at the C-terminus (*tra1-Δ1*and *tra1-Δ2*) (**Figure 9**). A serine mutation was introduced at the C-terminus to test for the effect of a polar residue and be a direct comparison with the alanine mutation which results in a phenotype, likely due to improper folding. Another substitution mutation made at the C-terminus was changing the terminal phenylalanine to an arginine (*tra1-F3744R*), to determine the effect of a positively charged residue at the C-terminus of Tra1. The last substitution mutation made was a switch between the last two residues of Tra1 (*tra1-WF-FW)*. For many PIKKs the last two residues are a phenylalanine followed by a tryptophan; however, in Tra1, these residues are reversed with a tryptophan followed by a phenylalanine. While Mec1 shares certain sequence similarity with Tra1, the Tti2-F328S suppressor is surprisingly unable to suppress the *mec1-W2368A* phenotype. Mec1 also contains the phenylalanine followed by a tryptophan pattern at its C-terminus and may explain why the *mec1-W2368A* phenotype cannot be suppressed by Tti2-F328S. Therefore the order of the last two residues of Tra1 may be a unique feature of Tra1.

To further explore the role of the C-terminal carboxyl group of Tra1, two deletion mutations were made where the last residue or the last two residues were deleted. The choice to

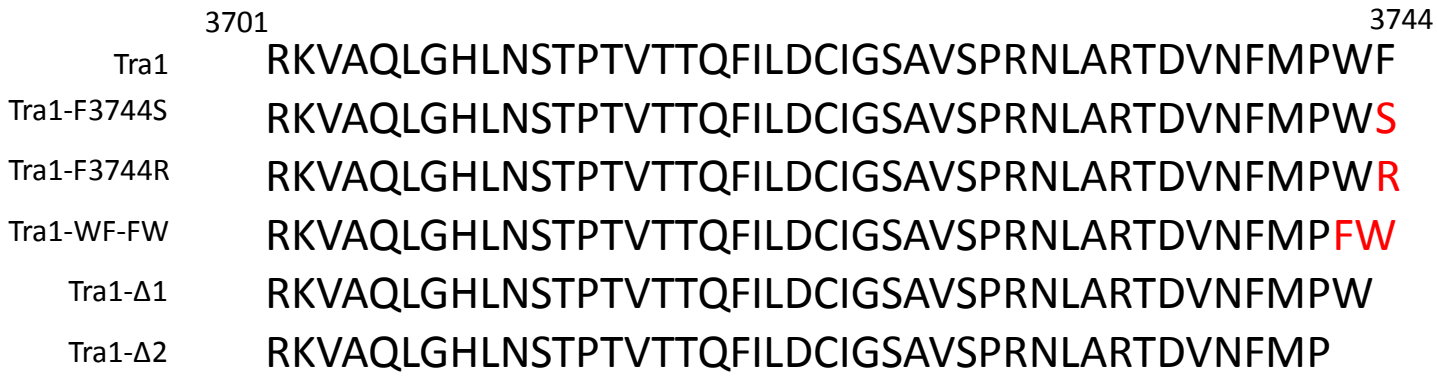

Figure 9. Diagram of mutations created in Tra1.

remove two residues from the C-terminus of Tra1 was based on the structure which shows several helices located in this region. The helical structure of the C-terminal end of the protein would cause the carboxyl group to point out in different directions as the amino acids are being deleted. This change in direction of the carboxyl group could cause structural instability; therefore to ensure that any phenotype seen from these mutations is not due to the carboxyl group pointing in the wrong direction, two mutations were created.

2. Results:

The Tra1 substitution and deletion mutations were genomically integrated into a diploid *TRA1* strain. The resulting yeast strain contains one wildtype allele and one mutated allele. To determine viability of the cells containing the *tra1* mutation, the diploid cells were sporulated by subjecting the cells to a low nitrogen environment. This environment causes the diploid cell to sporulate into a tetrad of four haploid spores. These spores were dissected and plated on a YPD plate to grow at room temperature. Since each spore should have either a mutated or wildtype *tra1* allele, viability can be assessed based on how many spore colonies grow. To determine if a spore colony contains a wildtype or mutated allele, genotyping was done with the viable spore colonies. However, when making the mutation to the *TRA1* allele, a gene nearby called *GEP4* could be disrupted due to the mutagenesis process. To avoid misinterpreting inviability due to a change to the *GEP4* allele, wildtype *GEP4* was reintroduced into the cell on a plasmid. When the viable spores are genotyped for the mutation, they are also genotyped for the *GEP4* plasmid which contains a *LEU2* marker. Only those spore colonies containing the *GEP4* plasmid were used for the viability assay results.

To determine if Tti2-F328S would suppress the lethality of the *tra1-F3744S* mutation, I sporulated the diploid cells and then checked for the presence of *tra1-F3744S* spore colonies. The *tra1-F3744S* mutation is linked to *HIS3,* and the *GEP4* plasmid or *GEP4* with *tti2-F328S* (*GEP4/tti2-F328S*) plasmid contains a *LEU2* gene. For the *tra1-F3744S* mutation, none of the spore colonies with the serine mutation in the *tra1* allele were viable (**Table 1**). To assess if the Tti2-F328S suppressor was able to rescue the *tra1-F3744S* mutation, *tti2-F328S* was introduced into the diploid strain prior to sporulation on a plasmid along with *GEP4*. When the Tti2-F328S suppressor was introduced into the strain, seven *tra1-F3744S* haploid cells were viable (**Table 2**). To ensure that the spore colonies were haploid, they were mated with a tester alpha and A mating strain. If the spore cells only mate with one of the tester strains, then it is a true haploid cell. The *tra1* allele of the haploid cells was subsequently sequenced after PCR from the genome to ensure the presence of the mutation.

Growth of a haploid strain containing *tra1-F3744S* and the *tti2-F328S* suppressor was analyzed to see if the mutation results in a phenotype (**Figure 10**). The strain was grown to stationary phase in a one milliliter YPD culture. The culture was serially diluted in water, the first dilution being a 100 times dilution followed by three serial 10-fold dilutions. Three microliters of each dilution was spotted onto YPD plates grown at 30°C or 37°C, and onto a YPD plate containing 6% ethanol grown at 30°C. A wildtype haploid spore colony was grown and plated alongside the *tra1-F3744S* spore colony as a control. The *tra1-F3744S* strain grows slowly on 6% ethanol plates and on YPD plates at 37°C (**Figure 10**).

A western blot was performed to determine if the level of Tra1-F3744S protein changes in the presence or absence of the Tti2-F328S suppressor. A diploid strain containing one wildtype

Table 1. Summary of sporulation results for *tra1* mutations containing the *GEP4* plasmid.

Mutation	Total Spores	Spores Containing *GEP4* plasmid	Viable Spores Containing the Mutation
tra1-F3744S	80	15	0
tra1-F3744R	112	20	0
tra1-WF-FW	80	34	2
tra1-Δ1	101	27	0
tra1-Δ2	96	12	0

Table 2. Summary of sporulation results for *tra1* mutations containing the *GEP4/tti2-F328S* plasmid.

Mutation	Total Spores	Spores Containing *GEP4/tti2-F328S* plasmid	Viable Spores Containing the Mutation
tra1-F3744S	32	9	7
tra1-F3744R	28	5	0
tra1-WF-FW	56	16	9
tra1-Δ1	72	12	0
tra1-Δ2	96	16	0

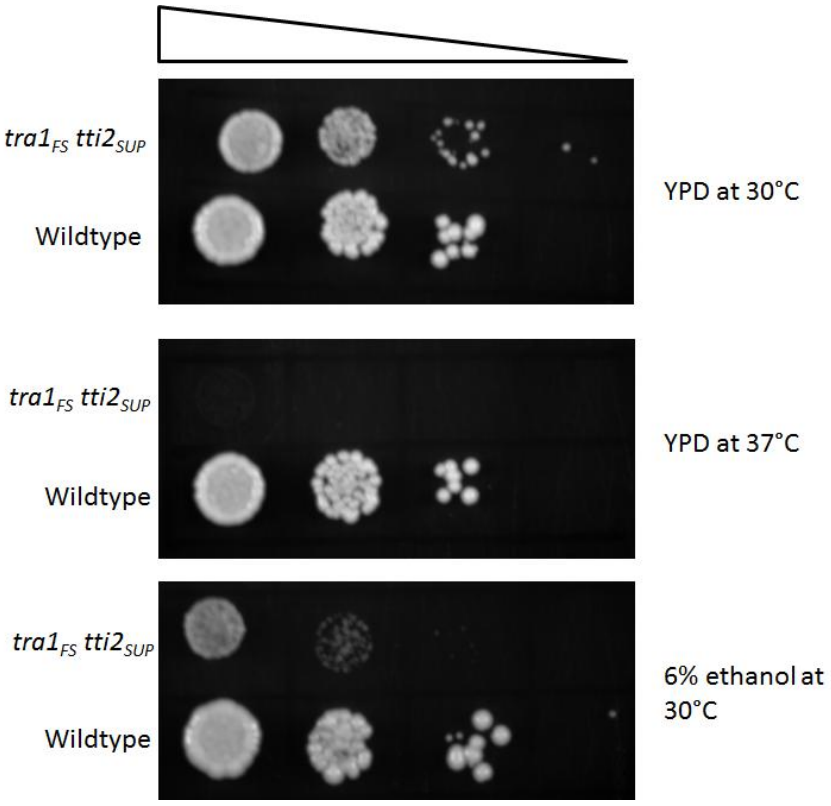

Figure 10. Growth of the *tra1-F3744S* cells with Tti2-F328S suppressor under stress conditions. A wildtype *TRA1* strain (Wildtype) and the *tra1-F3744S* mutant strain containing the Tti2-F328S suppressor ($tra1_{FS}$ $tti2_{SUP}$) were grown in 1mL of YPD media at 30°C until stationary phase. Both strains are found in a haploid background with only one copy of *TRA1* present. The cultures were grown to stationary phase before being diluted once 100-fold followed by three serial dilutions of 10-fold. Three microliters of each dilution was plated onto either a YPD plate grown at 30°C or 37°C, or a YPD plate containing 6% ethanol grown at 30°C.

allele and one FLAG tagged *tra1-F3744S* allele was grown in the presence or absence of the *tti2-F328S* suppressor. The cultures were grown for eight hours at 30°C or 37°C before lysing the cells using glass beads. Fifty micrograms of protein from the whole cell lysate was separated by electrophoresis on a 5% SDS polyacrylamide gel and transferred to a PVDF membrane. The membrane was blotted for using an anti-FLAG antibody. The protein was visualised by chemiluminesence. For a protein loading control, the bottom of the 5% SDS-PAGE gel was removed before the protein was transferred to the PVDF membrane and stained with Coomassie Brilliant Blue stain (**Figure 11 B**). The protein levels of Tra1-F3744S at 30°C do not change whether the cells are grown in the absence or presence of the Tti2-F328S suppressor (compare lanes 4 and 5) (**Figure 11 A**). Although the levels of the Tra1-F3744A mutant do not increase in the presence of the suppressor at 30°C, the degradation pattern disappears which equally shows an increase in Tra1-F3744A stability (**Figure 11 A**). This advocates for a greater loss of activity with Tra1-F3744S than for Tra1-F3744A. This hypothesis is additionally supported by the results seen at 37°C. The level of Tra1-F3744S alone is lower than that of wildtype (compare lane 4 to lane 3) (**Figure 11 A**). The Tti2-F328S suppressor increases the level of Tra1-F3744S (compare lane 4 to lane 5) (**Figure 11 A**). The increased levels of Tra1-F3744S in the presence of Tti2-F328S are near wildtype (compare lane 5 to lane 3) (**Figure 11 A**). However, this increase in protein is not sufficient to completely rescue the slow growth phenotype of Tra1-F3744S at 37°C (**Figure 10**).

The *tra1-F3744R* mutation was also assessed for viability. For *tra1-F3744R,* no viable spore colonies contained the arginine mutation (**Table 1**). The same result was seen for spores containing the Tti2-F328S suppressor (**Table 2**). This result suggests that the arginine mutation

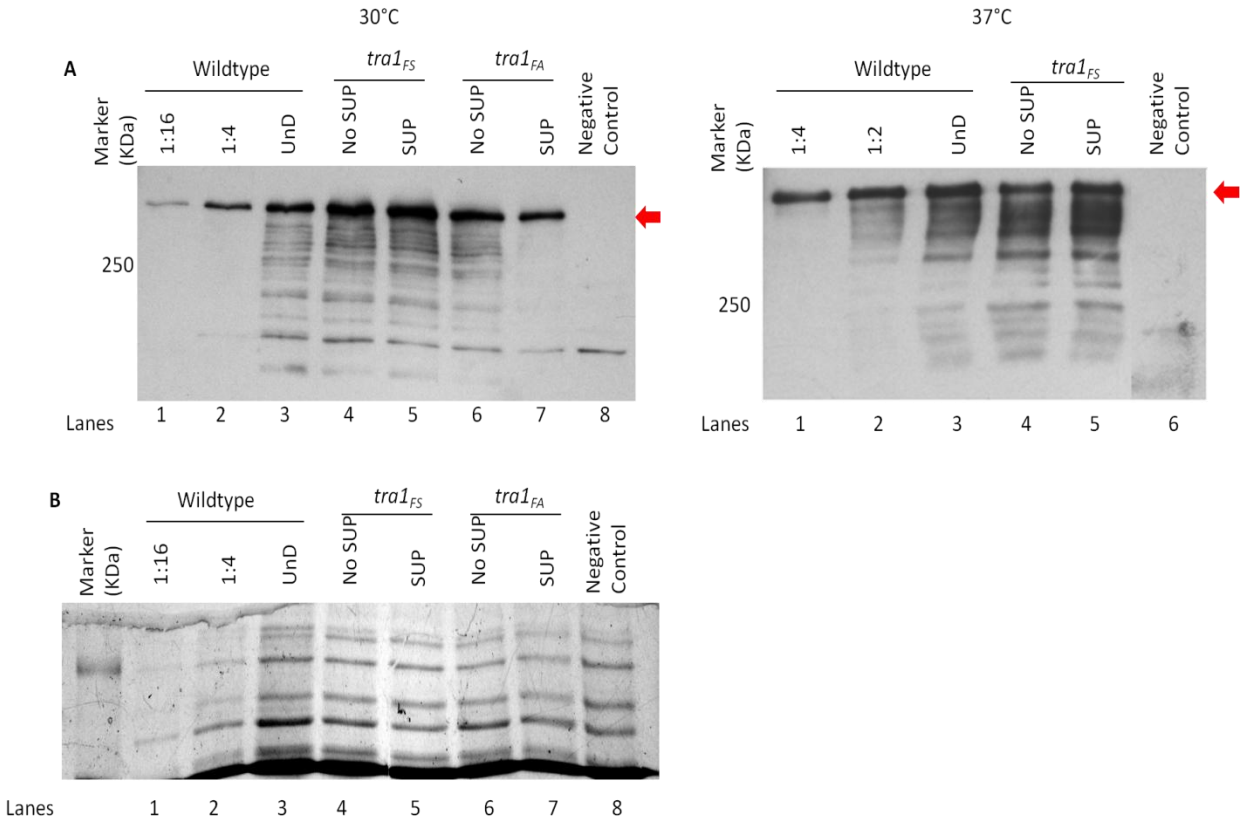

Figure 11. Western blot of Tra1-F3744S mutant with and without Tti2-F328S suppressor. ***A.*** Diploid strains of the Tra1-F3744S (*tra1*$_{FS}$) mutation, in which one allele contained wildtype *TRA1* and the other allele contained the FLAG tagged *tra1* mutation gene, were grown in 10 mL of YPD either at 30°C (left) or 37°C (right). Both a strain containing the *GEP4/tti2-F328S* suppressor (SUP) and a strain containing only *GEP4* (No SUP) were grown. After 8 hours of growth, the cells were lysed using glass beads and 50 µg of protein from the crude extract was separated by electrophoresis on a 5% SDS polyacrylamide gel. The gel was then transferred to a PVDF membrane where the protein was immunoblotted for using a FLAG antibody. Tra1 was visualised on the PVDF membrane using chemiluminescence. A strain containing FLAG tagged wildtype *TRA1* (wildtype) and a strain containing untagged *TRA1* (negative control) were used as controls. The Tra1-F3744A mutant (*tra1*$_{FA}$) was also separated alongside the Tra1-F3744S mutant (*tra1*$_{FS}$) at 30°C to help illustrate a change in protein levels of the Tra1 (433 kDa) protein in the presence or the absence of the Tti2-F328S suppressor. The wildtype sample was serially diluted from 50µg (UnD) either 1:4 and 1:16 for the 30°C or 1:2 and 1:4 for the 37°C. The Tra1 protein is indicated by the red arrow. ***B.*** The bottom of the SDS PAGE gels was cut from the gel prior to transferring the protein to the PVDF membrane. The bottom gel was stained with Coomassie Brilliant Blue stain as a protein loading control. The gel corresponds to the 30ºC samples.

interrupts the C-terminus of Tra1 to an extent greater than the other substitution alleles or affects a function not suppressible by Tti2-F328S. The positively charged side chain of the arginine amino acid may prevent the C-terminal tail from orienting into the proper conformation for stability and/or may disrupt a crucial interaction. If the terminal residue interacts with the activation loop of the PI3K domain, as shown in the mTOR structure, then the positive side chain may prevent the C-terminus from interacting with the PI3K domain (Yang *et al*., 2013).

The next step for Tra1-F3744R would be to check for protein expression levels. Unfortunately, I was unable to obtain a diploid strain where the *tra1-F3744R* gene was FLAG tagged. I did transform *tra1-F3744R* into a diploid strain where both *TRA1* alleles are FLAG tagged; however, the background signal from the remaining *TRA1* FLAG tagged allele makes the results difficult to interpret.

The same viability assay was also used to determine the viability of the *tra1-WF-FW* cells. Two *tra1-WF-FW* spore colonies could be identified with the *tra1-WF-FW* mutation (**Table 1**). In the presence of the Tti2-F328S suppressor, nine *tra1-WF-FW* spore colonies were viable and genotyped as true haploids containing the *tra1-WF-FW* gene by mating each spore colony with tester A and alpha strain (**Table 2**). The *tra1* allele from the *tra1-WF-FW* spore colonies was sequenced to verify the presence of the mutation.

The growth assay for the *tra1-WF-FW* mutation was performed similarly to those done for *tra1-F3744S*. A culture of the *tra1-WF-FW* haploid strain containing either the *GEP4* plasmid or the *GEP4/tti2-F328S* plasmid were grown and serially diluted. The dilutions were spotted onto a YPD plate grown at 30°C or 37°C (**Figure 12**). From these growth assays, the *tra1-WF-FW* strain without the suppressor grows slowly on YPD at 37ºC (**Figure 12**). This slow

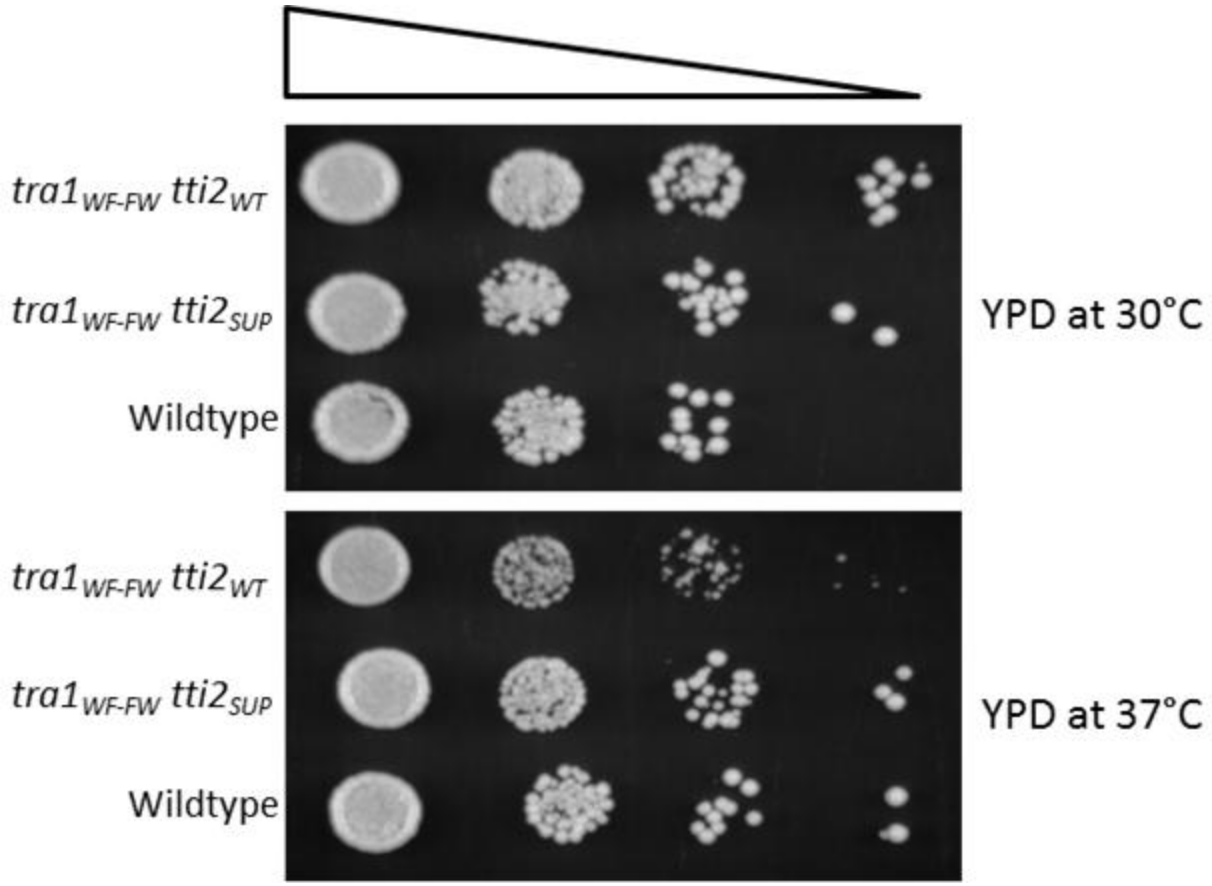

Figure 12. Growth of the *tra1-WF-FW* mutation cells in the presence or absence of the Tti2-F328S suppressor under stress conditions. A wildtype *TRA1* strain (Wildtype) and the *tra1-WF-FW* mutation strain were grown in 1 mL of YPD media at 30°C until stationary phase in the absence ($tra1_{WF\text{-}FW}$ $tti2_{WT}$) or presence ($tra1_{WF\text{-}FW}$ $tti2_{SUP}$) of Tti2-F328S suppressor. Both strains are found in a haploid background with only one copy of *tra1* present. The saturated cultures were then diluted once 100-fold followed by three serial dilutions of 10-fold. Three microliters of each dilution was plated onto YPD plates and grown at 30°C or 37°C.

growth is suppressed by *tti2-F328S* (**Figure 12**).

To see if there is any effect on protein stability of Tra1-WF-FW a western blot was performed. **Figure 13 A** shows the protein levels of Tra1-WF-FW with and without the Tti2-F328S suppressor, grown at 30°C or 37°C. **Figure 13 B** shows the loading controls. The protein levels for Tra1-WF-FW are higher in cells containing the Tti2-F328S (compare lane 4 to lane 5) (**Figure 13 A**). The change in protein levels between the two Tra1-WF-FW samples resembles the change seen by the Tra1-F3744A mutation at 37°C (compare lanes 4 and 5 to lanes 6 and 7) (**Figure 13 A)**. Although the suppressor increases the protein levels of Tra1-WF-FW, these levels are still lower than wildtype (compare lane 5 to lane 3) (**Figure 13 A**).This result would suggest that the suppressor aids in the stability and expression of the protein, similar to the *tra1-F3744A* mutation.

To understand the effect of the carboxyl group of Tra1, two deletion mutations were made: *tra1-Δ1*and *tra1-Δ2*. These mutations were created similarly to the substitution mutations and were integrated into the yeast genome. Likewise, viability assays were performed by sporulating the diploid cells containing the mutation. Neither of the two deletion mutations, *tra1-Δ1* nor *tra1-Δ2*, were viable in the absence or presence of Tti2-F328S (**Tables 1 and 2**).

The Tra1-Δ1 and Tra1-Δ2 protein expression levels were analysed using western blots in a diploid background. The strains were grown both at 30°C or 37°C (**Figure 14 A** and **Figure 15 A**). **Figures 14 B and 15 B** show the loading controls for Tra1-Δ1 and Tra1-Δ2, respectively. The presence of Tti2-F328S did not increase the expression levels seen for Tra1-Δ1 nor Tra1-Δ2 (compare lane 4 to lane 5) (**Figure 14 A** and **Figure 15 A**). However, *tra1-Δ1*and *tra1-Δ2* strains

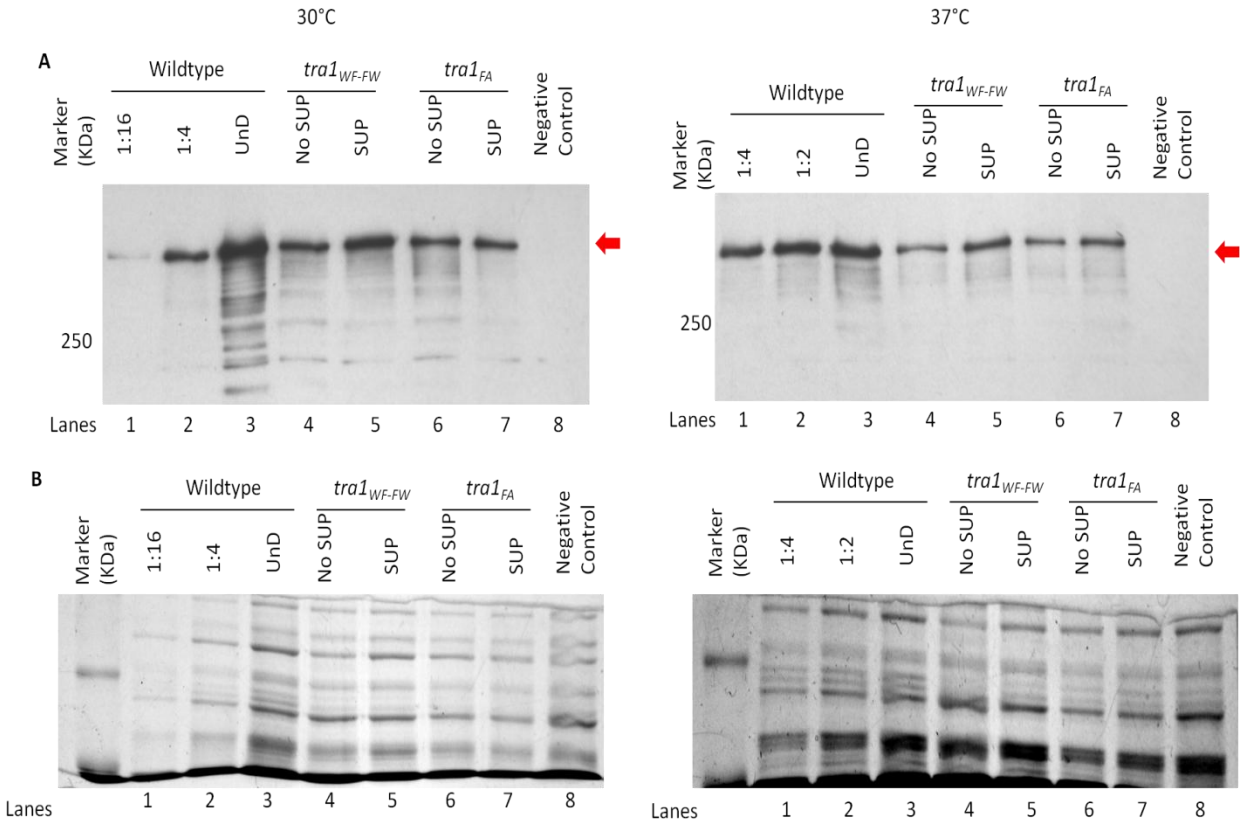

Figure 13. Western blot of the Tra1-WF-FW mutation in the absence or presence of the Tti2-F328S suppressor. *A.* Diploid strains of the Tra1-WF-FW ($tra1_{WF-FW}$) mutation, in which one allele contained wildtype *TRA1* and the other allele contained the FLAG tagged *tra1* mutation gene, were grown in 10 mL of YPD either at 30°C (left) or 37°C (right). A strain containing the *GEP4*/*tti2-F328S* suppressor (SUP) and a strain containing only *GEP4* (No SUP) were grown. After 8 hours of growth, the cells were lysed using glass beads and 50 µg of protein from the crude extract was separated by electrophoresis on a 5% SDS polyacrylamide gel. The gel was then transferred to a PVDF membrane where the protein was immunoblotted for using a FLAG antibody. Tra1 (433 kDa) was visualised on the PVDF membrane using chemiluminescence. A strain containing FLAG tagged wildtype *TRA1* (wildtype) and a strain containing untagged *TRA1* (negative control) were used as controls. The Tra1-F3744A mutation ($tra1_{FA}$) was also separated alongside the Tra1-WF-FW mutations to help illustrate a change in protein levels of the Tra1 protein in the presence or absence of the Tti2-F328S suppressor. The wildtype sample was serially diluted from 50µg (UnD) to 1:16 and 1:4 at 30°C or 1:2 and 1:4 at 37°C. The Tra1 protein is indicated by the red arrow. ***B.*** The bottom of the SDS PAGE gels was cut from the gel prior to transferring the protein to the PVDF membrane. The bottom gel was stained with Coomassie Brilliant Blue stain as a protein loading control. The left gel corresponds to the 30ºC samples and the right gel is the 37ºC samples.

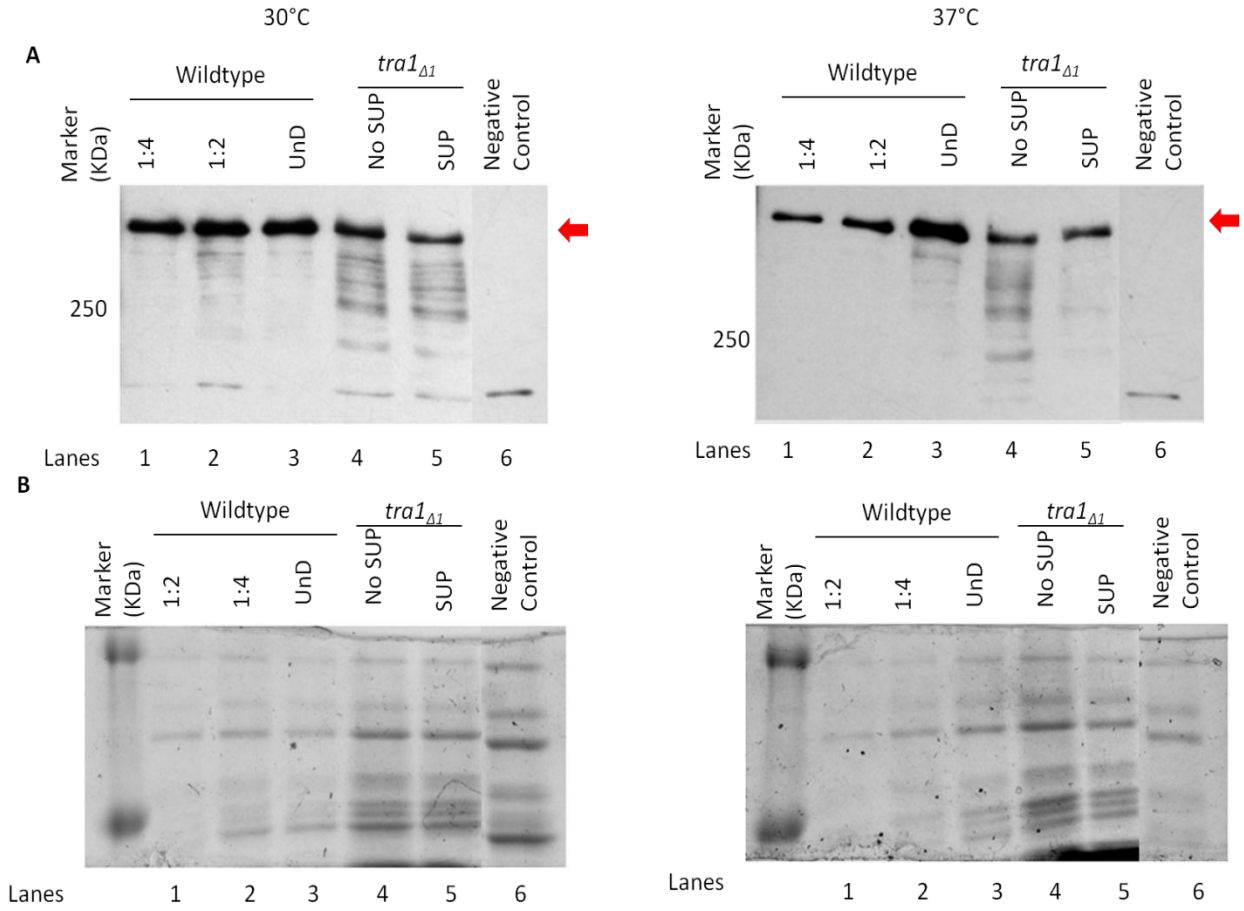

Figure 14. Western blot of the Tra1-Δ1 deletion mutation in the absence or presence of the Tti2-F328S suppressor. ***A.*** Diploid strains of the Tra1-Δ1 mutation ($tra1_{\Delta1}$), in which one allele were grown in 10 mL of YPD either at 30°C (left) or 37°C (right). A strain containing the *GEP4/tti2-F328S* suppressor (SUP) and a strain containing only *GEP4* (No SUP) were grown. After 8 hours of growth, the cells were lysed using glass beads and 50 µg of protein from the crude extract was separated by electrophoresis on a 5% SDS polyacrylamide gel. The gel was then transferred to a PVDF membrane where the protein was immunoblotted for using a FLAG antibody. Tra1 (433 kDa) was visualised on the PVDF membrane using chemiluminescence. A strain containing FLAG tagged wildtype *TRA1* (wildtype) and a strain containing untagged *TRA1* (negative control) were used as controls. The wildtype sample was serially diluted from 50µg (UnD) to 1:2 and 1:4. The Tra1 protein is indicated by the red arrow. ***B.*** The bottom of the SDS PAGE gels was cut from the gel prior to transferring the protein to the PVDF membrane. The bottom gel was stained with Coomassie Brilliant Blue stain as a protein loading control. The left gel corresponds to the 30ºC samples and the right gel is the 37ºC samples.

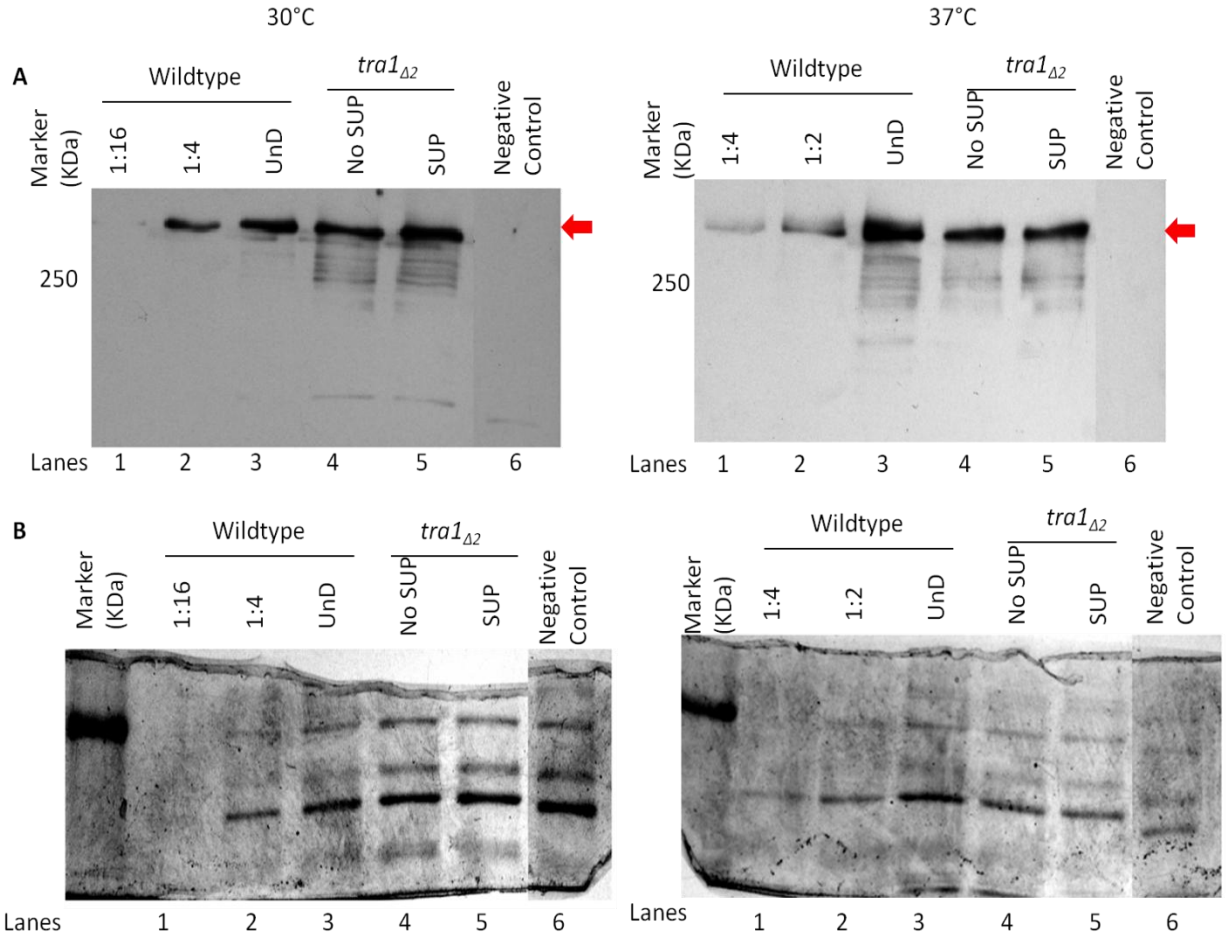

Figure 15. Western blot of the Tra1-Δ2 deletion mutation in the absence or presence of Tti2-F328S suppressor. ***A.*** Diploid strains of the Tra1-Δ2 mutation ($tra1_{\Delta 2}$), in which one allele contained wildtype *TRA1* and the other allele contained the FLAG tagged *tra1* mutation gene, were grown in 10 mL of YPD either at 30°C (left) or 37°C (right). A strain containing the *GEP4/tti2-F328S* suppressor (SUP) and a strain containing only *GEP4* (No SUP) were grown. After 8 hours of growth, the cells were lysed using glass beads and 50 µg of protein from the crude extract was separated by electrophoresis on a 5% SDS polyacrylamide gel. The gel was then transferred to a PVDF membrane where the protein was immunoblotted for using a FLAG antibody. Tra1 (433 kDa) was visualised on the PVDF membrane using chemiluminescence. A strain containing FLAG tagged wildtype *TRA1* (wildtype) and a strain containing untagged *TRA1* (negative control) were used as controls. The wildtype sample was serially diluted from 50µg (UnD) to 1:16 and 1:4 at 30°C or 1:2 and 1:4 at 37°C. The Tra1 protein is indicated by the red arrow. ***B.*** The bottom of the SDS PAGE gels was cut from the gel prior to transferring the protein to the PVDF membrane. The bottom gel was stained with Coomassie Brilliant Blue stain as a protein loading control. The left gel corresponds to the 30ºC samples and the right gel is the 37ºC samples.

both showed a decrease in protein expression compared to wildtype, particularly at 37°C (compare lane 4 and 5 to lane 3) (**Figure 14 A** and **Figure 15 A**).

Chapter 4:

1. Rationale:

Tti2 is part of the TTT complex which also includes Tti1 and Tel2. The exact function of this complex is unknown but it interacts with Hsp90, as well as members of the PIKK family, including Tra1 (Takai *et al*., 2010). Furthermore, Takai *et al*., (2010) have shown that the interaction of the TTT complex with PIKK proteins is short lived and occurs shortly after the PIKK protein is synthesized. This datum would suggest a role of the TTT complex in the folding of PIKK proteins. However, how the TTT complex helps with protein folding and the role of each individual protein in the complex remains unknown. As previously stated, Tti2-F328S suppresses two mutations within the Tra1 FATC domain, and, at least for *tra1-F3744A*, increases the protein levels thus reinforcing the hypothesis that the *tti2-F328S* suppressor has a role in protein folding.

A comprehensive characterization of the Tti2 protein would provide a better understanding of the relationship between the *tti2-F328S* suppressor and the stabilization of Tra1-F3744A. Very little is currently known about Tti2. No structure or domain analysis has been revealed and no functional analysis has been undertaken. Therefore a *tti2* truncation mutation analysis was performed to elucidate its domain features. Plasmid shuffling assays were done with the *tti2* truncation mutations to establish what regions are required for viability followed by co-immunoprecipitation experiments to resolve which of these regions retain the ability to interact with the TTT complex binding partners.

With a better understanding of the functions of Tti2, we can start to piece together how Tti2-F328S suppresses the *tra1-F3744A* mutation as well as gather evidence with regards to the overall function of wildtype Tti2 and its effects on wildtype Tra1.

2. Results:

To begin the analysis of wildtype Tti2, a set of *tti2* gene truncation mutations were made in order to determine the regions necessary for viability. **Figure 16** illustrates the regions that were deleted from Tti2. The N-terminal deletions, as well as, the internal Tti2 piece were generated using PCR with primers flanking the regions of interest. The PCR products were then ligated into a *LEU2*-containing centromeric plasmid. For the internal deletion (using *Bst*BI) and the 1-165 mutation (using *Eco*RI), the enzymes cut at two sites and the gene was ligated back together after the removal of the middle or end region. For the 1-238 fragment, the gene was digested with *Nde*I then the overhanging ends blunted before ligation, therefore causing a frame shift to the gene after base pair 716 (residue 238). For Tti2-1-238, the frame shift added an additional 15 amino acids to the sequence while Tti2-1-165 contains an additional 27 amino acids. Much like the other deletions, the C-terminal deletions and the internal deletion were ligated into a *LEU2*-containing centromeric plasmid.

To check for viability of the *tti2* truncation mutations, plasmid shuffling was used. The plasmids harbouring the *tti2* mutations were individually transformed into a *S. cerevisiae* strain where *tti2* is deleted from its genome and instead contains wildtype *TTI2* on a plasmid with a *URA3* marker. These transformed cells containing both plasmids were grown to stationary phase

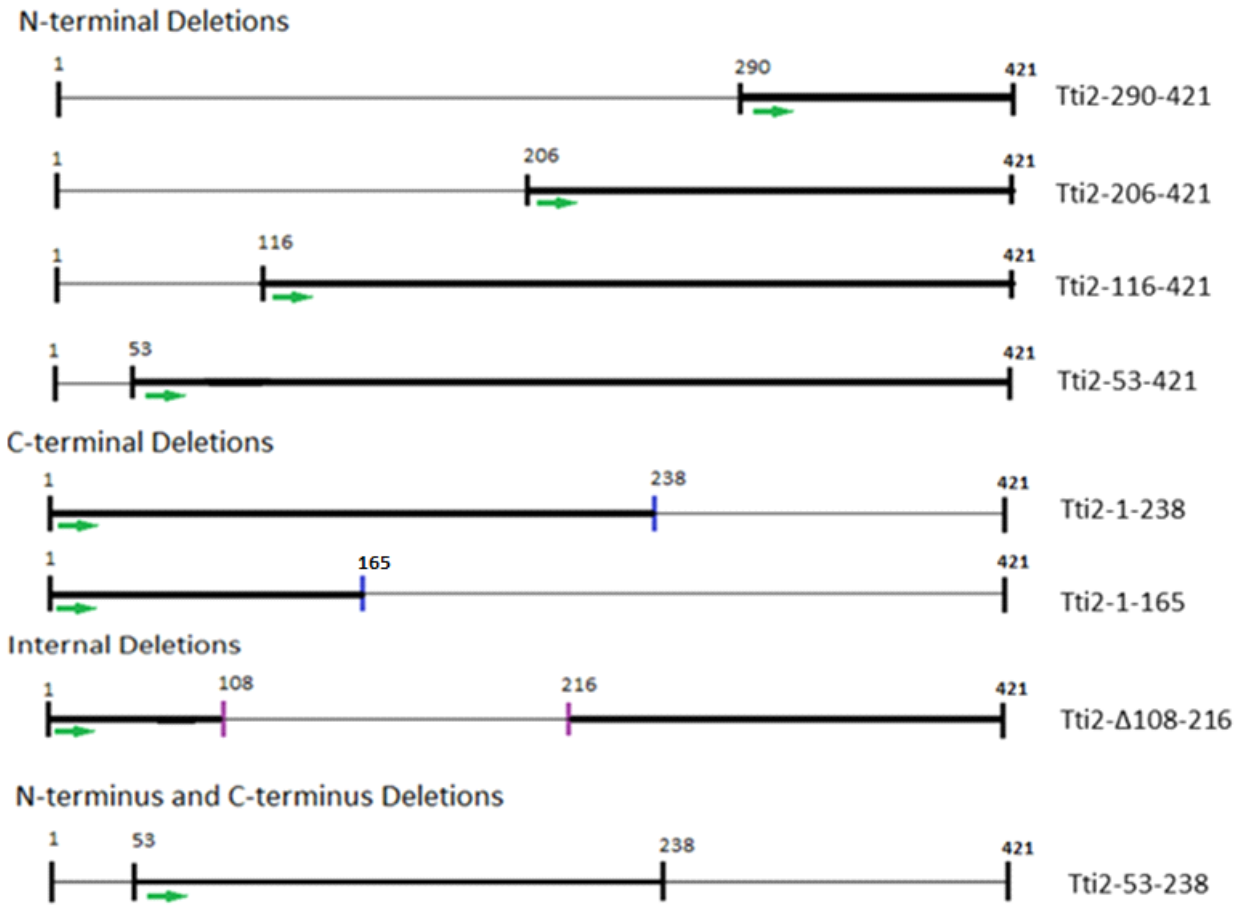

Figure 16. Map of Tti2 truncation mutations. The thick black line encompasses the expressed region of the Tti2 protein**.** The residue numbers of Tti2 are indicated above the bars.

in selective media to retain the *tti2* mutation plasmid. The cells from the selective media cultures were grown in YPD media to enable the loss of the wildtype *TTI2* plasmid. These cultures were again grown to stationary phase and then plated on a 5-fluoroorotic acid (5-FOA) plate. If the cells lose the wildtype *TTI2* plasmid and the *tti2* truncation mutation can support viability, then the cells will grow on the 5-FOA plate. The wildtype *TTI2* on a *LEU2* centromeric plasmid was transformed into the same yeast *tti2* deletion strain as a positive control. Of the deletion alleles only the *tti2-53-421* supported viability (**Figure 17**). This demonstrates that the very N-terminus of the protein is not necessary for function. Since the *tti2-1-238* mutation is not viable, this suggests that the Tti2-F328S suppressor mutation falls in a region required for function.

Protein expression levels were examined for the *tti2* truncation mutations by western blotting. The myc-tagged- *tti2* plasmids were transformed into a yeast strain containing a genomic copy of wildtype *TTI2* within its genome. This allows for all of the truncation mutations to be assessed for protein expression, even those mutations that are not viable. The transformed cells were grown in YPD media and then lysed using glass beads in the presence of protease inhibitors. Seventy micrograms of protein from the crude lysate was separated by electrophoresis on a 12.5% SDS polyacrylamide gels and transferred to a PVDF membrane. The protein was immunoblotted for using an anti-myc antibody and Tti2 was detected by chemiluminesence. A negative control strain lacking tagged Tti2 and a positive control containing myc tagged wildtype Tti2 were included. **Figure 18** shows that six of the *tti2* truncation mutations are expressed: Tti2-53-421 (lane 3), Tti2-116-421 (lane 4), Tti2-53-238 (lane 7), Tti2-1-165 (lane 8), Tti2-1-238 (lane 9), and Tti2-Δ108-216 (lane 10). For Tti2-116-421, Tti2-53-238, and Tti2-Δ108-216, the protein levels are lower than wildtype levels which suggests that the reason for inviability may

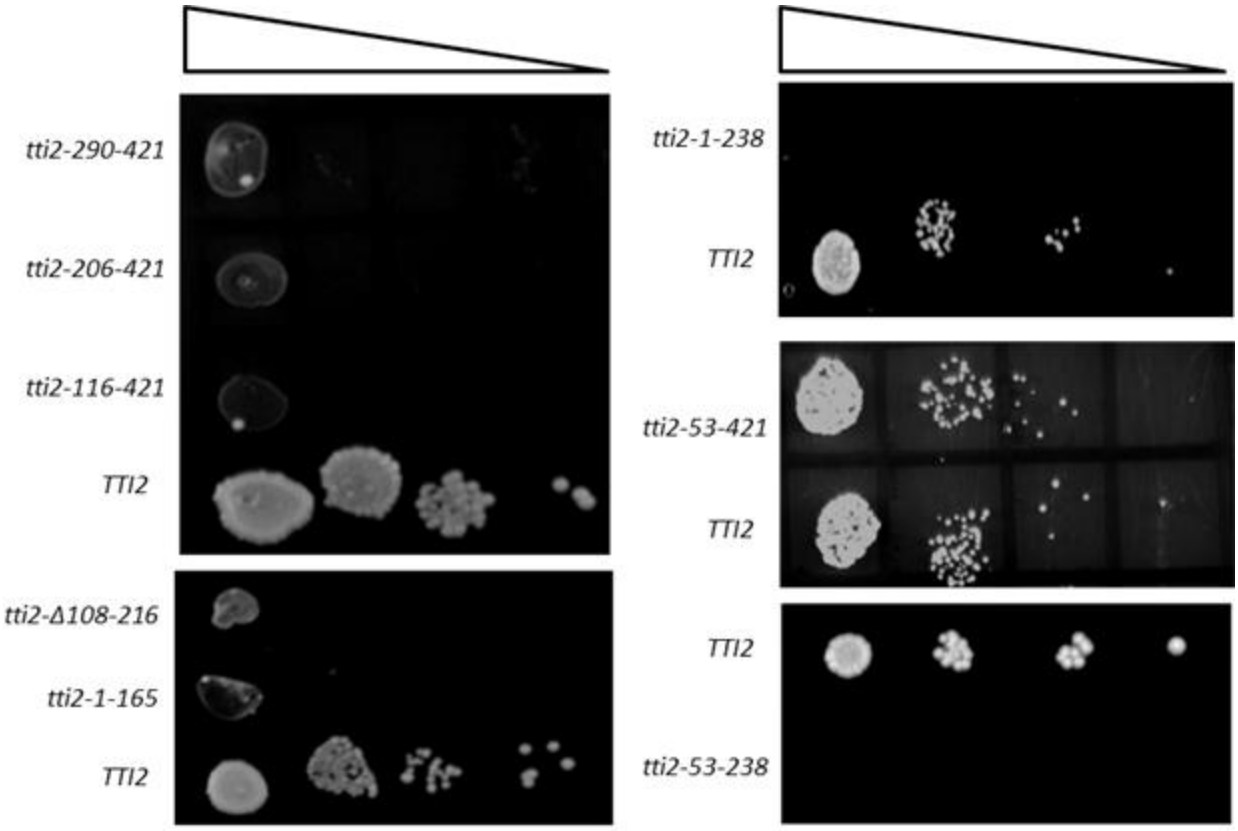

Figure 17. Viability assay of *tti2* truncation mutations grown on 5-FOA after plasmid shuffling. Each *tti2* truncation mutation on a *LEU2*-containing centromeric plasmid (*tti2-290-421, tti2-206-421, tti2-116-421, tti2-Δ108-216, tti2-1-165, tti2-1-238, tti2-53-421, tti2-53-238*) was transformed into a *tti2* deletion strain where the wildtype *TTI2* is found on a *URA3* plasmid. After growing the strains with the *tti2* truncation plasmids in selective media, the cells were transferred to YPD media and grown to stationary phase at 30°C. The cultures were diluted once 100 fold then subsequently serially diluted 3 times at 10 fold (left to right). Each dilution was plated on a 5-FOA plate to check for viability. A control wildtype *TTI2* on a *LEU2*-containing centromeric plasmid (*TTI2*) was also transformed into the Tti2 deletion strain, grown, and plated similarly to the mutations.

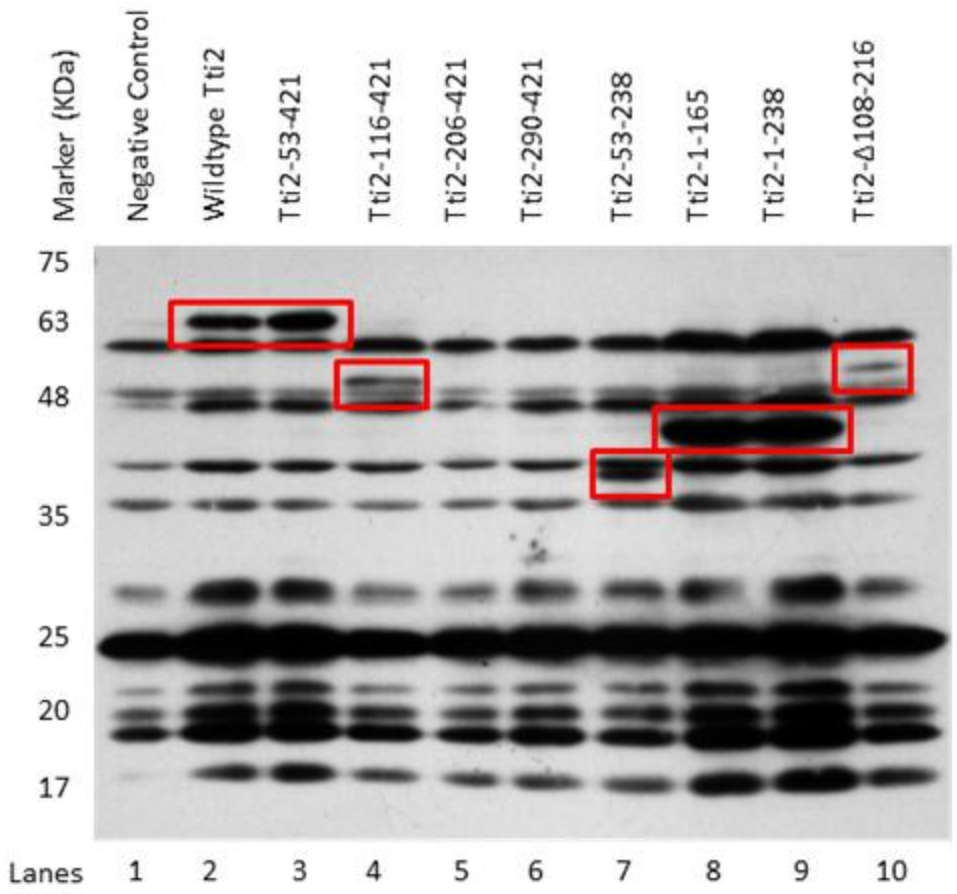

Figure 18. Western blot of Tti2 truncation mutations. The *tti2* truncation plasmids and a wildtype *TTI2* control plasmid were transformed into a wildtype background yeast strain. The strains were grown for 8 hours in 10 mL of YPD at 30°C. The cells were isolated and lysed using glass beads. Seventy micrograms of protein from the crude extracts were separated by electrophoresis on 12.5% SDS-polyacrylamide gels. The gels were then transferred to a PVDF membrane and the Tti2 protein was immunoblotted using the anti-myc antibody. Chemiluminescence was used to visualise the protein. As a control, a yeast strain was transformed with a plasmid lacking myc tagged *TTI2* (Negative Control), as well as, a plasmid harbouring myc tagged wildtype *TTI2* (Wildtype Tti2). The expressed Tti2 truncation mutations are highlighted by a red box (WT Tti2 – 60 kDa).

be due to protein instability (compare lanes 4, 7, and 10 with lane 2) (**Figure 18**). Tti2-53-421 (lane 3), Tti2-1-238 (lane 9) and Tti2-1-165 (lane 8) all expressed near wildtype levels (lane 2). For the Tti2-1-165 mutation, the protein migrated with lower mobility on the gel than expected (lane 8). The *tti2-1-165* gene was sequenced and shown to be correct.

To determine if the *tti2-53-421*containing strain shows any phenotype under stress conditions, it was grown at 30°C on YPD plates containing either 6% ethanol, 0.2M hydroxyurea (interferes with the DNA replication pathway), 200µg/µL of 6-azauracil (interferes with transcription elongation), or 2nM rapamycin (interferes with signal transduction and amino acid utilization) and on a YPD plate at 30°C or 37°C (Hampsey, 1997). *tti2-53-421* results in a slight slow growth phenotype at 37°C but not in any of the other stress conditions (**Figure 19**). These results indicate that the first 52 amino acids from the N-terminus of Tti2 can be deleted with only a minor temperature sensitivity phenotype. This is consistent with the N-terminal region of the protein being less highly conserved in the fungal species as shown in the sequence alignment of **Figure 20**. The highest degree of conservation can be found within the central region of the protein.

Co-immunoprecipitation experiments were performed to determine if any of the truncation mutations retained the ability to interact with other members of the TTT complex. All of the expressed alleles of Tti2 were examined with the exception of *tti2-Δ108-216* in the Tel2 co-IP and *tti2-53-238* in the Tti1 co-IP. The *tti2* truncations were expressed in a strain containing wildtype *TTI2* and genomically encoded TAP tagged *TTI1*. These transformed strains were grown in 500 mL YPD cultures and lysed by grinding in liquid nitrogen. The crude cell extracts

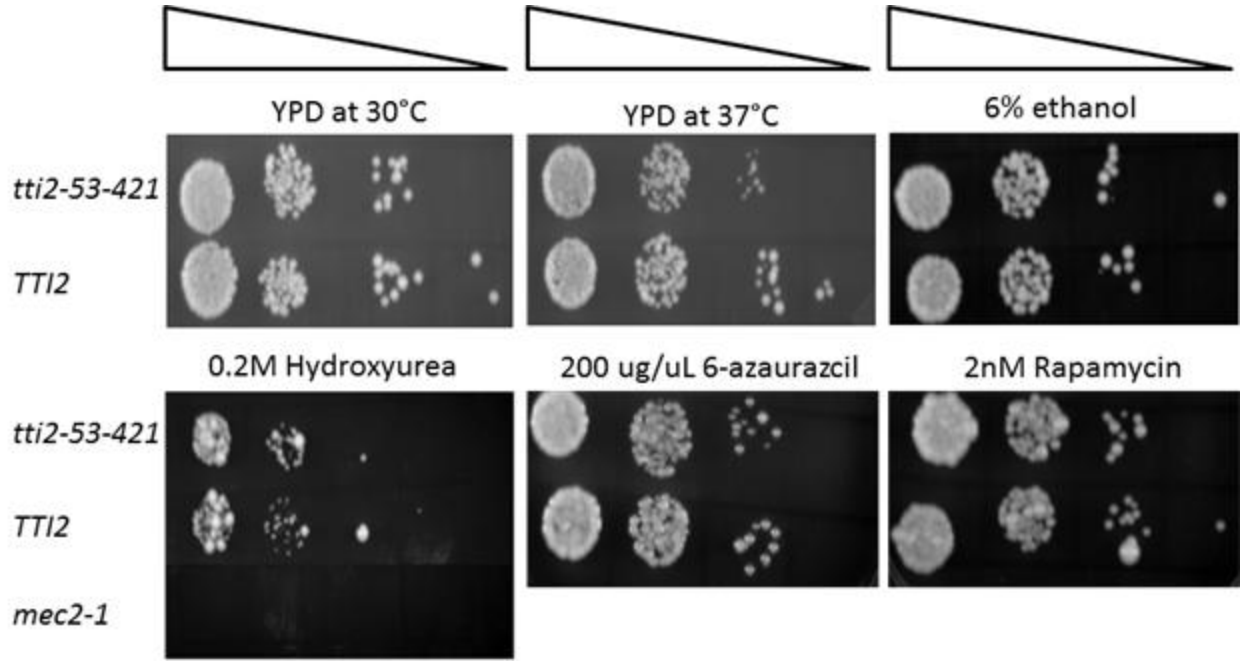

Figure 19. Growth of assay of *tti2-53-421* truncation mutation strain under stress conditions. The *tti2* deletion strain containing either the wildtype *TTI2* plasmid or the *tti2-53-421* plasmid were grown in 1 mL of YPD media at 30°C until stationary phase. The cultures were then diluted once 100-fold followed by 3 serial dilutions of 10-fold (from left to right). Three microliters of each dilution was plated onto either a YPD plate grown at 30°C or 37°C, and a YPD plate containing either 6% ethanol, 0.2M hydroxyurea, 200µg/µL of 6-azauracil, or 2nM rapamycin. Each plate was grown at 30°C unless otherwise stated. *mec2-1* is a control strain used to validate the hydroxyurea plates, Weinert *et al.*, (1994).

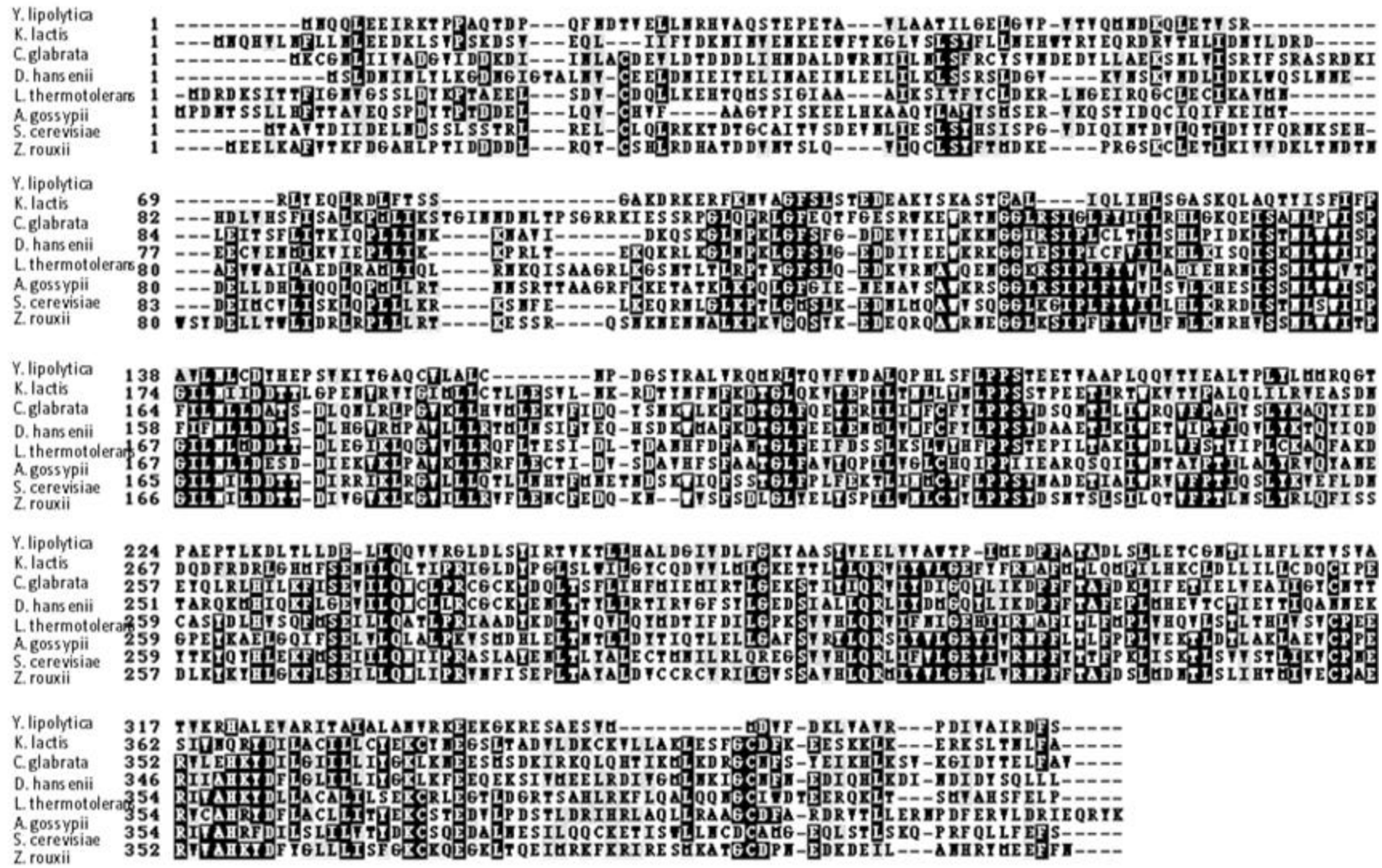

Figue 20. MUSCLE Alignment of Tti2 orthologs from fungl species.

were chromatographed over an IgG column which binds to the TAP tag. Three washes were performed before eluting Tti1 off the column using the Tobacco Etch Virus protease (TEV). The eluted protein was precipitated using trichloroacetic acid (TCA) and 2% sodium deoxycholate (DOC). All of the precipitated protein was separated by electrophoresis on a 12.5% SDS polyacrylamide gel along with 70 µg of protein from the crude lysate (**Figure 21**). An anti-myc antibody was used to detect Tti2. The input levels of the crude cell extracts indicate that each of the proteins is present (lanes 4 to 8) (**Figure 21 A, C**). For Tti2-53-421, the ratio of input to protein bound to Tti1 was similar to wildtype Tti2 (**Figure 21 A and B**). Densitometry indicated that the ratio was 0.4 to 0.5 fold increase in the inputs (**Figure 22, 30 second exposure**). For the other mutations, the amount bound to Tti1 is lower than the amount in the inputs (lane 5 to 8) (**Figure 21 C and D**). The protein band intensities for Tti2-1-238 and Tti2-1-165 dropped below the background intensity signal (**Figure 22, 5 minute exposure**). The fold change of Tti2-116-421 and Tti2-Δ108-216 were 35.7 and 39.4, respectively, and the background fold change (-TAP control) was 15.7 (**Figure 22, 5 minute exposure**). Therefore, I conclude that only Tti2-53-421 is able to interact with Tti1.

To ensure that the Tti1 TAP tagged molecule was present within all the transformed cells used for the co-immunoprecipitation experiments, the same co-immunoprecipitation membranes were blotted with an anti-calmodulin binding protein (CBP) antibody (**Figure 23**). Within the TAP molecule bound to Tti1 is a calmodulin binding peptide which can be detected using this antibody. Tti1 was present in each of the samples used for the co-immunoprecipitation experiment with the exception of the untagged Tti1 control.

The interaction datum with Tel2 is shown in the form of a histogram indicating the ratio of input versus co-immunoprecipitated (**Figure 24**). The interaction datum with Tel2 is shown in

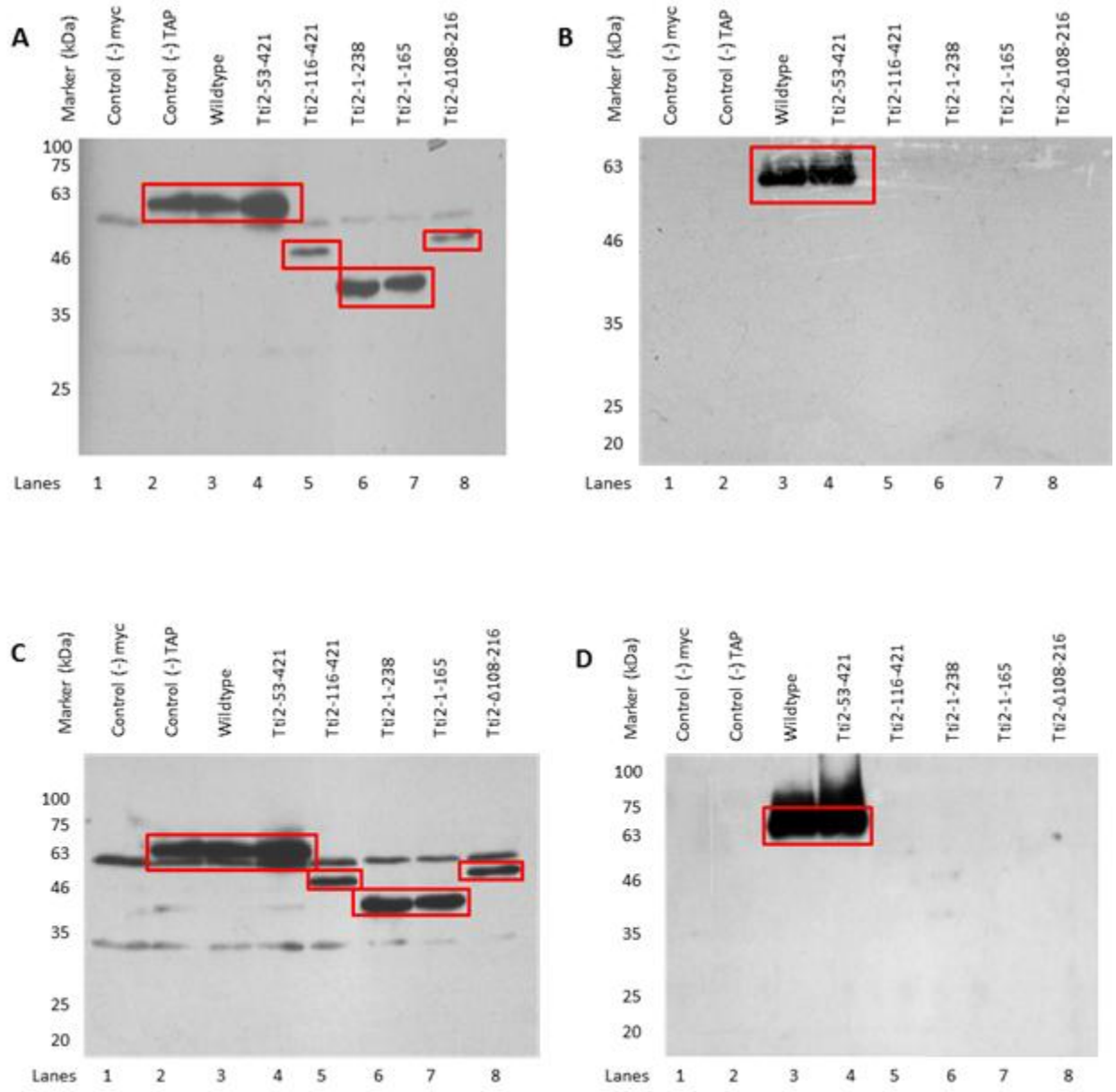

Figure 21. Co-immunoprecipitation assay of myc$_9$-tagged *tti2* truncation mutations with TAP-tagged Tti1 protein to check for interaction. The plasmids containing the *tti2* truncations were transformed into a TAP-tagged Tti1 *S. cerevisiae* strain. The strains were grown in YPD media until stationary phase. The yeast cells were lysed and 30 mg of the protein extract was chromatographed on 600 µL of IgG agarose resin. TEV enzyme was used to cleave Tti1 from the TAP tag which allows Tti1 to elute off the column. The protein within the elution sample was precipitated using TCA and DOC. All of the precipitated protein (**B, D**) and 50µg of the protein lysate (**A, C**) was separated by electrophoresis on a 12.5% polyacrylamide gel. The protein on the gel was then transferred to a PVDF membrane. Tti2 was probed via an anti-myc antibody and

chemiluminescence was used to visualize the protein (**A and B-** 30 second exposure; **C and D** – 5 minute exposure). The wildtype control is a plasmid containing the wildtype *TTI2* with a myc tag and TAP-tagged *TTI1*. The negative controls are a wildtype strain with no myc tagged *TTI2* but retains the TAP tagged *TTI1* (control –myc) and a wildtype strain with myc tagged *TTI2* but no TAP tagged *TTI1* (control –TAP). The bands enclosed in the red boxes are Tti2 (WT Tti2 – 60 kDa).

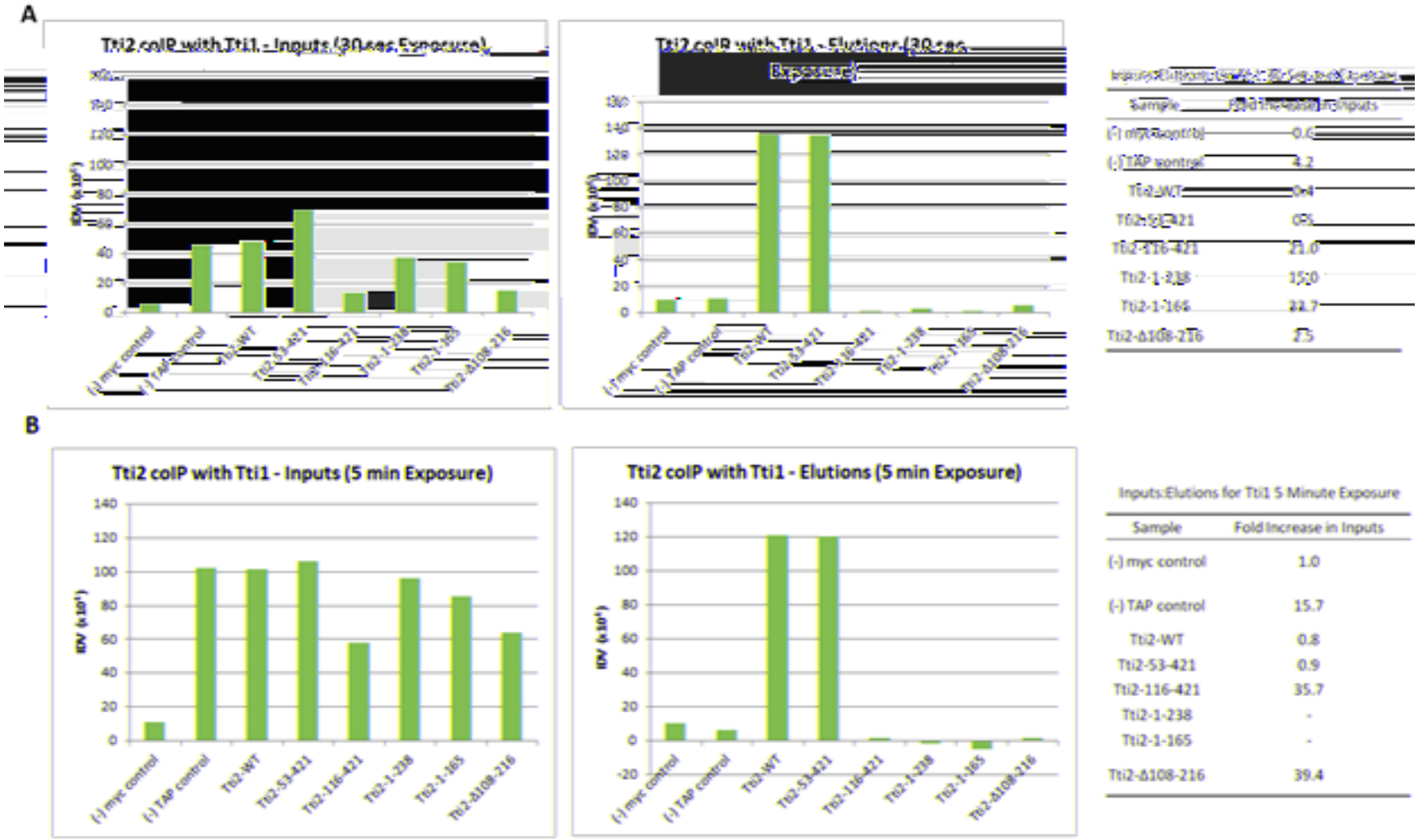

Figure 22. Histograms of the Tti1 co-immunoprecipitation densitometry datum. ***A***. The densitometry datum of the input and elution samples after exposing the film for 30 seconds. ***B.*** The densitometry datum of the input and elution samples after exposing the film for 5 minutes. IDV is equal to the sum of the pixel value of each band minus the background. The tables list the fold change from the elution samples to the input samples. Samples with negative values were not calculated.

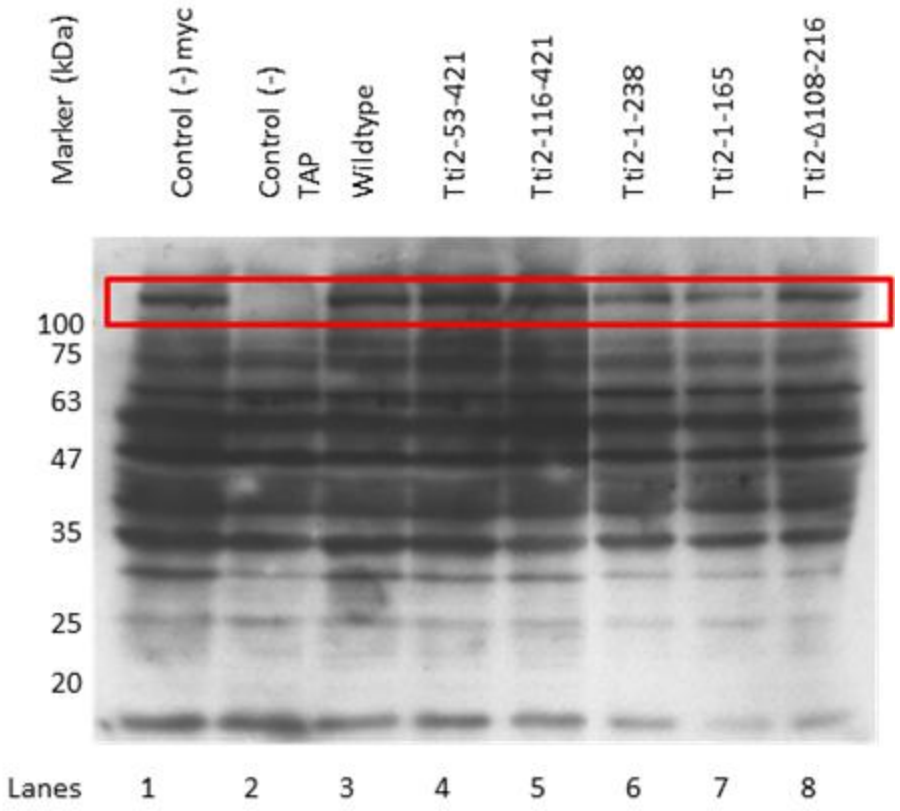

Figure 23. Re-probe of TAP tagged Tti1 and myc$_9$ tagged Tti2 co-immunoprecipitation experiment using CBP antibody. The input membrane used in the IP experiment was stripped of the myc antibody before re-blotting using an anti-CBP primary antibody. Chemiluminescence was used to visualize the protein (5 second exposure). The bands enclosed in the red boxes are Tti1 (119 kDa). Negative controls are a wildtype strain with no myc tagged *TTI2* but retains the TAP tagged *TTI1* (control –myc) and a wildtype strain with myc tagged *TTI2* but no TAP tagged *TTI1* (control –TAP). Wildtype is a plasmid containing the wildtype *TTI2* with a myc tag and TAP-tagged *TTI1*.

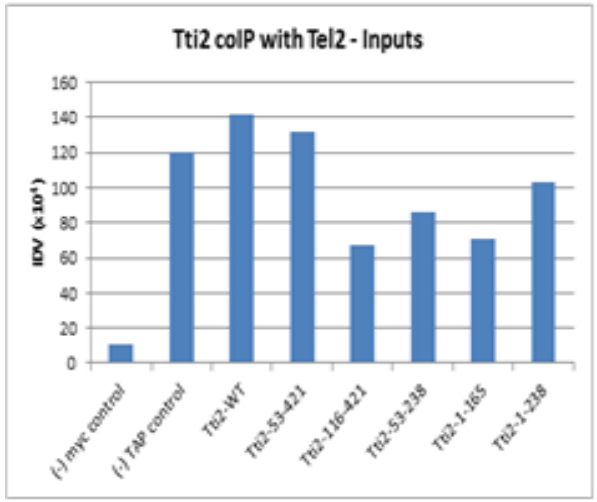

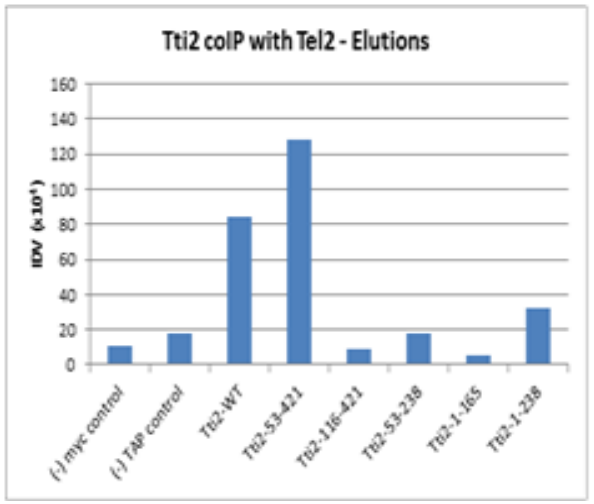

Inputs:Elutions for Tel2

Sample	Fold Increase in Inputs
(-) myc control	0.9
(-) TAP control	6.8
Tti2-WT	1.7
Tti2-53-421	1.0
Tti2-116-421	7.3
Tti2-53-238	4.8
Tti2-1-165	14.4
Tti2-1-238	3.2

Figure 24. Histograms of the Tel2 co-immunoprecipitation densitometry datum. The densitometry datum of the input and elution samples after exposing the film for 5 minutes. IDV is equal to the sum of the pixel value of each band minus the background. The table lists the fold change from the elution samples to the input samples.

the form of a histogram indicating the ratio of input versus co-immunoprecipitated (**Figure 24**). The ratios of input to elution of Tti2-53-421 is approximately 1.0 fold difference in the input than elution samples while the ratio for wildtype Tti2 is approximately 1.7 fold more in the input than elution samples (**Figure 24**). This indicates that Tti2-53-421 interacts with Tel2 at least as efficiently as the wildtype Tti2. Tti2-53-238 and Tti2-1-238 show a ratio of 4.8 and 3.2 fold more input than elution protein, respectively (**Figure 24**). This suggests that Tti2-53-238 and Tti2-1-238 interact with Tel2 but with low affinity (**Figure 24**). Tti2-1-165 and Tti2-116-421 did not appear to interact with Tel2. The densitometry intensity signal of Tti2-1-165 and Tti2-116-421 were 14.4 and 7.3, respectively, and the background fold change (-TAP control) was 6.8 (**Figure 24**). This datum suggests that the 53-238 region of Tti2 is required for interaction with Tel2. A portion of this region is missing from both Tti2-1-165 and Tti2-116-421. The *tti2-116-421* mutation suggests that the region of Tti2 between amino acids 53 to 116 is equally crucial for Tel2 binding (**Figure 25**). An anti-CBP western blot was performed to determine the level of Tel2 TAP tagged protein present in the samples (**Figure 26**). All of the samples, with the exception of the untagged Tel2 control, showed the presence of the Tel2 protein.

The results from the experiments performed with the *tti2* truncation mutations are summarized in **Table 3**.

Chapter 5:

1. Rationale

Mec1 is an integral component of the DNA repair pathway, as well as, crucial for DNA replication fork stability (Lopes *et al*., 2001). This protein is a member of the PIKK family and is an active kinase with many phosphorylation targets (Emili 1998; Tseng *et al*., 2006; Morrison *et*

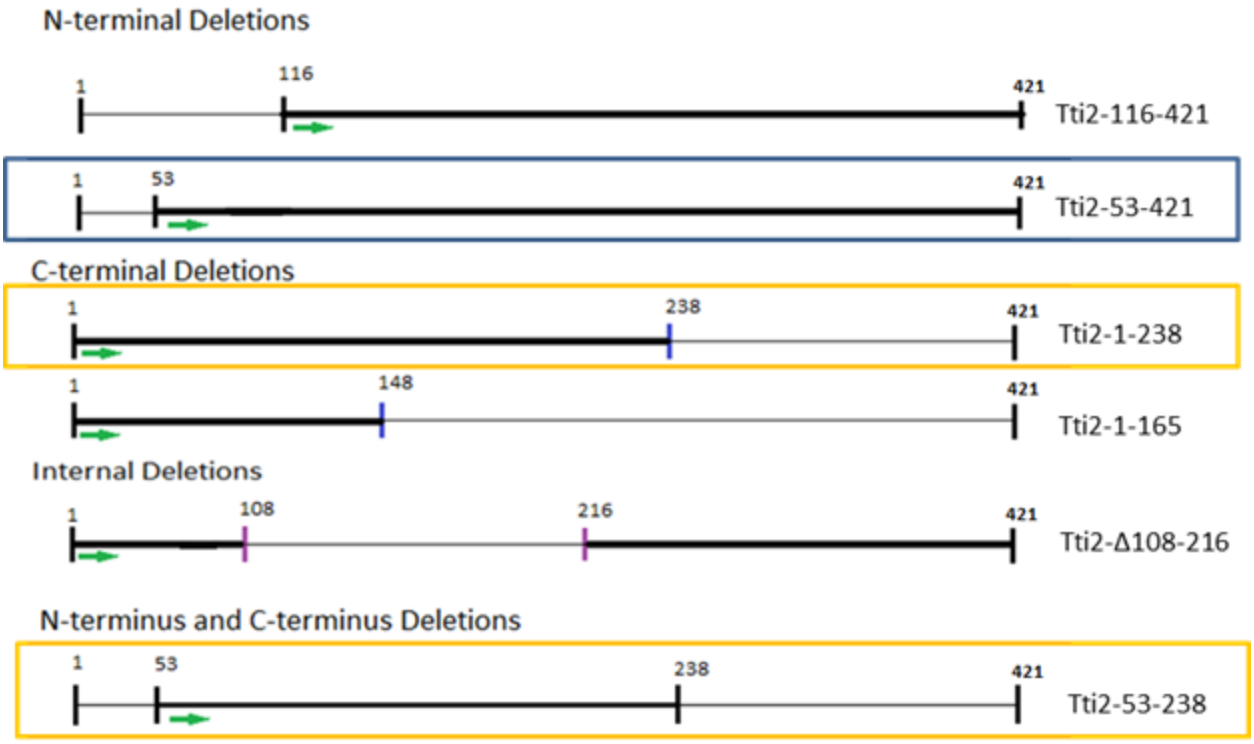

Figure 25. Schematic depicting the region of Tti2 required for interaction with Tel2 and Tti1. Schematic of the Tti2 protein sequences used in the co-immunoprecipitation experiments. The protein sequences boxed in blue are those that interact with both Tel2 and Tti1. The protein sequences boxed in orange are those that only interact with Tel2.

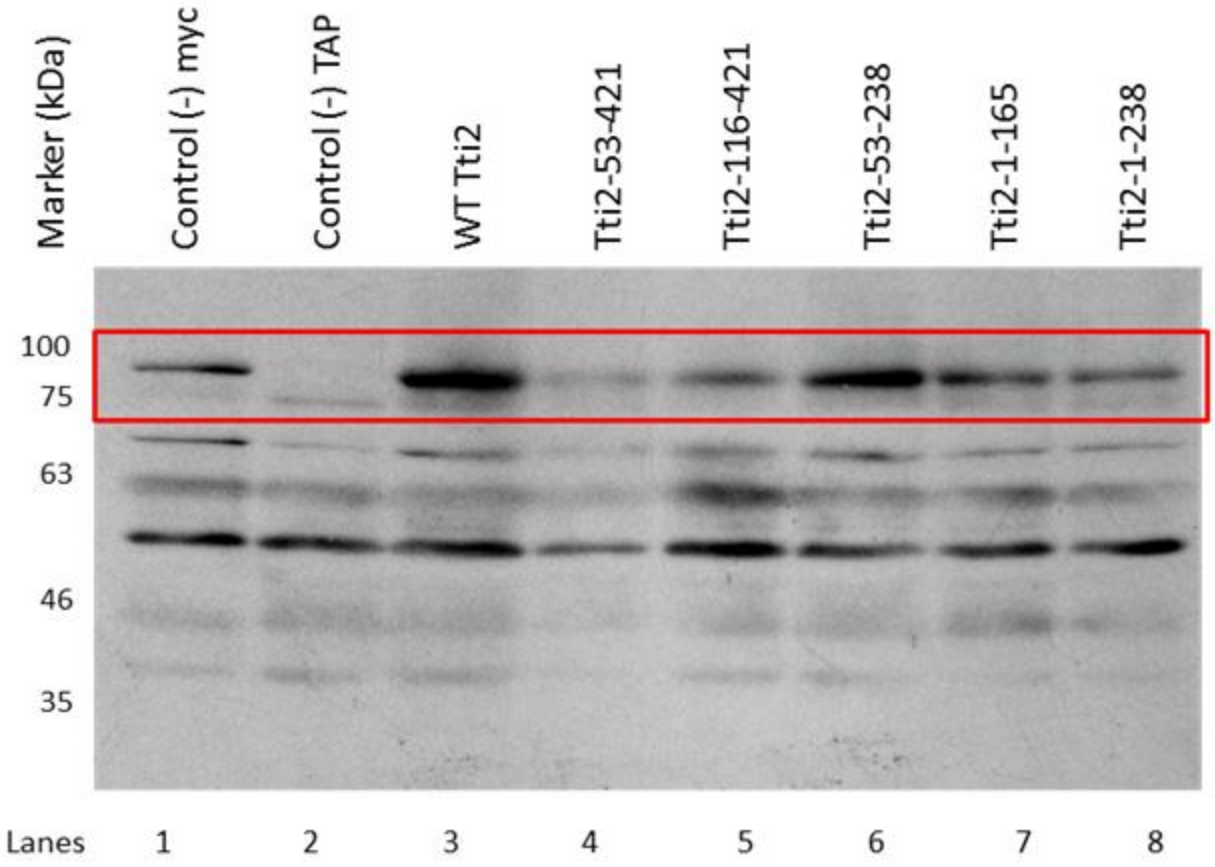

Figure 26. Re-probe for TAP tagged Tel2 in the myc$_9$ tagged Tti2 co-immunoprecipitation experiment. The input membrane used in the IP experiment was stripped of the myc antibody before re-blotting using an anti-CBP primary antibody. Chemiluminescence was used to visualize the protein (30 second exposure). The bands enclosed in the red boxes are Tel2 (79 kDa). Negative controls are a wildtype strain with no myc tagged *TTI2* but retains the TAP tagged *TEL2* (control –myc) and a wildtype strain with myc tagged *TTI2* but no TAP tagged *TEL2* (control –TAP). Wildtype is a plasmid containing the wildtype *TTI2* with a myc tag and TAP-tagged *TEL2*.

Table 3. Summary of *tti2* truncation mutations and their viability, expression, and interaction status.

Mutation	Viable	Expressed	Interacts with Tel2	Interacts with Tti1
tti2-53-421	Yes	Yes	Yes	Yes
tti2-116-421	No	Yes	No	No
tti2-206-421	No	No	-	-
tti2-290-421	No	No	-	-
tti2-1-165	No	Yes	No	No
tti2-1-238	No	Yes	Yes	No
tti2-Δ108-216	No	Yes	-	No
tti2-53-238	No	Yes	Yes	-

al., 2007). Although its function is known and the pathways in which Mec1 is involved have been identified, the molecular mechanism for Mec1-dependent protein phosphorylation is poorly understood. It is hypothesised that the Mec1 protein phosphorylation activity relies on its C-terminus (Nakada *et al.,* 2005). Similar to Tra1, a series of Mec1 mutations have been generated including a substitution at the C-terminal residue of Mec1, *mec1-W2368A*. This *mec1-W2368A* mutation, like *tra1-F3744A*, is viable yet grows slowly under stress conditions (Dasilva *et al.,* In press). The expression of this mutation is less than the wildtype suggesting that the phenotype is due to problems with *mec1-W2368A* folding and stability (DaSilva et al., In press). These results suggest that the C-terminus of Mec1, much like the C-terminus of Tra1, is important for cell viability and protein expression. We pursued further analysis of the Mec1 mutation because unlike Tra1, Mec1 has kinase activity that can be measured.

Interestingly, Tti2-F328S, a suppressor of Tra1-F3744A, does not suppress the *mec1-W2368A* phenotype (Genereaux *et al*., 2012). This is not believed to be the result of a specific interaction between Tti2-F328S and Tra1-F3744A since this suppressor can also suppress *tra1-L3733A*. As we expected the *mec1* mutations to fold incorrectly, we screened for suppressors of the slow growth properties caused by Mec1-W2368A. Additionally, finding a suppressor of Mec1-W2368A would increase our understanding of the proteins and pathways involved with regulation of Mec1.

2. Results

Extragenic suppressors that would allow growth of a strain containing *mec1-W2368A* at 37°C were selected after mutagenizing cells with a short exposure to ultraviolet light (DaSilva *et al.,* In Press). Those cell colonies that showed faster growth at 37°C were isolated and backcrossed ten

times with the parent *mec1-W2368A* yeast strain. Backcrossing was performed to remove additional mutations from the suppressor genomes. After the backcrossing suppressor strains were sent for whole genome sequencing using Illumina sequencing technology. The suppressor discovery and backcrossing was performed by Julie Genereaux and Dr. Chris Brandl.

The Bowtie software was used to map the suppressor Illumina sequencing datum to a reference genome acquired from *Saccharomyces* Genome Database (SGD; http://www.yeastgenome.org) (Langmead *et al.*,2009). The sequence variants in the reads compared to the reference were identified and organized into a table using SAMtools (Li *et al*., 2009). The quality of the DNA sequence reads were assessed using the Phred score. Any variant within this table that did not meet a Phred quality score of 20 was eliminated from further analysis. A Phred score of 20 is equivalent to the presence of a single-nucleotide polymorphism (SNP) in 99% of the reads (Ewing *et al.*, 1998). High quality variants detected in the wildtype control were subtracted from the variants detected in the suppressor set to enrich for variants resulting in suppression. These remaining variants were examined to determine if they were intragenic or extragenic. Only those intragenic variants were analysed to determine if the base change resulted in an amino acid change. Those variants that predicted an amino acid change within a gene were considered potential suppressors.

From the nine samples sent for sequencing, three of these samples had a variant within a gene that was known to suppress a Mec1 mutation and were not analysed further. These three mutations are *sml1-L62ochre* (TAA), *rfx1-S213N*, and *rfx1-S462L* (Zhao *et al*., 1998; Huang *et al*., 1998). The discovery of these known suppressor genes added confidence to the method used for the suppressor variants screening.

Of the remaining six samples, one sample had a potential novel suppressor, a mutation in the *rpn3* gene causing a leucine to proline change at residue 140 (Rpn3-L140P). To validate this mutation as the suppressor, the *rpn3* gene was amplified and sequenced from the suppressor strain, in addition to creating the Rpn3-L140P mutation anew in the Mec1-W2368A background strain. Both were consistent with Rpn3-L140P being responsible for the suppression (DaSilva *et al*, In Press). Rpn3 is a component of the 19S regulatory cap of the 26S proteasome (Finley *et al*., 1998). The specific role of Rpn3 is unclear but the cap is thought to be important in the recruitment of proteins to the proteasome for degradation (Finley *et al*., 1998). As reviewed in Hoyt and Coffino, (2004) and Sorokin *et al.,* (2009), the proteasome can degrade both ubiquitinated (ubiquitin-dependent pathway) and non-ubiquitinated (ubiquitin-independent pathway) protein.

To further ensure that Rpn3-L140P was the suppressor mutation, sequence coverage of the suppressor sample was analysed using the IGV (Integrative Genomics Viewer) program (Robinson *et al.,* 2011). IGV is a program which visually displays mapped reads along the reference sequence to demonstrate coverage - the number of reads aligning to a base in the reference sequence. This allows for areas of low coverage to be easily seen. IGV also displays any base substitutions that may be present within the suppressor sample compared to the reference genome. From the linkage analysis it was clear that the suppressor, if not Rpn3-L140P, was closely linked to this mutation (DaSilva et al, In Press). Therefore, I focussed on analysing the coverage, 40,000 bases downstream and upstream of *rpn3*. Within the 80,000 base pair region, there were no regions of significant low coverage and there was only one base substitution found which causes a silent mutation within the *zrg8* gene (**Figure 27**). This

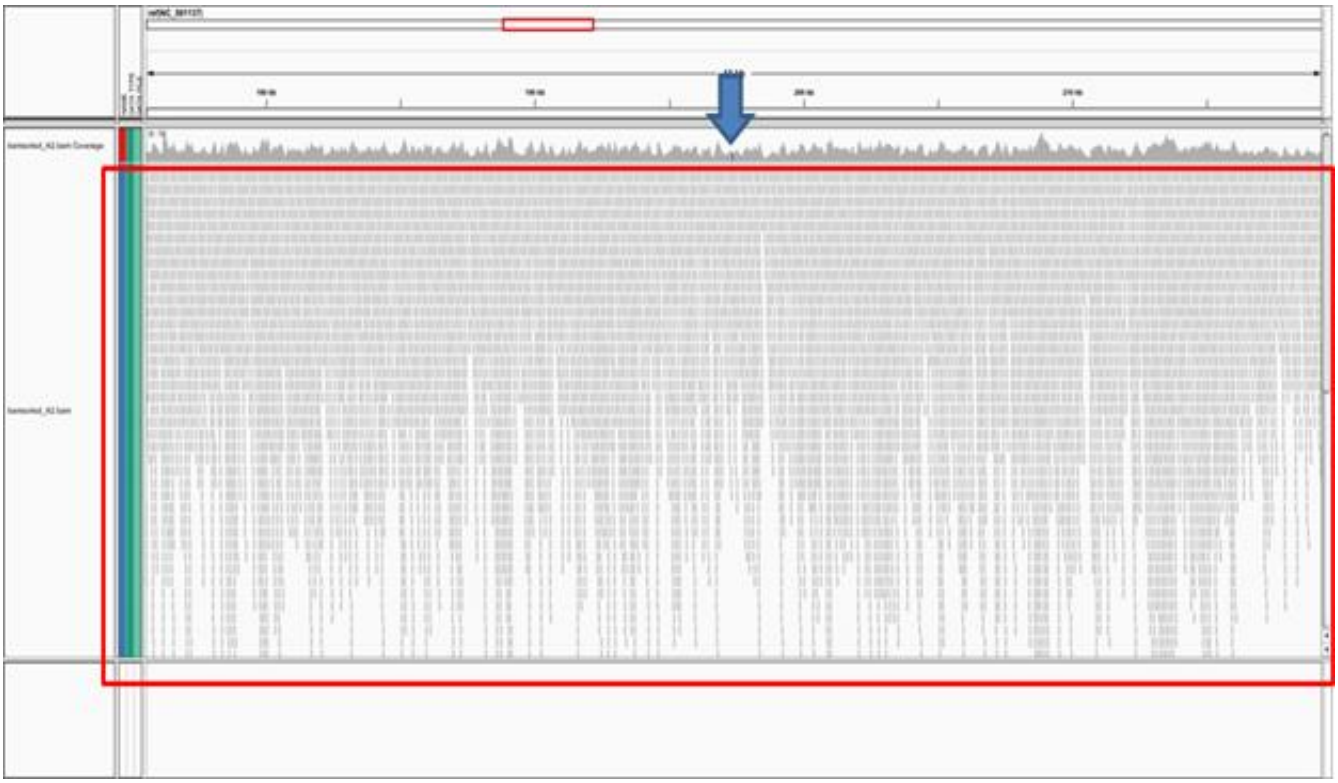

Figure 27. Mapped reads to the region 40 kb downstream and upstream of the *rpn3-L140P* mutation using IGV. The blue arrow indicates the location of the *rpn3-L140P* mutation and the red box encloses the mapped reads

increased the confidence that Rpn3-L140P is the suppressor of Mec1-W2368A within this sample.

The suppressor sequencing reads from the Rpn3-L140P sample were also analysed using Novoalign to ensure that there were no insertion or deletion (indel) mutations that could be responsible for the suppression (Hercus, 2013). From the Novoalign datum, there appears to be no indels within 50,000 base pairs upstream and 50,000 base pairs downstream. There was only one indel detected on chromosome V located approximately 75,000 bases upstream of the *rpn3* gene predicting a thymine insertion within a string of poly Ts. The evidence for this thymine insertion is of very low quality and occurs in only one read of all five reads that map to this region. Thus, there are no significant indels occurring within chromosome V and this supports Rpn3-L140P as the suppressor of the Mec1-W2368A mutation.

From another suppressor sample, it appeared that Hkr1-V594A was a candidate for a potential suppressor. Hkr1 is a mucin gene involved in osmolarity regulation within the cell (Tatebayashi *et al.*, 2007). However, upon amplification and sequencing of the gene from four different haploid colonies, two which demonstrate slow growth at 37°C and two which grow similarly to the wildtype control, all four HKR1 genes contained the Hkr1-V594A mutation. Therefore, *hkr1* is not the suppressor gene for that sample.

Chapter 6: Discussion

1. Prelude

I will first discuss the effect that the C-*terminal tra1* mutations have on Tra1 activity and what this reveals about the function of the FATC domain. The Tti2 truncations will likewise be discussed with a focus on their impact on Tti2 function, the TTT complex, and cell viability. Lastly, two potential hypotheses for the mechanism of the Rpn3-L140P suppressor of Mec1-W2368A will be evaluated. Throughout, I will consider future work that could be undertaken.

2. Differences in cell viability and protein expression for the *tra1* C-terminal mutations

Three substitution mutations (*tra1-F3744S*, *tra1-F3744R*, and *tra1-WF-FW*) and two deletion mutations (*tra1-Δ1* and *tra1-Δ2*) were created at the C-terminus of *tra1*. Each mutation was assessed for cell viability and protein expression both in the presence or absence of the Tti2-F328S suppressor. Only *tra1-WF-FW* was able to support viability without the suppressor, while *tra1-F3744S* and *tra1-WF-FW* allowed for cell viability in the presence of Tti2-F328S.

The effect of Tra1-F3744S differed from the alanine mutation (*tra1-F3744A*) previously examined by Hoke *et al*., (2010). The *tra1-F3744A* mutation resulted in a phenotype when cells were grown under stress conditions. These phenotypes could be rescued in the presence of the Tti2-F328S (Hoke *et al*., 2010; Genereaux *et al*., 2012). Interestingly, Tra1-F3744S resulted in inviability in the absence of the suppressor and showed a phenotype when grown under stress conditions in the presence of the Tti2-F328S suppressor. Potential causes for these differences were further examined by comparing the protein levels of Tra1-F3744S. The level of Tra1-F3744S increased in the presence of *tti2-F238S* when cells were grown at 37°C. This suggests a role for Tti2-F328S in Tra1-F3744S protein folding and/or stabilization. Tra1-F3744S levels in

the presence of the suppressor were comparable to wildtype, yet the F3744S mutation resulted in stress related growth defects. This may result from the *tra1-F3744S* mutation affecting the activity of Tra1 in addition to its folding. Tti2-F328S may aid with the folding of Tra1-F3744S but might not fix the interactions lost or compromised due to the polar group of the serine residue. To help support this possibility it would be valuable to examine the localization of Tra1-F3744S, as perhaps the deficiency results from an inability to transport the protein into the nucleus.

The *tra1-F3744R* mutation resulted in inviability in the presence or absence of the suppressor. The inability of the suppressor to assist Tra1-F3744R again would be consistent with the C-terminus of Tra1 playing a role beyond folding. The levels of Tra1-F3744R were not determined due to the inability to obtain *tra1-F3744R* on the FLAG tagged allele in a diploid strain. These protein levels should be examined in the future to determine if cell inviability is due to protein instability and what influence the suppressor has on Tra1-F3744R protein levels.

The *tra1-WF-FW* containing cells were viable in the presence or absence of the suppressor. In isolation Tra1-WF-FW resulted in slow growth at 37°C; this phenotype was suppressed by Tti2-F328S. As well, Tra1-WF-FW levels increased in the presence of the suppressor at 37°C, similar to Tra1-F3744A. Suppression of *tra1-WF-FW* by the Tti2-F328S would suggest that the mutation primarily affects folding. The subtleties of the role of the C-terminal residues are clearly revealed by this mutation as it represents the switching of what are commonly thought of as functionally similar residues. And similar to the *tra1-F3744A* mutation, the result with this allele suggests that once the suppressor is able to adjust the residues into a functional and stable orientation, the protein is able to function correctly. These experiments further illustrate the

specificity and importance of the FATC domain of Tra1. This specificity could be the result of the terminal residue making important interactions with the PI3K domain that are necessary for folding. A detailed structure of the Tra1 FAT-PI3K-FATC regions would be invaluable in further evaluating the function of the C-terminal residue.

It was seen from the crystal structure produced by Yang *et al.*, (2013) that the C-terminus of mTOR interacts with the PI3K domain. This and our mutational analyses imply that the terminal amino acid is important for PI3K function. Alternatively, it may be the carboxyl group that is required for function. The *tra1* deletion mutations were designed to test the role of the carboxyl group. Neither *tra1-Δ1* nor *tra1-Δ2* was viable in the presence or absence of the suppressor suggesting these deletions disrupt Tra1 activity or result in a folding defect that cannot be repaired by Tti2-F328S. The protein levels for each of the deletion mutations were below those levels seen for wildtype in the presence or absence of the Tti2 F328S suppressor. The deletion mutations show the importance of the interactions occurring at the C-terminus. Since there is no new amino acid being introduced into the sequence, it is unlikely that these mutations are sterically inhibited in their folding; however the terminal residue may still be involved in making key contacts for folding. Alternatively the result with the deletion derivatives may support a specific function for the C-terminal carboxyl. This lack of interaction may cause a loss of activity or it may prevent Tra1-Δ1 and Tra1-Δ2 from localizing to the nucleus. Kinase activity assays of Mec1-Δ1, Mec1-Δ2, and Mec1-Δ3 showed reduced activity compared to wildtype (DaSilva, *et al*., In press). Paralleling this datum with the *tra1*deletion mutations would also suggest that Tra1-Δ1 and Tra1-Δ2 influence protein activity.

Like Tra1, the *mec1* deletion mutations similarly showed a reduction in protein levels (DaSilva *et al*., In press). In addition, the nuclear localization of Mec1-Δ1, Mec1-Δ2, and Mec1-Δ3 was reduced (DaSilva *et al*., In press). This experiment should be repeated with the *tra1* deletion mutations. Additional mutations may help evaluate the role of the C-terminal carboxyl group. One potential mutation would be to remove the terminal phenylalanine and replace the penultimate tryptophan with a glutamic acid residue (Tra1-W3743E). If it is the carboxyl group that supports function for Tra1, then the glutamic acid side chain carboxyl may restore function to Tra1. It may be valuable to also perform this experiment with Mec1 protein as well where kinase assays could be analyzed.

The reduction in protein levels was equally seen with Mec1-W2368A suggesting that the C-terminus is not only important for Tra1 but for all PIKKs. The C-terminus of the FATC domain, however, is not present in PI3Ks (Yang *et al*., 2013). This indicates that the specificity and function of the terminal residue is unique to PIKKs and may be an important feature that differentiates the PIKKs from the PI3Ks.

3. Regions of Tti2 required for viability correlate with interaction to the TTT complex component Tti1

Very little is known about the structure and function of Tti2. The suppression of Tra1-F3744A by Tti2-F328S (Genereaux *et al*. 2012), helped elucidate some of the molecular properties of Tra1. To better understand the relationship between Tra1 and Tti2, details of Tti2 structure/function are required. From the viability assays and analysis of the protein levels, I demonstrated that the N-terminus of Tti2 (first 52 amino acids) can be deleted without any effect on protein level or cell viability. The *tti2-53-421* mutation only demonstrated a slight temperature sensitivity, which suggests that this region does not provide any essential function

for Tti2. None of the other mutations, encompassing deletions of the middle regions or C-terminal sequences supported viability and Tti2-206-421 and Tti2-290-421 were not expressed suggesting that there is a region between residues 116 and 206 that is required for protein stability. The expression of the *tti2* truncation mutations was lower than wildtype with the exception of Tti2-53-421. The lower Tti2 expression levels could contribute to cell inviability for these mutations. Tti2, Tel2, and Tti1 are part of the TTT chaperone complex (Hurov *et al.,* 2010; Takai *et al.,* 2010). Particularly, the TTT complex is thought to assist with the folding of PIKKs, among which Tra1 and Mec1 are essential proteins in yeast (Takai *et al.*, 2010). Insufficient TTT complex in the cell may deplete the PIKKs leading to growth defects or potentially cell death.

Tti2-1-165 migrated more slowly than expected on SDS-PAGE. The reason for this is unclear. When the plasmid was generated and the internal piece of *TTI2* was removed, it resulted in the protein shifting out of frame after residue 165. The frame shift caused an added 81 base pairs to be added to the 3' end of *tti2-1-165*. The extra 27 amino acids would add approximately 3.2 kDa to the molecular weight of Tti2-1-165. Similarly, Tti2-1-238 contained an extra 15 residues at its C-terminus contributing to an increase of approximately 1.7 kDa.

The ability of the Tti2 truncations to interact with the components of the TTT complex was determined using co-immunoprecipitation (co-IP) assays with TAP-tagged proteins. Co-IPs were performed with both Tel2 and Tti1. Tti2-53-421, Tti2-1-238, and Tti2-53-238 all co-immunoprecipitated with Tel2; although Tti2-1-238 and Tti2-53-238 bound less efficiently. Tti2-1-165 and Tti2-116-421 did not bind to Tel2. These results position the Tel2 interaction region between residues 53 and 238 of Tti2. The Tti1 co-IP demonstrated that Tti2-53-421 has a significantly greater ability to bind Tti1 than any of the other Tti2 truncations. This would

suggest interaction with Tti1 is an essential feature of Tti2 function. It is difficult to establish which region is required for binding to Tti1 since most of the truncation proteins did not bind. The lack of binding from the inviable *tti2* truncation mutations may be an added affect with the lowered protein expression. It may be these two facets working together that prevent the TTT complex from forming which then results in cell inviability.

To further explore the regions required for viability and TTT complex formation, more truncation mutations should be generated. The truncation mutations previously generated focussed more on narrowing the regions of viability at the N-terminus. *tti2-1-238* was initially thought to be viable, so additional truncations were not made at the C-terminus. They are now being made to refine the C-terminal mapping. Tti2-53-238 and Tti2-Δ108-216 should be co-IPed with Tti1 and Tel2, respectively, to gain a better understanding of these truncation mutations. Other co-immunoprecipitation assays can be performed with the other interacting proteins of the putative ASTRA complex. By identifying the regions that are required for viability and those which are required for an interaction with a binding partner, essential interactions can be determined.

4. Suppressor Identification Approach and Potential Mechanisms for Rpn3-L140P Suppression of Mec1-W2368A

a. Rpn3-L140P may disrupt the 26S proteasome and prevents Mec1-W2368A degradation

Rpn3 is a constituent of the 26S proteasome. Its function within the proteasome is unclear but it is a member of the 19S regulatory particle, which is thought to aid in recruiting proteins to the proteasome for degradation (Finley, 1998). There are two hypotheses as to how Rpn3-L140P could function to help stabilize Mec1-W2368A. The first is that the mutation in *rpn3* renders the

protein non-functional. If the 19S regulatory particle is no longer able to recruit proteins due to the loss of function of Rpn3-L140P, Mec1-W2368A may avoid degradation. If Mec1-W2368A is not readily degraded, this will give Mec1-W2368A more time to fold and it may give rise to a sufficient amount of functional protein. Experiments performed in the lab are consistent with Mec1 not being ubiquitinated suggesting that Mec1 is degraded by the ubiquitin-independent degradation pathway of the 26S proteasome or that Mec1 associates with another protein that is ubiquitinated and is carried to the proteasome via this secondary protein. In either case, the C-terminus of Mec1 is unchanged due to ubiquitination leaving the possibility that if the 26S proteasome malfunctions (due to the *rpn3-L140P* mutation), Mec1-W2368A could fold into the correct confirmation to support cell viability.

b. Rpn3 may act as a chaperone

The second hypothesis is that the *rpn3-L140P* mutation helps Mec1-W2368A fold through chaperone activity. It has been described in the literature that certain components of the 19S regulatory particle may function to unfold proteins which enables them to enter the proteasome for degradation (reviewed in Elsasser and Finley, 2005). These components include Rpt1-6, which contains functional similarity to ATPase ring complexes which are known to aid in folding (reviewed in Elsasser and Finley, 2005). It may be that, along with the Rpt1-6 subunits, Rpn3 works as a chaperone and possesses the ability to assist with proper protein folding of select proteins. Mec1 may be one of these proteins and the mutation in *rpn3-L140P* may work directly or through other mechanisms to assist with folding of the Mec1-W2368A protein.

Work performed by DaSilva *et al.,* (In press), favour the first model where Rpn3-L140P allows more time for Mec1-W2368A to fold. An experiment where the proteasome was inhibited

by MG-132 also resulted in an increase in Mec1-W2368A protein levels, similar to the increase seen with Rpn3-L140P. Further experiments will need to be undertaken to clarify which of these two hypotheses is correct. These experiments could include making mutations in other proteasomal components and assessing their effect on Mec1-W2368A expression levels. Alternatively, the components of the 19S proteasomal cap have shown function in transcription as well, suggesting another possible pathway for suppression to occur (Ferdous *et al.* 2001; Gonzalez *et al.* 2002).

C. Suppressor Identification Approach

The approach taken to analyse the suppressors was to align the Illumina whole genome sample datum to a reference *S. cerevisiae* genome. This sequence alignment was done with a program called Bowtie (Langmead *et al.*, 2009). Bowtie compares the sample datum to the reference genome and lists any position in the genome where a SNP (single-nucleotide polymorphism) occurs (Langmead *et al.*, 2009). This variants list was then formatted into a table using SAMtools (Li *et al.*, 2009). The table lists the nucleotide present in the genome, the SNP, and a quality or Phred score (Ewing *et al.*, 1998). The Phred score is used to further narrow the search for the suppressor mutation by discarding any SNP which shows a Phred score of less than 20. A Phred score of 20 or higher means that the SNP is present ≥99% of the time (Ewing *et al.*, 1998). After filtering the datum based on their Phred scores, the control sample was compared individually to each of the suppressor samples. Any SNP found in the suppressor sample that was also in the control sample was discarded. SNPs that fell in a non-coding region were equally discarded. The remaining SNPs were analyzed manually to determine the gene where the SNP occurs and if the nucleotide mutation results in an amino acid change.

Although this suppressor analysis approach has identified the novel Rpn3-L140P suppressor and three other known suppressors, there are certain limitations to the analysis which may have prevented the identification of the suppressor in the other samples. First, the Bowtie software used to identify the SNPs can only identify missense mutations, not insertions or deletions (indels). Other programs exist to examine sequencing data for indels. Novoalign is one such program and it was used to ensure the Rpn3-L140P suppressor dataset did not have any indels linked to *rpn3* (Hercus, 2013). This program can also be used to examine the other datasets in a similar manner. Second, the Phred score may have been too stringent for the potential suppressor variants. The suppressor sample datum should be re-examined with a lower Phred score to see what new variants arise. Third, only coding regions of the genome were analysed. The potential suppressor may lie within non-coding regulatory regions. The method of suppression may be a change in the expression level of a certain protein and not a direct mutation within the gene. Non-coding regions should be investigated for any potential variants that lie within a regulatory region of a gene. Gene expression analysis programs can also be used to determine if a certain gene is under or over expressed in the suppressor background compared to the control.

Overall, whole genome sequencing combined with bioinformatics is a powerful technique to identify suppressors within a genome. As the sequencing techniques and sequence analysis software improve, the possibility to identify suppressors also grows.

5. Conclusions

The experiments performed on the *tra1-F3744S, tra1-F3744R, tra1-WF-FW, tra1-Δ1,* and *tra1-Δ2* mutations indicate that the C-terminus of Tra1 possesses a sequence specificity that is important for proper protein function and for folding. The effect these mutations have on the cell

show the importance of the C-terminus of Tra1 while the inability of the suppressor to rescue some of these mutations is indicative of a role for the C-terminal residue beyond folding. The role of the carboxyl group in Tra1 appears to be important for function and should be further explored.

The truncation mutations of *tti2* show that the N-terminus of Tti2 is not required for cell viability and that the *tti2-F328S* suppressor mutation lies in a region that is crucial for function. The inviable truncation mutations had lower expression and their ability to bind Tti1 was drastically decreased. Tti2-53-238 and Tti2-1-238 retained their interaction with Tel2, which suggests the region for binding Tel2 is between residues 53-238. These results are consistent with the formation of the TTT complex being necessary for viability. More mutations must be analyzed to gain a better understanding of the domain boundaries of Tti2.

Rpn3-L140P was identified as a suppressor of the *mec1-W2368A* mutation using whole genome sequencing and bioinformatics. The mechanism by which the Rpn3-L140P suppressor functions to suppress the Mec1-W2368A phenotype is unclear. It may work to disrupt the 26S proteasome and therefore prevent Mec1-W2368A degradation or it may function as a chaperone and assist with Mec1-W2368A folding.

References

Abraham R.T. (2001). Cell Cycle Checkpoint Signaling through the ATM and ATR Kinases. *Genes Dev*. (15): 2177-2196.

Adam M., Robert F., Larochelle M., and Gaudreau L. (2001) H2A.Z is Required for Global Chromatin Integrity and for Recruitment of RNA Polymerase II under Specific Conditions. *Mol Cell Biol.* (21): 6270-6279.

Allard S., Utley R.T., Savard J., Clarke A., Grant P., Brandl C.J., Pillus L., Workman J.L., and CôtéJ. (1999) NuA4, an Essential Transcription Adaptor/Histone H4 Acetyltransferase Complex Containing Esa1p and the ATM-Related Cofactor Tra1p. *EMBO J.* (18): 5108-5119.

Auger A., Galarneau L., Altaf M., Nourani A., Doyon Y., Utley R.T., Cronier D., Allard S., and Côté J. (2008). Eaf1 is the Platform for NuA4 Molecular Assembly that Evolutionarily Links Chromatin Acetylation to ATP-Dependent Exchange of Histone H2A Variants. *Mol Cell Biol.* (28): 2257-2270.

Balasubramanian R., Pray-Grant M.G., Selleck W., Grant P.A., and Tan S. (2002) Role of the Ada2 and Ada3 Transcriptional Coactivators in Histone Acetylation. *J Biol Chem.* (277): 7989-7995.

Barbet N.C., Schneider U., Helliwell S.B., Stansfield I., Tuite M.F., and Hall M.N. (1996) TOR Control Translation Initiation and Early G1 Progression in Yeast. *Mol Biol Cell*. (7): 25-42.

Belotserkovskaya R., Sterner D.E., Deng M., Sayre M.H., Lieberman P.M. and Berger S.L. (2000) Inhibition of TATA-Binding Protein Function by SAGA Subunits Spt3 and Spt8 at Gcn4-Activated Promoters. *Mol Cell Biol.* (20): 634-647.

Berndt A., Miller S., Williams O., Le D.D., Houseman B.T., Pacold J. I., Gorrec F., Hon W-C., Liu Y., Rommel C., Gaillard P., Rückle T., Schwarz M.K., Shokat K.M., Shaw J.P., and Williams R.L. (2010) The p110δStructure: Mechanisms for Selectivity and Potency of New PI(3)K Inhibitors. *Nat Chem Biol*. (6): 117-124.

Bhaumik S.R. and Green M.R. (2002) Differential Requirement of SAGA Components for Recruitment of TATA-Box-Binding Protein to Promoter *in vivo*. *Mol Cell Biol.* (22): 7365-7371.

Bird A. W., Yu D.Y., Pray-Grant M.G., Qui Q., Harmon K.E., Megee P.C., Grant P.A., Smith M.M., and Christman M.F. (2002). Acetylation of histone H4 by Esa1 is Required for DNA Double-Strand Break Repair. *Nature.* (419): 411-415.

Bonnet J., Romier C., Tora L., and Devys D. (2008) Zinc-finger UBPs: Regulators of Deubiquitylation. *Trends Biochem Sci*. (33) 369-375.

Bosotti R., Isacchi A., and Sonnhammer E.L.L. (2000) FAT: a Novel Domain in PIK-Related Kinases. *Trends Biochem Sci*. (25): 225-227.

Boudreault A.A., Cronier D., Selleck W., Lacoste N., Utley R.T., Allard S., Savard J., Lane W.S., Tan S., and Côté J. (2003) Yeast Enhancer of Polycomb Defines Global Esa1-Dependent Acetylation of Chromatin. *Genes Dev*. (17): 1415-1428.

Brewerton S.C., Doré A.S., Drake A.C.B., Leuther K.K., and Blundell T.L. (2004) Structural Analysis of DNA-PKcs: Modelling of the Repeat Units and Insights into the Detailed Molecular Architecture. *J Struct Biol.* (145): 295-306.

Brown E.J. and Baltimore D. (2003) Essential and Dispensable Roles of ATR in Cell Cycle Arrest and Genome Maintenance. *Genes Dev*. (17): 615-628.

Brown C. E., Howe L., Sousa K., Alley S.C. Carrozza M.J., Tan S., and Workman J.L. (2001). Recruitment of HAT Complexes by Direct Activator Interactions with the ATM-Related Tra1 Subunit. *Science*. (292): 2333-2337.

Budillon A., Di Gennaro E., Bruzzese F., Rocco M., Manzo G., and Caraglia M. (2007) Histone Deacetylase Inhibitors: A New Wave of Molecular Targeted Anticancer Agents. *Recent Pat Anti-Canc*. (2): 119-134.

Burtelow M.A., Roos-Mattjus P.M.K., Rauen M., Babendure J.R., and Karnitz L.M. (2001). Reconstitution and Molecular Analysis of the hRad9-hHus1-hRad1 (9-1-1) DNA Damage Responsive Checkpoint Complex. *J. Biol Chem* (276): 25903-25909.

Chittuluru J.R., Chaban Y., Monnet-Saksouk J., Carrozza M.J., Sapountzi V., Selleck W., Huang J., Utley R.T., Cramet M., Allard S., Cai G., Workman J.L., Fried M.G., Tan S., Côté J., and Asturias F.J. (2011). Structure and Nucleosome Interaction of the Yeast NuA4 and Piccolo-NuA4 Histone Acetyltransferase Complexes. *Nat Struct Mol Biol.* (18): 1196-1204.

Clapier C.R. and Cairns B.R. (2009). The Biology of Chromatin Remodeling Complexes. *Annu Rev Biochem.* (78): 273-304.

Clark D.J. and Felsenfeld G. (1992) A Nucleosome Core is Transferred out of the Path of a Transcribing Polymerase. *Cell*. (71): 11-22.

Cortez D., Guntuku S., Qin J., and Elledge S.J. (2001) ATR and ATRIP: Partners in Checkpoint Signalling. *Science*. (294): 1713-1716.

Dames S.A., Mulet J.M., Rathgeb-Szabo K., Hall M.N., and Grzesiek S. (2005) The Solution Structure of the FATC Domain of the Protein Kinase Target of Rapamycin Suggests a Role for Redox-dependent Structural and Cellular Stability. *J Biol Chem.* (280): 20558-20564.

Dames S.A. (2009). Structural Basis for the Association of the Redox-sensitive Target of Rapamycin FATC Domain with Membrane-mimetic Micelles. *J Biol Chem.* (285): 7766-7775.

Daniel J.A., Torok M.S., Sun Z-W., Schieltz D., Allis D., Yates III J.R., and Grant P.A. (2004) Deubiquitination of Histone H2B by a Yeast Acetyltransferase Complex Regulates Transcription. *J Biol Chem.* (279): 1867-1871.

DaSilva L., Pillon S., Genereaux J., Davey M.J., Gloor G.B., Karagiannis J., and Brandl C.J. The Extreme C-terminus of *Saccharomyces cerevisiae* Mec1 is Required for its Localization, Stability, and Function. Submitted to G3: Genes, Genomes, Genetics.

Delacroix S., Wagner J.M., Kobayashi M., Yamamoto K., and Karnitz L.M. (2007). The Rad9-Hus1-Rad1 (9-1-1) Clamp Activated Checkpoint Signaling via TopBP1.*Gene Dev.* (21):1472-1477.

Downs J.A., Allard S., Jobin-Robitaille O., Javaheri A., Auger A., Bouchard N., Kron S.J., Jackson S.P. and Côté J. (2004). Binding of Chromatin-Modifying Activities to Phosphorylated Histone H2A at DNA Damage Sites. *Mol Cell*. (16): 979-990.

Doyon Y. And Côté J. (2004) The Highly Conserved and Multifunctional NuA4 HAT Complex. *Curr Opin Genet Dev.* (14): 147-154.

Dubrana K., van Attikum H., Hediger F., and Gasser S.M. (2007). The Processing of Double-Strand Breaks and Binding of Single-Strand-Binding Proteins RPA and Rad51 Modulate the Formation of ATR-Kinase Foci in Yeast. *J Cell Sci.* (120): 4209-4220.

Dudley A.M., Gansheroff L.J., and Winston F. (1999a) Specific Components of the SAGA Complex are Required for Gcn4- and Gcr1-Mediated Activation of *his4-912δ*Promoter in *Saccharomyces cerevisiae*. *Genetics*. (151): 1365-1378.

Edgar C.R. (2004). MUSCLE: Multiple Sequence Alignment with High Accuracy and High Throughput. *Nucleic Acids Res.* (32): 1792-1797.

Eisenmann D.M., Arndt K.M, Ricupero S.L., Rooney J.W., and Winston F. (1992). SPT3 Interacts with TFIID to Allow Normal Transcription in *Saccharomyces cerevisiae*. *Genes Dev*. (6): 1319-1331.

Eisenmann D.M., Chapon C., Roberts S.M., Dollard C., and Winston F. (1994) The *Saccharomyces cerevisiae* SPT8 Gene Encodes a Very Acidic Protein that is Functionally Related to SPT3 and TATA-Binding Protein. *Genetics* (137): 647-657.

Elsasser S. and Finley D. (2005) Delivery of Ubiquitinated Substrates to Protein-Unfolding Machines. *Nature Cell Biol*. (7): 742-749.

Emili A. (1998). MEC1-Dependent Phosphorylation of Rad9p in Response to DNA Damage. *Mol Cell*. (2): 183-189.

Ewing B., Hillier L., Wendl M.C., and Green P. (1998) Base-Calling of Automated Sequencer Traces Using *Phred*. I. Accuracy Assessment. *Genome Res.* (8): 175-185.

Ferdous, A., F. Gonzalez, L. Sun, T. Kodadek, and S. A. Johnston. (2001) The 19S regulatory particle of the proteasome is required for efficient transcription elongation by RNA polymerase II. *Mol.Cell* (7): 981-991.

Fishburn J., Mohibullah N., and Hahn S. (2005) Function of a Eukaryotic Transcription Activator During the Transcription Cycle. *Mol Cell*. (18): 369-378.

Flores O., Lu H., and Reinberg D. (1992) Factors Involved in Specific Transcription by Mammalian RNA Polymerase II. *J Biol Chem*. (267): 2786-2793.

Friedel A.M., Pike B.L., and Gasser S.M. (2009). ATR/Mec1: Coordinating Fork Stability and Repair. *Curr Opin Cell Biol.* (21): 237-244.

Genereaux J., Kvas S., Dobransky D., Karagiannis J., Gloor G.B., and Brandl C.J. (2012). Genetic Evidence Links the ASTRA Protein Chaperone Component Tti2 to the SAGA Transcription Factor Tra1. *Genetics*. (191): 765-780.

Ghaemmaghami S., Huh W.K., Bower K., Howson R.W., Belle A., Dephoure N., O'Shea E.K., and Weissman J.S. (2003) Global Analysis of Protein Expression in Yeast. *Nature*. (425): 737-741

Glickman M.H., Rubin D.M., Coux O., Wefes I., Pfeifer G., Cjeka Z., Baumeister W., Fried V.A., and Finley D. (1998) A Subcomplex of the Proteasome Regulatory Particle Required of Ubiquitin-Conjugate Degradation and Related to the COP9-Signalosome and eIF3. *Cell*. (94): 615-623.

Glickman M.H., Rubin D.M., Fried V.A., and Finley D. (1998) The Regulatory Particle of the *Saccharomyces cerevisiae* Proteasome. *Mol Cell Biol*. (18): 3149-3162.

Gonzalez, F., A. Delahodde, T. Kodadek, and S. A. Johnston, 2002 Recruitment of a 19S proteasome subcomplex to an activated promoter. Science 296: 548-550.

Govind C.K., Zhang F., Qui H., Hofmeyer K., and Hinnebusch A.G. (2007) Gcn5 Promotes Acetylation, Eviction, and Methlyation of Nucleosomes in Transcribed coding Regions. *Mol Cell*. (25): 31-42.

Grant P.A., Schieltz D., Pray-Grant M.G., Steger D., Reese J.C., Yates III J.R., and Workman J.L. (1998a) A Subset of TAF_{II}s are Integral Components of the SAGA Complex Required for Nucleosome Acetylation and Transcriptional Stimulation. *Cell*. (94): 45-53.

Grant P.A., Eberharter A., John S., Cook R.G., Turner B.M., and Workman J.L. (1999) Expanded Lysine Acetylation Specificity of Gcn5 in Native Complexes. *J Biol Chem*. (274): 5895-5900.

Hampsey M. (1997) A Review of Phenotypes in *Saccharomyces cerevisiae*. *Yeast*. (13): 1099-1133.

Helmlinger D., Marguerat S., Villén J., Swaney D.L., Gygi S.P., Bähler J., and Winston F. (2011) Tra1 has Specific Regulatory Roles, Rather than Global Functions, Within the SAGA Co-activator Complex. *EMBO J*. (0): 1-10.

Helmlinger D. (2012) New Insights into the SAGA Complex from Studies of the Tra1 Subunit in Budding and Fission Yeast. *Biochem Soc Symp*. (3): 13-18.

Henry K.W., Wyce A., Lo W-S., Duggan L.J., Emre N.C.T., Kao C-F., Pillus L., Shilatifard A., Osley M.A., and Berger S.L. (2003) Transcriptional Activation via Sequential Histone H2B Ubiquitylation and Deubiquitylation, Mediated by SAGA-Associated Ubp8. *Genes Dev*. (17): 2648-2663.

Hercus C., 2013 www.novocraft.com(last accessed date June, 2013).

Hirao A., Kong Y-Y., Matsuoka S., Wakeham A., Ruland J., Yoshida H., Liu D., Elledge S.J. and Mak T.W. (2000) DNA Damage-Induced Activation of p53 by the Checkpoint Kinase Chk2. *Science*. (287): 1824-1827.

Hoke S.M.T., Guzzo J., Andrews B., and Brandl C.J. (2008) Systematic Genetic Array Analysis Links the *Saccharomyces cerevisiae* SAGA/SLIK and NuA4 Component Tra1 to Multiple Cellular Processes. *BMC Genetics* (9): 46-60.

Hoke S.M.T, Mutiu A.I., Genereaux J., Kvas S., Buck M., Yu M., Gloor G.B., and Brandl C.J. (2010) Mutational Analysis of the C-terminal FATS Domain of *Saccharomyces cerevisiae* Tra1. *Curr Genet*. (56): 447-465.

Holstege F.C.P., VanderVliet P.C., and Timmers H.T.M. (1996) Opening of a RNA Polymerase II Promoter Occurs in Two Distinct Steps and Requires the Basal Transcript Ion Factors IIE and IIH. *EMBO J*. (15): 1666-1677.

Horiuchi J., Silverman N., Marcus G.A., and Guarente L. (1995) ADA3, a Putative Transcriptional Adaptor, Consists of Two Separable Domains and Interacts with ADA2 and GCN5 in a Trimeric Complex. *Mol Cell*. (15): 1203-1209.

Hoyt M.A., an Coffino P. (2004) Ubiquitin-Free Routes in the Proteasome. *Cell Mol Life Sci*. (61): 1596-1600.

Huang M.X., Zhou Z., and Elledge S.J. (1998) The DNA Replication and Damage Checkpoint Pathways Induce Transcription by Inhibition of the Crt1 Repressor. *Cell*. (94): 595-605.

Huang S., Bjornsti M-A., and Houghton P.J. (2003) Rapamycins: Mechanism of Action and Cellular Resistance. *Cancer Biol Ther*. (2): 222-232.

Hurov K.E., Cotta-Ramusino C., and Elledge S.J. (2010) A Genetic Screen Identifies the Triple T complex Required for DNA Damage Signaling and ATM and ATR Stability. *Genes Dev*. (24): 1939-1950.

Jackson S.P. (1996) The Recognition of DNA Damage. *Curr Opin Genet Dev*. (6): 19-25.

Jiang X., Sun Y., and Chen S. (2006) The FATC Domain of PIKK Proteins are Functionally Equivalent and Participate in the Tip60-Dependent Activation of DNA-PKcs and ATM. *J Biol Chem*. (281): 15741-15746.

Kanemaki M., Kurokawa Y., Matsu-ura T., Makino Y., Masani A., Okazaki K., Morishita T., and Tamura T. (1999) TIP49b, a New Ruvb-like DNA Helicase, is Included in a Complex Together with Another RuvB-like DNA Helicase, TIP49a. *J Biol Chem.* (274):22437-22444.

Kanoh J. and Yanagida M. (2007) Tel2: a Common Partner of PIK-Related Kinases and a Link Between DNA Checkpoint and Nutritional Response? *Genes Cells.* (12): 1301-1304.

Keith C.T. and Schreiber S.L. (1995) PIK-Related Kinases: DNA Repair, Recombination and Cell Cycle Checkpoints. *Science*. (270): 50-51.

Keogh M-C., Mennella T.A., Sawa C., Berthelet S., Krogan N.J., Wolek A., Podolny V., Carpenter L.R., Greenblatt J.F., Baetz K., and Buratowski S. (2006) The *Saccharomyces cerevisiae* Histone H2A Variant Htz1 is Acetylated by NuA4. *Genes Dev*. (20): 660-665.

Khöler A., Pascual-García P., Llopis A., Zapater M., Posas F., Hurt E., and Rodríguez-Navarro S. (2006) The mRNA Export Factor Sus1 is Involved in Spt/Ada/Gcn5 Acetyltransferase-Mediated H2B Deubiquitinylation through its Interaction with Ubp8 and Sgf11. *Mol Biol Cell.* (17): 4228-4236.

Khöler A., Schneider M., Cabal G.G., Nehrbass U., and Hurt E. (2008) Yeast Ataxin-7 Links Histone Deubiquitination with Gene Gating and mRNA Export. *Nat Cell Biol.* (10): 707-715.

Killeen M., Coulombe B., and Greenblatt J. (1992) Recombinant TBP, Transcription Factor IIB, and RAP30 are Sufficient for Promoter Recognition by Mammalian RNA Polymerase II. *J Biol Chem*. (267): 9463-9466.

Kim S.G., Hoffman G.R., Poulogiannis G., Buel G.R., Jang Y.J., Lee K.W., Kim B-Y., Erikson R.L., Cantley L.C., Choo A.Y., and Blenis J. (2013). Metabolic stress Controls mTORC1 Lysosomal Localization and Dimerization by Regulating the TTT-Ruvb1/2 Complex. *Mol Cell*. (49): 172-185.

Knutson B.A. and Hahn S. (2011) Domains of Tra1 Important for Activator Recruitment and Transcription Coactivator Functions of SAGA and NuA4 Complexes. *Mol Cell Biol*. (31): 818-831.

Kobor M.S., Venkatasubrahmanyam S., Meneghini M.D., Gin J.W., Jennings J.L., Link A.J., Madhani H.D., and Rine J. (2004). A Protein Complex Containing the Conserved Swi2/Snf2-Related ATPase Swr1p Deposits Histone Variant H2A.Z into Euchromatin. *PLOS Biol*. (2): 0587-0599.

Langmead B, Trapnell C, Pop M, and Salzberg SL (2009) Ultrafast and Memory-Efficient Alignment of Short DNA Sequences to Human Genome. *Genome Biol*. 10(3):R25

Lasker K., Förster F., Bohn S., Walzthoeni T., Villa E., Unverdorberf P., Beck F., Aebersold R., Sali A., and Baumeister. (2011). Molecular Architecture of the 26S Proteasome Holocomplex Determined by an Integrative Approach. *PNAS*. (109): 1380-1387.

Lee K.K., Florens L., Swanson S.K., Washburn M.P., and Workman J.L. (2005) The Deubiquitylation Activity of Ubp8 is Dependent upon Sgf11 and its Association with the SAGA Complex. *Mol Cell Biol*. (25): 1173-1182.

Lempiäinen H. and Halazonetis T.D. (2009) Emerging Common themes in Regulation of PIKKs and PI3Ks. *EMBO J.* (28): 3067-3073.

Li H., Handsaker B., Wysoker A., Fennell T., Ruan J., Homer N., Marth G., Abecasis G., Durbin R., and 1000 Genome Project Data Processing Subgroup. (2009) The Sequence Alignment/Map (SAM) Format and SAMtools. *Bioinformatics* (25): 2078-2079.

Lopes M., Cotta-Ramusino C., Pellicioli A., Liberi G., Plevani P., Muzi-Falconi M., Newlon C.S., and Foiani M. (2001). The DNA Replication Checkpoint Response Stabilizes Stalled Replication Forks. *Nature*. (412): 557-561.

Lu P.Y.T., Lévesque N., and Kobor M.S. (2009) NuA4 and SWR1-C: Two Chromatin-Modifying Complexes with Overlapping Functions and Components. *Biochem Cell Biol*. (87): 799-815.

Luger K., Mäder A.W., Richmond R.K., Sargent D.F., and Richmond T.J. (1997). Crystal Structure of the Nucleosome Core Particle at 2.8Å Resolution. *Nature*. (389): 251-260.

Majka J., Niedziela-Majka A., and Burgers P.M.J. (2006). The Checkpoint Clamp Activates Mec1 Kinase During Initiation of the DNA Damage Checkpoint. *Mol Cell*. (24): 891-901.

Makino Y., Mimori T., Koike C., Kanemaki M., Kurokawa Y., Inoue S., Kishimoto T., and Tamura T. (1998) TIP49, Homologous to the Bacterial DNA Helicase RuvB, Acts as an Autoantigen in Human. *Biochem Bioph Res Co*. (245): 819-823.

Matsuoka S., Ballif B.A., Smogorzewska A., McDonals III E.R., Hurov K.E., Luo J., Bakalarski C.E., Zhao Z., Solimini N., Lerenthal Y., Shiloh Y., Gygi S.P., and Elledge S.J. (2007). ATM and ATR Substrates Analysis Reveals Extensive Protein Networks Responsive to DNA Damage. *Science*. (316): 1160-1166.

Maxon M.E., Goodrich J.A., and Tjian R. (1994) Transcription Factor IIE Binds Preferentially to RNA Polymerase IIa and Recruits TFIIH: a Model for Promoter Clearance. *Genes Dev*. (8): 515-524.

Mizzen C.A., Yang X-J., Kokubo T., Brownell J.E., Bannister A.J., Owen-Hughes T., Workman J.L., Wang L., Berger S.L., Kouzarides T., Nakatani Y., and Allis C.D. (1996) The $TAF_{II}250$ Subunit of TFIID has Histone Acetyltransferase Activity. *Cell* (87): 1261-1270.

Mordes D.A., Glick G.G., Zhao R., and Cortez D. (2008) TopBP1 Activates ATR Through ATRIP and a PIKK Regulatory Domain. *Genes Dev*. (22): 1478-1489.

Morita T., Yamashita A., Kashima I., Ogata K., Ishiura S., and Ohno S. (2007). Distant N- and C-terminal Domains are Required for Intrinsic Kinase Activity of SMG-1, a critical component of Nonsense-mediated mRNA Decay. *J Biol Chem*. (282) 7799-7808.

Morrison A.J., Kim J-A., Person M.D., Highland J., Xiao J., Wehr T.S., Hensley S., Bao Y., Shen J., Collins S.R., Weissman J.S., Delrow J., Krogan N.J., Haber J.E., and Shen X. (2007). Mec1/Tel1 Phosphorylation of the INO80 Chromatin Remodeling Complex Influences DNA Damage Checkpoint Responses. *Cell*. (130): 499-511.

Mutiu A.I., Hoke S.M.T., Genereaux J., Hannam C., MacKenzie K., Jobin-Robitaille O., Guzzo J., Côté J., Andrews B., Haniford D.B., and Brandl C.J. (2007) Structure/Function Analysis of the Phosphatidylinositol-3-Kinase Domain of Yeast Tra1. *Genetics*. (177): 151-166.

Nakada D., Hirano Y., Tanaka Y., and Sugimoto K. (2005) Role of the C-terminus of Mec1Checkpoint Kinase in Its Localization to Sites of DNA Damage. *Mol Biol Cell*. (16): 5227-5235.

Noma K., Allis C.D., and Grewal S.I.S. (2001) Transitions in Distinct Histone H3 Methylation Patterns at the Heterochomatin Domain Boundaries. *Science*. (293): 1150-1155.

Ozols J. (1990) Amino-Acid Analysis. *Methods Enzymol*. (182): 587-601.

Perry J. and Kleckner N. (2003) The ATRs, ATMs, and TORs are Giant HEAT Repeat Proteins. *Cell*. (112): 151-155.

Pray-Grant M.G., Schieltz D., McMahon S.J., Wood J.M., Kennedy E.L., Cook R.G., Workman J.L., Yates III J.R., and Grant P.A. (2002) The Novel SLIK Histone Acetyltransferase Complex Functions in the Yeast Retrograde Response Pathway. *Mol Cell Biol*. (22): 8774-8786.

Pray-Grant M.G., Daniel J.A., Schieltz D., Yates III J.R., and Grant P.A. (2005) Chd1 Chromodomain Links Histone H3 Methylation with the SAGA- and SLIK-dependent Acetylation. *Nature*. (433): 434-438.

Qi J. and Zhao F. (2010) http://ingap.sourceforge.net/(last accessed date, June 2013)

Ranish J.A., Yudkovsky N., and Hahn S. (1999) Intermediates in Formation and Activity of the RNA Polymerase II Preinitiation Complex: Holoenzyme Recruitment and a Postrecruitment Role for the TATA Box and TFIIB. *Genes Dev.* (13): 49-63.

Rea S., Eisenhaber F., O'Carroll D., Strahl B.D., Sun Z-W., Schmid M., Opravil S., Mechtler K., Ponting C.P., Allis C.D., and Jenuwein T. (2000) Regulation of Chromatin Structure by Site-Specific Histone H3 Methyltransferase. *Nature*. (406): 593-599.

Reinberg D. And Roeder R.G. (1987) Factors Involved in Specific Transcription by Mammalian RNA Polymerase II. *J Biol Chem*. (262): 3310-3321.

Rigaut G., Shevchenko A., Rutz B., Wilm M., Mann M., and Séraphin B. (1999) A Generic Protein Purification Method for Protein Complex Characterization and Proteome Exploration. *Nature Biotech* (17): 1030-1032.

Rivera-Calzada A., Maman J.P., Spagnolo L., Pearl L.H., and Llorca O. (2005). Three-Dimensional Structure and Regulation of the DNA-Dependent Protein Kinase Catalytic Subunit (DNA-PKcs). *Structure*. (13): 243-255.

Robinson J.T., Thorvaldsdóttir H., Winckler W., Guttman M., Lander E.S., Getz G., and Mesirov J.P. (2011) Integrative Genomics Viewer. *Nature Biotechnology* (29): 24-26.

Rodriguez-Navarro S. (2009). Insights into SAGA Function During Gene Expression. *EMBO Rep.* (10) 843-850.

Rodriguez J. And Tsukiyama T. (2013). ATR-like kinase Mec1 Facilitates both Chromatin Accessibility at DNA Replication Forks and Replication Fork Progression During Replication Stress. *Genes Dev*. (27): 74-86.

Ruediger R., Hentz M., Fait J., Mumby M., and Walter G., (1994). Molecular Model of the A Subunit of Protein Phosphatase 2A: Interaction with Other Subunits and Tumor Agents. *J Virol*. (68): 123-129.

Saleh A., Lang V., Cook R., and Brandl C.J. (1997) Identification of Native Complexes Containing the Yeast Coactivator/Repressor Proteins NGG1/ADA3 and ADA2. *J Biol Chem.* (272) 5571-5578.

Saleh A., Schieltz s., Ting N., McMahon S.B., Litchfield D.W., Yates III J.R., Lees-Miller S.P., Cole M.D., and Brandl C.J. (1998) Tra1p is a Component of the Yeast Ada·Spt Transcriptional Regulatory Complexes. *J Biol Chem.* (273): 26559-26565.

Samara N.L. and Wolberger C. (2011) A New Chapter in the Transcription SAGA. *Curr Opin Struct Biol.*(21): 767-774.

Shen X., Mizuguchi G., Hamiche A., and Wu C. (2000) A Chromatin Remodeling Complex Involved in Transcription and DNA Processing. *Nature*. (406): 541-544

Shevchenko A., Roguev A., Schaft D., Buchanan L., Habermann B., Sakalar C., Thomas H., Krogan NJ., Shevchenko A., and Stewart A.F. (2008). Chromatin Central: Towards the Comparative Proteome by Accurate Mapping of the Yeast Proteomic Environment. *Genome Biol*. (9): R167.

Sibanda B.L., Chirgadze D.Y., and Blundell T.L. (2010). Crystal Structure of DNA-PKcs Reveals a Large Open-Ring Cradle Comprised of HEAT Repeats. *Nature*. (463): 118-122.

Sommer L.A.M., Schaad M., and Dames S.A. (2013) NMR-and CD-Monitored Lipid-Binding Studies Suggest a General Role for the FATC Domain as Membrane Anchor of Phosphatidyl-Inositol-3 Kinase-Related Kinases (PIKKs). *J Biol Chem*. (288): 20046-20063.

Sorokin A.V., Kim E.R., and Ovchinnikov L.P. (2009) Proteasome System of Protein Degradation and Processing. *Biochemistry-Moscow+*. (74): 1411-1442.

Stirling P.C., Bloom M.S., Solanki-Patil T., Smith S., Sipahimalani P., Li z., Kofoed M., Ben-Aroya S., Myung K., and Hieter P. (2011). The Complex Spectrum of Yeast Chromosome Instability Genes Identifies Candidate CIN Cancer Genes and Functional Roles for ASTRA Complex Components. *PLOS Genet.* (7): 1-10.

Strahl B.D. and Allis C.D. (2000). The Language of Covalent Histone Modifications. *Nature* (403): 41-45.

Steinboeck F., Bogusch A., Kaufmann A., and Heidenreich E. (2007). The Nuclear Actin-Related Protein of *Saccharomyces cerevisiae*, Arp4, Directly Interacts with the Histone Acetyltransferase Esa1p. *J Biochem.*(141): 661-668.

Takahashi T., Hara K., Inoue H., Kawa Y., Tokunaga C., Hidayat S., Yoshino K., Kuroda Y., and Yonezawa K. (2000). Carboxyl-terminal Region Conserved Among Phosphoinositide-Kinase-Related Kinases is Indispensable for mTOR Function *in vivo* and *in vitro*. *Genes Cell*. (5): 765-775.

Takai H., Xie Y., de Lange T., and Pavletich N.P. (2010) Tel2 Structure and Function in the Hsp90-dependent Maturation of mTOR and ATR Complexes. *Genes Dev*. (24): 2019-2030.

Tatebayashi K., Tanaka K., Yang H-Y., Yamamoto K., Matsushita Y., Tomida T., Imai M., and Saito H. (2007). Transmembrane Mucins Hkr1 and Msb2 are putative osmosensors in the SHO1 branch of yeast HOG pathway. *EMBO J*. (26): 3521-3533.

Tseng S-F., Lin J-J., and Teng S-C. (2006). The Telomerase-Recruitment Domain of the Telomere Binding Protein Cdc13 is Regulated by Mec1p/Tel1p-Dependent Phosphorylation. *Nucleic Acids Res.*(34): 6327-6336.

Wandelt C. and Grummt I. (1983) Formation of Stable Preinitiation Complexes is Prerequisite for Ribosomal DNA Transcription *in vitro*. *Nucleic Acids Res.* (11): 3795-3809.

Weinert T.A., Kiser G.L., and Hartwell L.H. (1994) Mitotic Checkpoint Genes in Budding Yeast and the Dependence of Mitosis on DNA Replication and Repair. *Genes Dev*. (8): 652-665.

Wu P-Y. J. and Winston F. (2002) Analysis of Spt7 Function in the *Saccharomyces cerevisiae* SAGA Coactivator Complex. *Mol Cell Biol*. (22): 5367-5379.

Yamashita A., Ohnishi T., Kashima I., Taya Y., and Ohno S. (2001) Human SMG-1, a Novel Phosphatidylinositol 3-Kinase-Related Protein Kinase, Associates with Components of the mRNA Surveillance Complex and is Involved in the Regulation of Nonsense-Mediated mRNA Decay. *Genes Dev.* (15): 2215-2228.

Yang H., Rudge D.G., Koos J.D., Vaidialingam B., Yang H.J., and Pavletich N.P. (2013) mTOR Kinase Structure, Mechanism and Regulation. *Nature.* (497): 217-224.

Zhao X., Muller E.G.D., Rothstein R. (1998) A Suppressor of Two Essential Checkpoint Genes Identifies a Novel Protein that Negatively Affects dNTP Pools. *Mol Cell*. (2): 329-340.

Zou L. And Elledge S.J. (2003). Sensing DNA Damage through ATRIP Recognition of RPA-ssDNA Complexes. *Science*. (300): 1542-1548.

Supplemental Data

```
########################################
# ARRAY DATA FOR MEC SUPPRESSORS #
########################################
#declare 10 elements for three different arrays that will be applied to the SAMPLE and NAME variables
ARRAYNAMES=( MEC8182 A2 A3 A4 B1 B2 B3 C2 C3 C6 )
ARRAYBARCODES=( CCAACA CATTTT CAAAAG CACGAT ATTCCT ATGAGC CAGGCG CACTCA
CGGAAT ACTGAT )
ARRAYNUMBER=( '002' '002' '001' '002' '001' '002' '002' '002' '002' '002' )
# get number of elements in the array
ELEMENTS=${#ARRAYNAMES[@]}
# echo each element in array
# for loop
for (( i=0;i<$ELEMENTS;i++)); do
#due to the {i} within the variables, they must be within the for loop since the for loop denotes the {i}
#assign variables to array so when the loop runs it will go through all the elements in the array.
SAMPLE=Sample_${ARRAYNAMES[${i}]}/${ARRAYNAMES[${i}]}_${ARRAYBARCODES[${i}]}_L006_R1
_${ARRAYNUMBER[${i}]}.fastq
NAME=${ARRAYNAMES[${i}]}
#script used to run the mapping program
if [ -e $DATA/$NAME/map_best3_$NAME.sam ]; then
echo "$DATA/$NAME/map_best3_$NAME.sam file exists"
else
#gunzip $DATA/$SAMPLE.gz
if [ -e $DATA/$SAMPLE ]; then
#if the file is unzipped, run through program
#make new directory to store the mapped data file
mkdir $DATA/$NAME
bowtie -S -v 3 -t $DATA/$IDX -q $DATA/$SAMPLE $DATA/$NAME/map_best3_$NAME.sam
else
#if not unzipped, the file will be unzipped before going through the mapping program
gunzip $DATA/$SAMPLE.gz
mkdir $DATA/$NAME
bowtie -S -v 3 -t $DATA/$IDX -q $DATA/$SAMPLE $DATA/$NAME/map_best3_$NAME.sam
fi
fi
#make sure that this portion of the script is out of the previous "if" statement
#if it is not, it will go through the frist statement, noting the file exists and stop
#when it is out of that statement, it will continue on to make a bam file if the file already exists
#or if not, it will do the mapping then convert to bam
#converting to BAM - same strategy as with mapping
#if sorted BAM file exists, echo filename
#if not then sort it using samtools function
if [ -e $DATA/$NAME/map_best3_$NAME.bam ]; then
echo "$DATA/$NAME/map_best3_$NAME.bam file exists"
else
echo "making map_best3_$NAME.bam file"
samtools view -bS $DATA/$NAME/map_best3_$NAME.sam > $DATA/$NAME/map_best3_$NAME.bam
fi
#sort the bam files and index to be able to do a pileup
#the pileup will group the variants so that they can be analyzed through a variant filter to get a Phred
score
#Phred score tells us the certainty of the variant
if [ -e $DATA/$NAME/bamsorted_$NAME.bam ]; then
```

```
echo "$DATA/$NAME/raw_pileup_$NAME.txt file exists"
else
echo "making $DATA/$NAME/raw_pileup_$NAME.txt"
#sort the bam files
#samtools sort <in> <out>
#don't need to end the new sorted filename with .bam since it will be added automatically
samtools sort $DATA/$NAME/map_best3_$NAME.bam $DATA/$NAME/bamsorted_$NAME
#index the bam files
samtools index $DATA/$NAME/bamsorted_$NAME.bam
#run the pileup of the variants
#vcf is for variant call format
samtools pileup -vcf $YEAST/yeast.fsa $DATA/$NAME/bamsorted_$NAME.bam >
$DATA/$NAME/raw_pileup_$NAME.txt
fi
#to filter through variants and keep those with a Phred quality score of 20 or more
if [ -e $DATA/$NAME/filtered_pileup_$NAME.txt]; then
echo "$DATA/$NAME/filtered_pileup_$NAME.txt file exists"
else
echo "making $DATA/$NAME/filtered_pileup_$NAME.txt"
#create new file of all the filtered variants
samtools.pl varFilter $DATA/$NAME/raw_pileup_$NAME.txt | awk '$6>=20' >
$DATA/$NAME/filtered_pileup_$NAME.txt
fi
done
```

Figure S1: Shell script to map the Illumina dataset to *S. cerevisiae* reference genome. The Bowtie software was used to map the Illumina reads to the reference genome obtained from SGD. SNPs were identified by the program and a table of variants was created using SAMtools. Phred scores above 20 were isolated and saved in a new file: filtered_pileup_$NAME.txt . This script (bc_supp.sh) was written by Dr. Greg Gloor and Stephanie Kvas, modified by Samantha Pillon.

```
#!/usr/bin/env perl -w
use strict;
my $variants = $ARGV[0]; #pilup output
my $ft = $ARGV[1]; #YAR066W NC_001133 221049 221660 Yar066wp
#build an index of all positions inside genes
my %feat;
open (IN, "< $ft") or die;
while(my $l = <IN>){
chomp $l;
my @l = split/\t/, $l;
if ($l[3]){
my $mx = $l[2]; $mx = $l[3] if $l[3] > $l[2];
my $mn = $l[2]; $mn = $l[3] if $l[3] < $l[2];
for (my $i = $mn; $i < $mx; $i++){
$feat{$l[1]}{$i} = $l[0];
}
}
}
close IN;
my %var;
open (IN, "< $variants") or die;
while(my $l = <IN>){
chomp $l;
my @l = split/[\t\|]+/, $l;
if (exists $feat{$l[1]}{$l[2]}){
print "$feat{$l[1]}{$l[2]}\t$l\n";
}else{
print "extragenic\t$l\n";
}
}
close IN;
```

Figure S2: Perl script to assign gene names to each SNP. This script (parse_yeast.pl) was written by Dr. Greg Gloor.

```
#!/usr/bin/env perl -w
use strict; #enforces good programing practices
use warnings;
=com
This program literally compares two files and makes a third file containing the differences between the
two files.
This program will be used to compare the polymorphisms between wild-type whole-genome sequencing
data and the
suppressors. Therefore, this will be used to narrow down the number of suppressor mutations.
=cut
my $filename = $ARGV[0]; #specify wild-type file to compare to
my $filename2 = $ARGV[1]; #specify second file to compare to
my %results = ();
print "enter wild type first, then mutant\noutput by command redirection\n" if !$ARGV[0];
exit if !$ARGV[0];
open FILE1, "$filename" or die "Could not open file: $! \n";
while(my $line = <FILE1>){
chomp $line;
my @l = split/\t/, $line;
my $var = join ("", @l[0 .. 3]); #generate a unique name
$results{$var} = $line;
}
close(FILE1);
print "in mut, not wt\n";
open FILE2, "$filename2" or die "Could not open file: $! \n";
while(my $line =<FILE2>) {
chomp $line;
my @l = split/\t/, $line;
my $var = join ("", @l[0 .. 3]); #generate a unique name
print "$line\n" if (!exists $results{$var} && $l[3] =~ /[ACGT]/);
}
close(FILE2);
%results = ();
exit if !$ARGV[0];
open FILE1, "$filename2" or die "Could not open file: $! \n";
while(my $line = <FILE1>){
chomp $line;
my @l = split/\t/, $line;
my $var = join ("", @l[0 .. 3]); #generate a unique name
$results{$var} = $line;
}
close(FILE1);
print "in wt, not mut\n";
open FILE2, "$filename" or die "Could not open file: $! \n";
while(my $line =<FILE2>) {
chomp $line;
my @l = split/\t/, $line;
my $var = join ("", @l[0 .. 3]); #generate a unique name
print "$line\n" if (!exists $results{$var} && $l[3] =~ /[ACGT]/);
}
close(FILE2);
```

Figure S3: Perl script to eliminate variants found in wildtype control sample. This script (Final_Comparisons.pl) was written by Stephanie Kvas and modified by Samantha Pillon.

```
#!/usr/bin/env perl -w
use strict;
# Need to realign A2 supp (RPN3) to check for indels
# used novoalign which can be accessed from Greg's folders through the path
# /Users/ggloor/bin/novoalign
####### Indexing
# First must make an index that can be used by novoalign
# basic format from novoalign manual
# novoindex indexfile.nix sequencefiletouseasreference.fsa
/Users/ggloor/bin/novoindex /Users/spillon3/Project_ChrisB/data/Novoalign_Data/index.nix
/Users/spillon3/yeast.fsa
# Once index is made can then start aligning sequences
######## Aligning Sequences
# must follow illumina formating
# in manual, tells to follow
# novoalign -d indexfile.nix -f sequencefile.fastq
# -d is the database name -f is the file name
# can save file in SAM format by adding
# -o SAM > alignments.sam
# this makes the full line read as
# novoalign -d indexfile.nix -f sequencefile.fastq -o SAM > alignments.sam
# novoalign command line for A2 supp sample
~/Downloads/novocraft/novoalign -d ~/Project_ChrisB/data/Novoalign_Data/index.nix-f
~/Project_ChrisB/data/Sample_A2/A2_CATTTT_L006_R1_002.fastq -o SAM >
~/Project_ChrisB/data/Novoalign_Data/A2alignment.sam
# run sam file through inGAP program to visualise the indels.
# need to also run WT/control sample to help filter out indels
# to open inGAP
java -mx2000m -jar inGAP_3_0_1/inGAP.jar
```

Figure S4: Perl script for Novoalign sequence alignment to check for indels in *rpn3* suppressor sample. The *rpn3* suppressor sample datum aligned with Novoalign and then the indels present are viewed using inGAP. This script (novoalign.pl) was written by Samantha Pillon.

Table S1: *S. cerevisiae* Strains

Strain Number	Description	Plasmids	Reference
BY4743	*MAT a/α his3Δ1/his3Δ1 leu2Δ0/leu2Δ0 lys2Δ0/LYS2 MET15/met15Δ0 ura3Δ0/ura3Δ0*		Winzeler et al., 1997
CY4398	*MAT a/α HIS3/his3Δ1 leu2Δ0/leu2Δ0 MET15/MET15 URA3/ura3Δ0 TRA1/TRA1*		Genereaux *et al*., 2012
CY4353	*MAT a his3Δ1ura3Δ0 leu2Δ0* TRA1-HIS3		Hoke *et al*., 2010
CY6070	*MAT a ura3Δ0 LEU2 LYS2 tti2Δ*	CB2319	This work
CY6145	Isogenic to CY6070	CB2494	This work
CY6497	Isogenic to CY4398 with FLAG5 tagged *tra1-F3744S* allele		This work
CY6499	*MAT α HIS3 leu2Δ0 MET15 ura3Δ0 tra1-F3744S*	CB2331	This work
CY6514	Isogenic to CY4398 with untagged *tra1-F3744R* allele		This work
CY6507	Isogenic to CY4398 with FLAG5 tagged *tra1-WF-FW* allele		This work
CY6503	*MAT α HIS3 leu2Δ0 MET15 URA3 tra1-WF-FW*	CB1932	This work
CY6504	*MAT α HIS3 leu2Δ0 MET15 ura3Δ0 tra1-WF-FW*	CB2331	This work
CY6508	Isogenic to CY4398 with FLAG5 tagged *tra1-Δ1* allele		This work
CY6509	Isogenic to CY4398 with FLAG5 tagged *tra1-Δ2* allele		This work
CY6513	Isogenic to CY6070	CB2327	This work
CY4118	*MATa his3Δ1 leu2Δ0 met15Δ0 ura3Δ0* TEL2-TAP fusion		Ghaemmaghami *et al*., 2003
CY4119	*MATa his3Δ1 leu2Δ0 met15Δ0 ura3Δ0* TTI1-TAP fusion		Ghaemmaghami *et al*., 2003
CY4419	Isogenic to BY4743 except TRA1/URA3-Flag5-TRA1-HIS3		Genereaux *et al*., 2012
CY4421	Isogenic to BY4743 except TRA1/URA3-Flag5-tra1-F3744A-HIS3		Genereaux *et al*., 2012
CY6076	*MAT*a *ura3Δ0 his3Δ0 leu2Δ0 mec1-W2368A-HIS3*		Genereaux *et al*., 2012
CY6267	Isogenic with CY6076 except contain suppressor of Mec1-W2368A		DaSilva, In Press

Table S2: Oligonucleotides used in this study

Name	Sequence (5'-3')	Description
4225-7	GCATTAATTGAAGCTGATAATGAAGAACTGAAC	Forward primer used to amplify and sequence *tra1* C-terminus
4479-1	ATACGAGCTCTTTGAGGCTTTCTCTACCTTC	Reverse primer used to amplify and sequence *tra1* C-terminus
6173-1	GACGTTATACGCATTGGAATG	Forward primer to generate *tti2-290-421* mutation
6173-2	ACAGTTCTCTAGTACTGGTTTA	Forward primer to generate *tti2-206-421* mutation
6173-3	ACCCACGCTTGGAATGTCTT	Forward primer to generate *tti2-116-421* mutation
6223-1	AATATGCCGCTCACTCCATATCTCCAGGAG	Forward primer to generate *tti2-53-421* and *tti2-53-238* mutations
6312-1	ATACGAGCTCTCAGGCTATTGTTTCATCAGCATTG	Reverse primer to generate *tti2-53-238* mutation
5693-2	ATACGAGCTCTGCATTTGTCTGTGTCTGTGT	Reverse primer to generate *tti2*
4249-3	GCGGCCGCAAACGCAGCGCATGATGATG	Forward primer to generate *tra1*
6238-1	CATGCCATGGTCCTAGAGCTGATACATGGGT	Forward primer to generate *tra1-F3744S* mutation
6238-2	CATGCCATGGAGATAGAGCTGATACATGGGT	Forward primer to generate *tra1-F3744R* mutation
6241-1	ATTCCATGGCTACCAGAATGGCATGAAGTTCACGTCTG	Reverse primer to generate *tra1-WF-FW*
5747-1	CCCGAGCTCTTGATTGTTAGCAATACCG	Reverse primer to generate *tra1*
6260-1	CATGCCATGGTAGAGCTGATACATGGGTTAG	Forward primer to generate *tra1-Δ1*
6260-2	ATTCCATGGCTATGGCATGAAGTTCACGTCTG	Reverse primer to generate *tra1-Δ2*
6529-1	GTAGTACCTTCTGCCTATGC	Forward primer to check *hkr1* for suppressor mutation
6529-2	GGCAGCAAAAGTTGATGGAG	Reverse primer to check *hkr1* for suppressor mutation

Table S3: DNA constructs used in this study

Name	Description
CB2321	*LEU2* centromeric plasmid containing the *tti2-1-238* (myc tagged) gene without the *URA3* marker
CB2320	*LEU2* centromeric plasmid containing the *tti2-1-165* (myc tagged) gene without the *URA3* marker
CB2134	*LEU2* centromeric plasmid containing *TTI2* (myc tagged) gene used to make *tti2* truncations
CB2327	*LEU2* centromeric plasmid containing *TTI2* (myc tagged) gene without the *URA3* marker
CB1932	*LEU2* centromeric plasmid containing the *GEP4* gene
CB2331	*LEU2* centromeric plasmid containing the *GEP4* and *tti2-F328S* genes
CB2115	Parent plasmid of CB2134 used in the cloning of *tti2* truncations
pGEM	T-Easy Vector used for cloning *tti2* and *tra1* mutations (Promega)
CB2147	*TRA1* template used to make *tra1* substitution and deletion mutations
CB2151	$tra1_{FA}$ template used to make *tra1* substitution and deletion mutations
CB2319	*TTI2* tagged with *URA3* gene on a plasmid; to use for plasmid shuffling assay
CB2485	*LEU2* centromeric plasmid containing the *tra1-F3744S* gene (with *HIS3*)
CB2486	*LEU2* centromeric plasmid containing the *tra1-F3744R* gene (with *HIS3*)
CB2487	*LEU2* centromeric plasmid containing the *tra1-WF-FW* gene (with *HIS3*)
CB2488	*LEU2* centromeric plasmid containing the *tra1-Δ1* gene (with *HIS3*)
CB2489	*LEU2* centromeric plasmid containing the *tra1-Δ2* gene (with *HIS3*)
CB2490	*LEU2* centromeric plasmid containing the *tti2-Δ108-216* (myc tagged) gene without the *URA3* marker
CB2491	*LEU2* centromeric plasmid containing the *tti2-290-421* (myc tagged) gene without the *URA3* marker
CB2492	*LEU2* centromeric plasmid containing the *tti2-206-421* (myc tagged) gene without the *URA3* marker
CB2493	*LEU2* centromeric plasmid containing the *tti2-116-421* (myc tagged) gene without the *URA3* marker
CB2494	*LEU2* centromeric plasmid containing the *tti2-53-421* (myc tagged) gene without the *URA3* marker
CB2495	*LEU2* centromeric plasmid containing the *tti2-53-238* (myc tagged) gene without the *URA3* marker

Curriculum Vitae

Samantha A. Pillon

Education:

Master of Science (Biochemistry)

The University of Western Ontario, London Ontario August 2013

Bachelor of Medical Science (Honours Specialization – Biochemistry)

The University of Western Ontario, London Ontario May 2011

Honours/Awards

Western Graduate Research Scholarship (WGRS) September 2011-August 2013

Related Work Experience

Teaching Assistant (Biochemistry 3380)

The University of Western Ontario, London Ontario January 2012-April 2013

Honours Thesis Student

The University of Western Ontario, London Ontario September 2010-April 2011

Summer Student

The University of Western Ontario, London Ontario May 2010-August 2010

Publications

DaSilva, LF., **Pillon, S.***, Genereaux, J., Davey, MJ., Gloor, GB., Karagiannis, J., and Brandl, CJ. The Extreme C-terminus of *Saccharomyces cerevisiae* Mec1 is required for its Localization, Stability and Function. *In press*.